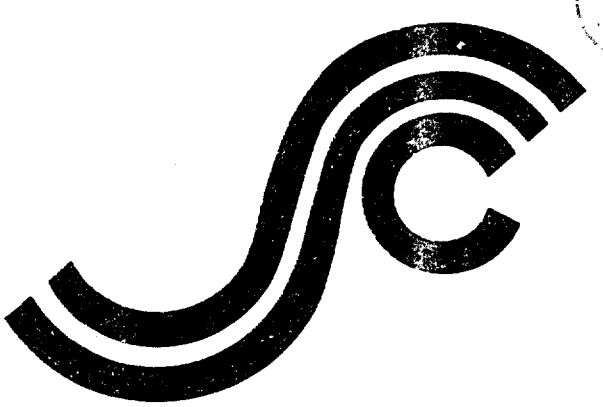
AD-A236 599

DTIC

SSC-363

UNCERTAINTIES IN STRESS ANALYSIS ON MARINE STRUCTURES



A-1

91-01866

This document has been approved
for public release and sale; its
distribution is unlimited

SHIP STRUCTURE COMMITTEE

1991

91 6 11 144

SHIP STRUCTURE COMMITTEE

The SHIP STRUCTURE COMMITTEE is constituted to prosecute a research program to improve the hull structures of ships and other marine structures by an extension of knowledge pertaining to design, materials, and methods of construction.

RADM J. D. Sipes, USCG, (Chairman)
Chief, Office of Marine Safety, Security and Environmental Protection
U. S. Coast Guard

Mr. Alexander Malakhoff
Director, Structural Integrity Subgroup (SEA 55Y)
Naval Sea Systems Command

Dr. Donald Liu
Senior Vice President
American Bureau of Shipping

Mr. H. T. Haller
Associate Administrator for Ship-building and Ship Operations
Maritime Administration

Mr. Thomas W. Allen
Engineering Officer (N7)
Military Sealift Command

CDR Michael K. Parmelee, USCG,
Secretary, Ship Structure Committee
U. S. Coast Guard

CONTRACTING OFFICER TECHNICAL REPRESENTATIVES

Mr. William J. Siekierka
SEA 55Y3
Naval Sea Systems Command

Mr. Greg D. Woods
SEA 55Y3
Naval Sea Systems Command

SHIP STRUCTURE SUBCOMMITTEE

The SHIP STRUCTURE SUBCOMMITTEE acts for the Ship Structure Committee on technical matters by providing technical coordination for determinating the goals and objectives of the program and by evaluating and interpreting the results in terms of structural design, construction, and operation.

AMERICAN BUREAU OF SHIPPING

Mr. Stephen G. Arntson (Chairman)
Mr. John F. Conlon
Dr. John S. Spencer
Mr. Glenn M. Ashe

MILITARY SEALIFT COMMAND

Mr. Albert J. Attermeyer
Mr. Michael W. Touma
Mr. Jeffery E. Beach

MARITIME ADMINISTRATION

Mr. Frederick Seibold
Mr. Norman O. Hammer
Mr. Chao H. Lin
Dr. Walter M. Maclean

NAVAL SEA SYSTEMS COMMAND

Mr. Robert A. Sielski
Mr. Charles L. Null
Mr. W. Thomas Packard
Mr. Allen H. Engle

U. S. COAST GUARD

CAPT T. E. Thompson
CAPT Donald S. Jensen
CDR Mark E. Noll

SHIP STRUCTURE SUBCOMMITTEE LIAISON MEMBERS

U. S. COAST GUARD ACADEMY

LT Bruce Mustain

U. S. MERCHANT MARINE ACADEMY

Dr. C. B. Kim

U. S. NAVAL ACADEMY

Dr. Ramswar Bhattacharyya

STATE UNIVERSITY OF NEW YORK MARITIME COLLEGE

Dr. W. R. Porter

WELDING RESEARCH COUNCIL

Dr. Martin Prager

NATIONAL ACADEMY OF SCIENCES - MARINE BOARD

Mr. Alexander B. Stavovy

NATIONAL ACADEMY OF SCIENCES - COMMITTEE ON MARINE STRUCTURES

Mr. Stanley G. Stiansen

SOCIETY OF NAVAL ARCHITECTS AND MARINE ENGINEERS - HYDRODYNAMICS COMMITTEE

Dr. William Sandberg

AMERICAN IRON AND STEEL INSTITUTE

Mr. Alexander D. Wilson

Member Agencies:

United States Coast Guard
Naval Sea Systems Command
Maritime Administration
American Bureau of Shipping
Military Sealift Command

Ship Structure Committee

An Interagency Advisory Committee
Dedicated to the Improvement of Marine Structures

Address Correspondence to:

Secretary, Ship Structure Committee
U. S. Coast Guard (G-MTH)
2100 Second Street, S.W.
Washington, D.C. 20593-0001
PH: (202) 267-0136
FAX: (202) 267-4816

SSC-363
SR-1326

April 10, 1991

UNCERTAINTIES IN STRESS ANALYSIS ON MARINE STRUCTURES

Marine structures are designed to withstand the extreme responses caused by external loads. It is important that we understand the extent to which uncertainties associated with stress analysis influence design considerations and structural reliability. This report surveys the state of knowledge concerning uncertainties in the analysis of marine structures. It emphasizes the critical roles of extreme loads and modeling methods. This information should prove to be quite useful for naval architects and design engineers.

J. B. SIPES
Rear Admiral, U.S. Coast Guard
Chairman, Ship Structure Committee

Technical Report Documentation Page

1. Report No.	2. Government Accession No.	3. Recipient's Catalog No.
SSC - 363		

4. Title and Subtitle

UNCERTAINTIES IN STRESS ANALYSES ON MARINE STRUCTURES

5. Report Date April 1991

6. Performing Organization Code

7. Author(s) E. Nikolaidis and P. Kaplan

8. Performing Organization Report No. SR-1326

9. Performing Organization Name and Address
Aerospace and Ocean Engineering Dept.
Virginia Polytechnic Institute and State University
Blacksburg, VA 24061

10. Work Unit No. (TRAIS)

11. Contract or Grant No. DTCG 23-88-R-20020

12. Sponsoring Agency Name and Address
Ship Structure Committee
U.S. Coast Guard
2100 Second Street, SW
Washington D.C. 20593

13. Type of Report and Period Covered Final Report

14. Sponsoring Agency Code G - M

15. Supplementary Notes

Sponsored by the Ship Structure Committee and its Member Agencies

16. Abstract

A survey of the state of knowledge on uncertainties in stress analyses on marine structures is presented. Uncertainties are classified and methods for modeling them are presented. Modeling uncertainties and their effects on extreme design loads are emphasized. Uncertainties in the following steps of stress analysis are quantified and ranked in terms of relative importance:

- Description of loading environment
- Evaluation of loads
- Combination of loads
- Structural analysis
- Fatigue

A 5 year research program is proposed for reducing uncertainties. This program consists of 14 tasks which have been prioritized in terms of expected benefits, risk and cost.

17. Key Words

Uncertainty analysis, structural reliability, design loads, MARINE ENGINEERING

18. Distribution Statement
Available from:
National Technical Information Service
U.S. Department of Commerce
Springfield, VA. 22151

19. Security Classif. (of this report)	20. Security Classif. (of this page)	21. No. of Pages	22. Price
Unclassified	Unclassified	110	

Form DOT F 1700.7 (8-72) Reproduction of completed page authorized

METRIC CONVERSION FACTORS

Approximate Conversions to Metric Measures

Symbol	When You Know	Multiply by	To Find	Symbol
	LENGTH			
in	inches	*2.5	centimeters	cm
ft	feet	30	centimeters	cm
yd	yards	0.9	meters	m
mi	miles	1.6	kilometers	km
	AREA			
in^2	square inches	6.5	square centimeters	cm^2
ft^2	square feet	0.09	square meters	m^2
yd^2	square yards	0.8	square meters	m^2
mi^2	square miles	2.6	square kilometers	km^2
	acres	0.4	hectares	ha
	MASS (weight)			
oz	ounces	28	grams	g
lb	pounds	0.45	kilograms	kg
	short tons (2000 lb)	0.9	tonnes	t
	VOLUME			
tsp	teaspoons	5	milliliters	ml
Tbsp	tablespoons	15	milliliters	ml
fl oz	fluid ounces	30	milliliters	ml
c	cups	0.24	liters	l
pt	pints	0.47	liters	l
qt	quarts	0.95	liters	l
gal	gallons	3.8	liters	l
ft^3	cubic feet	0.03	cubic meters	m^3
yd^3	cubic yards	0.76	cubic meters	m^3
	TEMPERATURE (exact)			
°F	Fahrenheit temperature	5/9 (after subtracting 32)	Celsius temperature	°C

*1 in = 2.54 (exactly). For other exact conversions and more detailed tables, see NBS Misc. Publ. 286, Units of Weights and Measures, Price $2.25, SD Catalog No. C13.10:286



Approximate Conversions from Metric Measures

Symbol	When You Know	Multiply by	To Find	Symbol
	LENGTH			
mm	millimeters	0.04	inches	in
cm	centimeters	0.4	inches	in
m	meters	3.3	feet	ft
m	meters	1.1	yards	yd
km	kilometers	0.6	miles	mi
	AREA			
cm^2	square centimeters	0.16	square inches	in^2
m^2	square meters	1.2	square yards	yd^2
km^2	square kilometers	0.4	square miles	mi^2
ha	hectares (10,000 m^2)	2.5	acres	
	MASS (weight)			
g	grams	0.035	ounces	oz
kg	kilograms	2.2	pounds	lb
t	tonnes (1000 kg)	1.1	short tons	
	VOLUME			
ml	milliliters	0.03	fluid ounces	fl oz
l	liters	2.1	pints	pt
l	liters	1.06	quarts	qt
l	liters	0.26	gallons	gal
m^3	cubic meters	35	cubic feet	ft^3
m^3	cubic meters	1.3	cubic yards	yd^3
	TEMPERATURE (exact)			
°C	Celsius temperature	9/5 (then add 32)	Fahrenheit temperature	°F

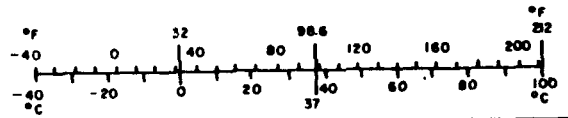


Table of Contents

Chapter/Section	Page
1.0 Introduction	1
1.1 Objective	2
1.2 Report outline	2
2.0 Types of Uncertainties	4
2.1 Classification	4
2.2 Models for modeling uncertainty	5
2.3 Effect of modeling uncertainties on lifetime extreme loads	8
3.0 Loading Environment	10
3.1 Ships	10
3.2 Offshore Platforms	16
4.0 Loads	19
4.1 Ships	19
4.1.1 Stillwater bending moments and shear forces	19
4.1.2 Uncertainties in short term vertical wave bending due to errors in response amplitude operators	23
4.1.3 Long term induced bending moments	25
4.1.4 Uncertainties in hydrodynamic pressure	28
4.2 Offshore platforms	30
5.0 Load Combinations	37
6.0 Structural Analysis	39
6.1 Ships	39
6.1.1 Uncertainties in F. E. A.	39
6.1.2 Uncertainties in F. E. A. in other engineering applications	42
6.1.3 Errors due to shear lag	42
6.1.4 Effect of joint flexibility and rigid beam lengths in transverse strength analysis of ships	48
6.2 Offshore platforms	48
7.0 Fatigue	51

7.1 Uncertainties in stress concentration factor 51
7.2 Uncertainties in cumulative fatigue damage 52
7.2.1 Relative importance of random uncertainties 54
7.2.2 Relative contribution of various types of uncertainty on fatigue damage 55

8.0 Conclusions 58

9.0 Research Plan for Future Efforts to Reduce Uncertainties in Estimated Load Effects on Marine Structures 61

10. References 78

Appendix A: Calculation of Uncertainties in Lifetime Maximum Loads or Load Effects 85

Appendix B: Combination of Slamming and Wave Induced Stresses: A Simulation Study 86

B.1 Introduction 86
B.2 Results and discussion 88
B.3 Conclusions 89

List of Figures

Figure 2.1 Probability Distribution of Bias of Extreme Wave Height.

Figure 2.2 Comparison Between Ditlevsen and Ang Models for Modeling Uncertainty.

Figure 3.1 Effect of Spectral Shape Variability on Mean Square Wave Induced Bending Moment.

Figure 3.2 Dependence of the Short Crestedness Bias on Various Parameters.

Figure 3.3 Directionality Bias.

Figure 3.4 Probability Distribution of Annual Expected Maximum (H_{max}) and Significant (H_{sig}) Wave Heights.

Figure 4.1 Calculated and Measured Response Amptitude Operators.

Figure 6.1 Sketch of SL-7 Model.

Figure 6.2 Loading Conditions.

Figure 6.3 Comparison of Twisting Angles Along the Ship Hull.

Figure 6.4 Longitudinal Warping Stresses in Frame 142.

Figure 6.5 Longitudinal Warping Stresses in Frame 290.

Figure 6.6 Shear Stresses at Frame 186.

Figure 6.7 Normal Bending Streses in Frame 186.

Figure B1 Maximum Wave Bending Moment vs. Significant Wave Height.

Figure B2 Design Bending Moment vs. Significant Wave Height.

Figure B3 Wave, Slamming and Combined Bending Moment Time History.

Figure B4 Maximum Combined Bending Moment Histograms.

Figure B5 Estimated Bias vs. Number of Simulated Time Histories.

List of Tables

2.1 Comparison Between The Ang and Cornell (74) and Ditlevsen Models for Modeling Uncertainty.

3.1 Uncertainties in Describing Loading Environment for Ships.

3.2 Uncertainties in Describing Environment for Offshore Platforms.

4.1 Variability in Stillwater Bending Moments.

4.2 Variability in Stillwater Shear Forces.

4.3 Uncertainties in Lifetime Extreme Bending Moments.

4.4 Relative Contribution of Various Types of Uncertainties to Total Uncertainty in Extreme Bending Moment.

4.5 Uncertainties in Long Term Vertical Wave Bending Moment.

4.6 Summary of Results on Uncertainties in Long Term Extreme Bending Moments.

4.7 Bounds for Bias of Response Amplitude Operator for Hydrodynamic Pressure on SL-7 Containership.

4.8 Uncertainties in Annual Maximum Loads for Drag and Inertia Dominated Platforms.

4.9 Total Coefficient of Variation of Global Force as a Function of Return Period.

4.10 Uncertainties Involved in Predicting Extreme Loads on a Vertical Pile in the North Sea.

4.11 Uncertainties in Wind, Current and Tide Loads.

4.12 Uncertainties in Extreme Global Loads on Offshore Platforms.

5.1 Bias and COV of Standard Methods for Combining Slamming and Wave Bending Moments.

6.1 Measured and Predicted Longitudinal Wave Bending Stress Amidships.

6.2	Uncertainties in F.E.A. on an SL-7 Containership.
6.3	Loading and Geometry Description.
6.4	Effective Breadth For Various Plate Thicknesses.
6.5	Loading and Geometry Description.
6.6	Effective Breadth For Various Stiffeners with Different Cross-Sectional Areas.
6.7	Bias and Scatter of Methods to Estimate Effective Breadth.
6.8	Uncertainties in Dynamic Analysis of Fixed Offshore Platforms.
7.1	Coefficient of Variation of Cumulative Fatigue Damage Due to Random Uncertainties ($N = 10^6$).
7.2	Uncertainties Involved in All Steps of Fatigue Analysis.
7.3	Uncertainties in Cumulative Fatigue Damage and Relative Contribution of Each Uncertainty in Table 7.2.
9.1	List of Tasks for Reducing Uncertainties.
B1	Data for Simulation Study
B2	Statistics of Maximum Value of Combined Bending Moment for Significant Wave Height: 6.14m, Ship Speed: 15 knots.
B3	Statistics of Maximum Value of Combined Bending Moment for Significant Wave Height: 9.6m, Ship Speed: 15 knots.
B4	(Same as B3, except for Wave Height: 13.07m)
B5	(Same as B3, except for Wave Height: 6.14m and Ship Speed: 18 knots)
B6	(Same as B5, except for Ship Speed: 20 knots)
B7	(Same as B6, except for Ship Speed: 25 knots)

Nomenclature

B	total bias
B_I	random bias
B_{II}	modeling bias
B_S	Bias due to spectral shape variability
B_{sc}	Bias due to shortcrestedness
B_d	Bias due to directionality of weather systems
B_H	Bias in visual observations
B_L	bias in response amplitude operator due to all uncertainties except from nonlinearities
$B_{S/H}$	bias due to uncertainty in sagging/hogging wave bending moment due to nonlinearities
B_M	bias due to manufacturing imperfections
B_F	bias in wave load applications
B_N	bias for errors in structural analysis
C_B	block coefficient
COV	coefficient of variation
D	fatigue damage
$E(B)$	expected value of B
H_s	significant wave height
$H(\omega)$	response amplitude operator at frequency ω
m	exponent in S-N equation ($N\ S^m = A$)

m_{ijk}	stillwater bending moment at the *ith* voyage which is applied to the *jth* ship, which belongs to the *kth* class
m_o	average load effect for all ships
$m_o + m_k$	average load effect for all ships in *kth* class
N	number of years or number of cyclic load applications
X	actual value of quantity of interest
X_o	value specified by design code
X_p	predicted value
$X^{(n)}$	maximum for n samples X_1, ..., X_n
ϵ	error between predictions and corresponding actual values
ϵ_i	variation of load effect from voyage to voyage
λ	effective breadth
ρ	correlation coefficient
σ	standard deviation

1.0 Introduction

Structural analysis of marine structures consists of the following steps:

a) description of the environment;

b) modeling of the applied loads;

c) load combination;

d) response analysis, where displacements, nominal forces applied to each structural member, and stresses are calculated;

e) fatigue analysis, where damage inflicted by cyclic loads is calculated.

The calculated load effects (demand) are compared to the strength of the structure (capacity), in order to assess its safety.

In design, the dimensions of the structural members are determined based on the requirement that the demand does not exceed the capacity.

Uncertainties are always involved in all the steps of structural analysis and also in evaluating strength. These uncertainties are due to the random character of the loading environment and the resulting loads, or due to inadequate knowledge of physical phenomena associated with loads.

Rational analysis and design of marine structures requires consideration of all the uncertainties involved in predicting load effects. In probabilistic methods, these uncertainties must be quantified in order to assess structural safety. For example, if a first order second moment (F.O.S.M.) method is used, we need at least the first two moments of all random variables associated with load effects in order to locate the design point and evaluate the safety index (Madsen, 86). Furthermore, the determination of the partial load and resistance factors, in the safety equation of a probabilistic design code, also requires quantification of all uncertainties (ISSC 85).

The development of probabilistic analysis methods and design codes increased the importance of quantifying uncertainties. Recent studies on offshore [Faulkner 83, ISSC 85, Das 86, Guedes Soares 82], as well as ship structures [Faulkner 81, ISSC 85, Kaplan 84, Guedes Soares 84], investigated errors in evaluating loads and load effects. The results of these studies can be used to assess the relative importance of the various types of uncertainties. For example, one of the conclusions drawn from Guedes Soares (82) for offshore structures, was that the uncertainty in the lifetime extreme wave height is the most significant. The error in predicting the most severe sea condition over the lifetime is one of the major ingedients of the above uncertainty.

Probabilistic theory and structural analysis have reached a state of maturity but there are still gaps in the state of knowledge on quantifying loads and their effects. As part of the total effort associated with rational ship and offshore study design based on probabilistic methods of analysis, a project aimed at quantifying the uncertainties in determining loads and load effects in marine structures was established by the Ship Structure Committee. The effort in this project concentrates on assessing the quality of procedures for predicting loading effects on marine structures by quantifying the errors involved. The following issues are emphasized and discussed in the present report summarizing the investigation:

a) what is the best way to model uncertainties?

b) what are the differences between random (natural) and modeling (subjective) uncertainties?

c) how do modeling uncertainties affect extreme loads?

d) what are the most important uncertainties?

1.1 Objective

The objective of this study is to quantify the error in stress analyses of marine structures, thus providing necessary information to establish safety criteria in design.

The work described herein is intended to locate the sources of error in all the steps of the load effect prediction procedure and to provide quantitative information on all types of error. The most important types of error are identified and ranked in terms of their influence in design. Finally, strategies are recommended for reducing the most important uncertainties.

1.2 Report outline

The information presented in this report is organized as follows:

In Chapter 2, we classify uncertainties into two categories, random (natural) and modeling, and we study the basic differences between these two types. Emphasis is given to the effect of modeling uncertainties on extreme loads. Furthermore, we review various methods for modeling uncertainties.

The uncertainties involved in describing the loading environment for ships and offshore platforms are considered in Chapter 3. For ships, we studied the uncertainty in spectral shape variability, short crestedness, directionality of weather systems, and visual observations. These uncertainties are quantified in terms of their effects on the short term longitudinal wave bending moment. For the case of offshore platforms, uncertainties in extreme wave heights are quantified.

Chapter 4 deals with uncertainties in loads and load effects. For the case of ships, most of the information is on uncertainties in short and long term stillwater and wave bending moments. Different ways for modeling uncertainties are compared. It is shown that we can dramatically reduce the variability, if we use the Guedes Soares model for uncertainty and distinguish between different types of ships, and between hogging and sagging. However, although Guedes Soares' idea for reducing uncertainties is correct, we believe that it has not been properly implemented in Guedes Soares (84) because, modeling uncertainties have not been correctly treated in his study.

For offshore platforms, we study uncertainties in extreme global loads. Important factors, such as current velocity and marine fouling are also considered.

Uncertainties in load combination procedures are considered in Chapter 5. The results from a Monte Carlo simulation study on the combination of wave and slamming induced bending moments are presented. The objective of this study is to assess the error associated with this process and its effect on extreme design loads.

Chapter 6 deals with uncertainties in structural analysis. The errors associated with finite element analysis (F.E.A.) of ships and offshore platforms, are quantified. Information is also provided on the errors in F.E.A. of other types of structures (automotive and aerospace structures).

Uncertainties in fatigue analyses are studied in Chapter 7. The study is confined to cumulative damage based approaches. We examine the contribution of the uncertainties, which are involved in all steps of fatigue analysis, to the overall uncertainty in fatigue damage. This allows to identify the most critical uncertainties. Finally, it is shown that the effect of random uncertainties on the cumulative damage is neglegible for both ships and offshore structures.

The conclusions from this study are summarized in Chapter 8. In this chapter, we also identify the most important uncertainties involved in all steps of stress analyses procedures. Random and modeling uncertainties are compared in terms of their effect on lifetime extreme loads and on fatigue damage.

In Chapter 9, we recommend a 5 year research program. The objective of this program is to expand the state of knowledge and reduce the most critical uncertainties. This program has been broken down into a number of tasks, which have been prioritized. The tasks have been prioritized in terms of the relative importance of the associated uncertainties, and the expected benefits, risk, and cost. A step by step procedure is presented for completing each task.

2.0 Types of Uncertainties

In this chapter we define two categories of uncertainties, random and modeling, and examine the differences between them. We also review various models for such uncertainties. Emphasis is given on the effect of modeling uncertainties in the extreme design loads.

2.1 Classification

Uncertainties in analysis of marine structures can be categorized into natural (random) and modeling types. The former are due to the statistical nature of the loading environment and the resulting loads, and they induce scatter in predictions. The latter are due to the imperfect knowledge on various phenomena, and idealizations and simplifications in analysis procedures. These uncertainties introduce both bias and scatter.

An example of a natural uncertainty is that associated with the wave elevation at a given position in the ocean. An example of a modeling uncertainty, is the error in calculating the stresses in a structure, when the applied loads are known. For this case, the error is only due to the assumptions and simplifications in structural analysis.

Modeling uncertainties are information sensitive, in the sense that they can be reduced as the knowledge of the associated physical phenomena expands, and the mathematical models representing them become more accurate. This is not the case with random uncertainties which do not decrease as we gather more information on fundamental science, but only as we obtain more data.

Both random and modeling uncertainties must be quantified and accounted for in reliability analysis and development of probabilistic design codes. In the following paragraph we explain why modeling uncertainties should be considered.

The reliability of a structural system depends on both load and strength variables. Each variable can be calculated with different degree of accuracy. For example, for most of the cases, the response of an offshore platform to dead loads can be evaluated with high accuracy, given that the loads are known, as opposed to the case of wave induced response which cannot be predicted with the same confidence. Therefore, when assessing structural safety and making design decisions, we must take into account the differences in the confidence levels associated with each load and strength variable. For example, in a probabilistic design code for offshore structures, the load factor for wave loads is larger than that for dead loads, because the modeling uncertainty associated with the former loads is larger. It should be noted, however, that the load factor associated with stillwater bending moments on ships should be large due to the high coefficient of variation (COV) associated with these loads.

2.2 Models for modeling uncertainty

Ang and Cornell (74) and Ditlevsen (82) proposed two different methods for treating modeling uncertainties. Ang's model is for both load and strength uncertainties. Ditlevsen's model was proposed for uncertainties associated with strength but it can also be applied to load variables.

In the following we present Ang's model.

Let X be the actual value of some quantity of interest and X_0 be the corresponding value specified by a design code. Then,

$$X = B_I B_{II} X_0, \tag{2.1}$$

where B_I is the ratio of the theoretically predicted value for this quantity, X_p, and X_0, and B_{II} is the ratio of X and X_p. B_I is a measure of natural (random) variability, which is also called type I uncertainty, and B_{II} is a measure of modeling uncertainty. The mean values of random variables B_I and B_{II}, $E(B_I)$ and $E(B_{II})$, are the biases corresponding to natural and modeling uncertainties, respectively. Assuming that the random and modeling uncertainties are statistically independent, and by using a first order second moment (F.O.S.M.) approximation, which is based on a linear expansion of the expression for B about the mean value of the random variables, we can quantify the total uncertainty in X as follows:

$$\begin{aligned} E(B) &= E(B_I)E(B_{II}), \text{ and} \\ COV_B &= (COV_{B_I}^2 + COV_{B_{II}}^2)^{\frac{1}{2}} \end{aligned} \tag{2.2}$$

where $B = B_I B_{II}$.

COV stands for the coefficient of variation of the quantity specified by the subscript.

As pointed out by Wirsching (81), equations (2.2) are valid for small coefficients of variation (less than 0.10) only. However, we adopted the above approximations because of the following reasons:

a) They have been employed in almost all studies on uncertainties in analyses on marine structures (Kaplan 84, Guedes Soares 84, Bea 89, Olufsen 90, Moses 85, 86)

b) In most cases, we do not know the exact probability distribution of random and modeling uncertainties. This does not allow to use more accurate methods, such as the Advanced First Order Second Moment Method to combine random and modeling uncertainties.

c) The estimates of the average bias and COV of various types of uncertainty are crude. Therefore, it is not reasonable to use more accurate (but also more complex) methods.

Random variables B_I and B_{II} are also assumed to be independent of X_0.

An example of quantifying modeling uncertainties is illustrated in Figure 2.1, which has been extracted from Bea (89). The quantity considered here is the maximum annual wave height in the northwest shelf of West Australia. The ratio of the measured over the predicted maximum wave height is shown in the horizontal axis. The maximum wave height is predicted using a hindcast method. The vertical axis represents the probability that the value of the ratio is less than some given number. Based on the information provided in Figure 2.1, the mean of B_{II}, which represents modeling uncertainty, is 1.1 and its coefficient of variation is 0.13. This means that on the average, hindcast methods predict a value for the annual maximum wave height, which is 10% smaller than the actual value. The coefficient of variation of 0.13 indicates that the ratio between the actual and predicted wave height ranges between 0.97 and 1.23 with probability 0.68.

A random variable, such as the stress in a particular structural member, is a function of other random variables, such as the wave height and the average wave period. Besides the errors involved in calculating these variables, errors are also involved in calculating the stress given the values of the latter random variables. Ang and Cornell (74) presented formulas, which are based on F.O.S.M. concepts, for quantifying the uncertainty associated with the above errors.

The Ditlevsen model is applicable to reduced random variables (Madsen, Krenk and Lind, 86), which are independent gaussian. We can obtain these variables from the original ones by employing Rosenblatt transformation (Rosenblatt 52). According to Ditlevsen (82), model uncertainty can be accounted for by the following equation,

$$X' = cX'_p + b \tag{2.3}$$

where c is a constant, and b is a gaussian random variable, which is statistically independent of X'. The prime indicates reduced random variables.

Ditlevsen, and Ang and Cornell models are compared in Table 2.1.

Clearly, Ditlevsen model is more general. The main difference between these two models, is that Ditlevsen model accounts for the statistical correlation between the error in predicting the value of a variable, $\epsilon = X' - X'_p$, and the value of the variable itself, while Ang's model assumes that the above random variables are independent. This is demonstrated in Figure 2.2, which is for the special case that X_p and X are lognormal. The value of X', which is equal to lnX, is plotted there as a function of X_p. The average of X' or lnX, as well as regions corresponding to this average $\pm$ one standard deviation, are plotted in this figure. It is observed that the error between actual values and predictions for lnX, which is represented by the width of the shaded region, is independent of lnX_p for the case of Ang's model.

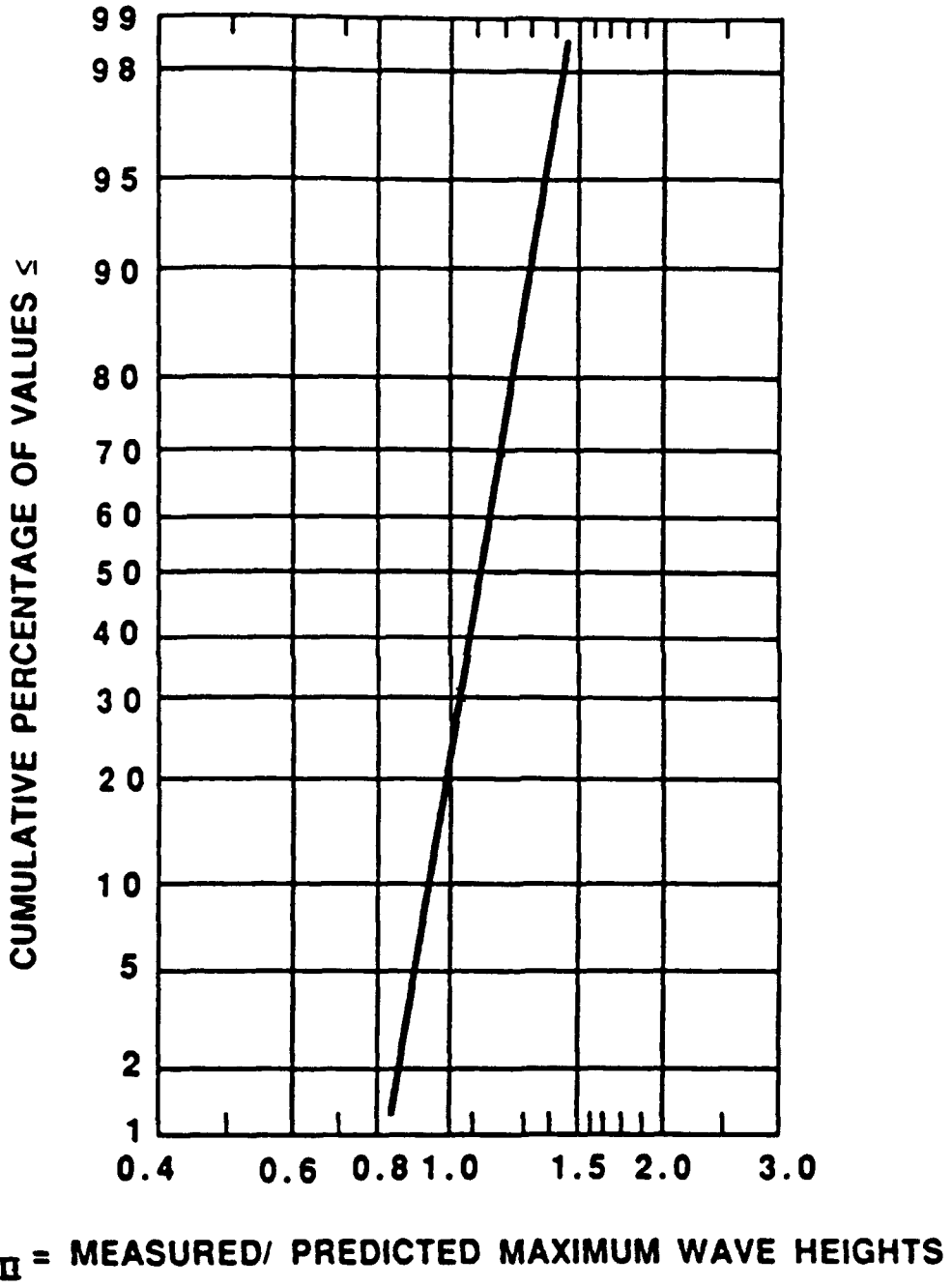
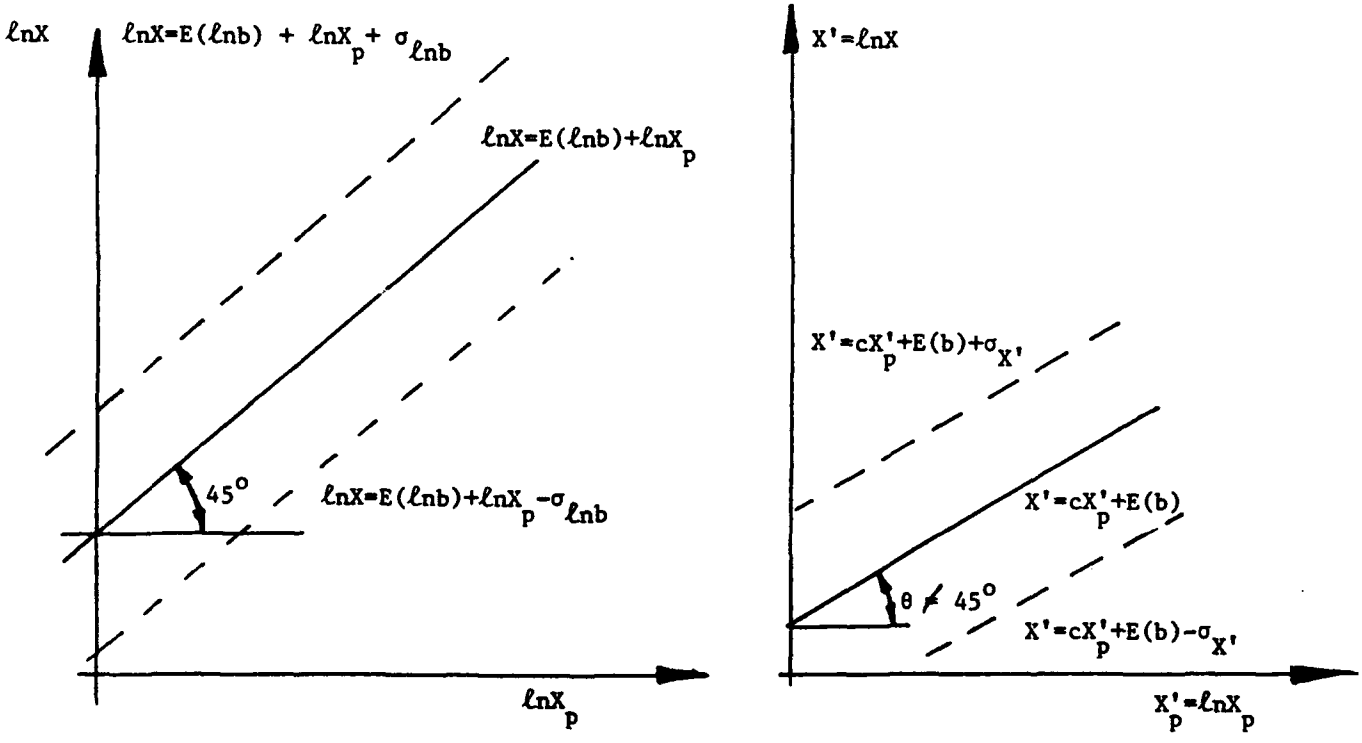


Fig. 2.1 Probability Distribution of Bias of Extreme Wave Height



Ang

Ditlevsen

Note: X is gaussian

Fig. 2.2 Comparison Between Ang and Ditlevsen Models for Modeling Uncertainty

Table 2.1. Comparison Between The Ang and Cornell and Ditlevsen Models for Modeling Uncertainty

Characteristic	Ditlevsen	Ang
Equation:	$X' = cX'_p + b$ c: constant b: random variable independent of X'_p	$X = BX_p$ B: random variable independent of X_p
Space in which model is applicable:	Reduced	Physical
Relation between statistics of actual and predicted values:	$E(X') = cE(X'_p) + E(b)$ $\sigma^2_{X'} = c^2\sigma^2_{X'_p} + \sigma^2_b$	$E(X) = E(B)E(X_p)$ $COV_x = (COV^2_B + COV^2_{X_p})^{\frac{1}{2}}$
Correlation between error and predicted value	$\rho_{\epsilon X'_p} = \frac{(c-1)\sigma^2_{X'_p}}{[(c-1)\sigma^2_{X'_p} + \sigma^2_b]^{\frac{1}{2}}}$	$\rho_{\epsilon X_p} = 0$

Notes:

a) ϵ denotes the error between prediction and measurements, i.e. $\epsilon = X' - X'_p$ (reduced space), or $\epsilon = X - X_p$ (physical space).

b) $\rho_{\epsilon X_p}$ denotes the correlation between ϵ and X_p.

c) For the special case of X_p and X being lognormal, Ditlevsen's model reduces to Ang's model for $c = 1$.

Although Ang's model is not as general as the Ditlevsen model, it is preferable, because it is simpler. It requires less information in order to determine the statistics of its parameters, and it is very convenient to use for the case that the variables involved are lognormal. Moreover, it is expected that random variable B is lognormally distributed, for most cases, because it is usually the product of several random variables. (Central Limit Theorem).

2.3 Effect of modeling uncertainties on lifetime extreme loads

In both ships and offshore platforms, it is important to distinguish between natural and modeling uncertainties, and the ways by which they affect the maximum lifetime loads and load effects.

In contrast to random uncertainties, modeling uncertainties in extreme loads or load effects do not decrease with the length of the return period increasing. Indeed, these uncertainties are systematic. Consequently, the modeling errors corresponding to two or more load applications are perfectly correlated. Therefore, the modeling error corresponding to the maximum of these loads does not reduce with the number of load applications increasing, as it is the case for independent or weakly correlated errors. Therefore, uncertainties in lifetime loads may be grossly underestimated if we treat modeling uncertainties as random.

We calculate uncertainties in the extreme value of some quantity X according to the following rule: Let $X_1, ..., X_n$ be n independent samples from a random variable and $X^{(n)}$ be their maximum value, i.e.

$$X^{(n)} = max\ (X_1, ..., X_n) \tag{2.4}$$

Then, the coefficient of variation of the maximum $X^{(n)}$ is:

$$COV_{X^{(n)}} = (COV_{II}^2 + COV_{I_{x^{(n)}}}^2)^{\frac{1}{2}} \tag{2.5}$$

where $COV_{I_{x^{(n)}}}$ is the coefficient of variation corresponding to natural uncertainties in the maximum $X^{(n)}$.

Equation (2.5) correctly implies that the two types of uncertainty, natural (random) and modeling, must be treated differently when studying the uncertainty in the extreme value of some load or load effect. Furthermore, the contribution of modeling uncertainties to the uncertainty in the maximum value, $X^{(n)}$, does not decrease as the number of samples, n, increases.

Olufsen and Bea (90), and Bea (89), have concluded in their work that uncertainties in maximum design loads and load effects have been seriously underestimated in the recently released API - PRAC 22 design code for offshore platforms. It is remarkable that the coefficients of variation of extreme global loads, which were derived from their studies, are almost 100% larger than those used by the developers of the API code. This is attributed to the way in which uncertainties were treated in developing this code.

In this report, we have estimated uncertainties in extreme loads by employing eq. (2.5) for both ships and offshore structures. We have demonstrated that, for most applications, this equation yields significantly larger uncertainties than those reported by some authors

including the developers of the API-PRAC 22 design code. We believe that, eq. (2.5) is more appropriate than the approach which is used in the API-PRAC 22 design code, because the former treats uncertainties in a more realistic way than the latter. Furthermore, we have shown that the effect of random uncertainties on fatigue life is phased out while the effect of modeling uncertainties does not decrease, with the length of the exposure time increasing. As a result, uncertainties in fatigue life are only due to modeling uncertainties. Random uncertainties do not affect fatigue reliability. The above observations demonstrate the importance of modeling uncertainties.

3.0 Loading Environment

The first step in stress analysis of a marine structure is to model the loading environment. In this chapter, we study environmental uncertainties associated with wave loads on ships and offshore platforms. For offshore platforms, we provide information on other types of loads such as those due to current velocity.

3.1 Ships

Guedes Soares (84) and Kaplan (84) studied uncertainties in ship loads and load effects. Guedes Soares (84) was the first to employ linear models relating the bias of some quantity associated with loads or load effects, to various parameters, such as the significant wave height and period. The coefficients in these linear models were calculated by regression on measured and predicted loads or load effects. All other studies on uncertainties assume that the bias is independent of all parameters. The main advantage of Guedes Soares' approach is that it yields smaller coefficients of variation for loads and load effects. Furthermore, the coefficient of variation decreases when the number of parameters, which are involved in the linear model for the bias, is increasing.

In this section we examine uncertainties in environmental description and their effects on short term loads and load effects.

The following uncertainties are involved in modeling the loading environment for the case of ships:

- uncertainty in wave spectra,
- uncertainty due to short crestedness,
- uncertainty due to directionality of the weather systems,
- uncertainty in visual observations of wave heights,
- uncertainty in wave heights due to correlation of subsequent wave peaks, and broadbandness of the wave spectrum,
- uncertainties due to heavy weather countermeasures.

Guedes Soares (84) and Kaplan (84) studied the uncertainty in wave spectra.

Guedes Soares (84) separated the uncertainty in wave spectra into three categories: statistical, fundamental and model uncertainty. Statistical uncertainty is associated with errors in estimating a spectrum from experimental measurements. Fundamental uncer-

tainty, which is also called spectral shape variability, is due to the variation of the shape of the spectrum for a specified sea state. Finally, model uncertainty is due to the discrepancy between the theoretical spectrum, which is used to describe a sea state, and the average of all actual spectra for that sea state.

Statistical uncertainty was modeled by assuming that the discrepancy between the ordinates of the actual and the theoretical spectrum can be represented by a gaussian random variable. The statistics of this variable are the same for all frequencies, and the random variables representing the discrepancies between spectral ordinates at different frequencies are statistically independent. This assumption was based on Haver and Moan's (83) results. The standard deviation of this variable for a particular frequency was taken equal to 0.525 multiplied by the corresponding spectral ordinate at that frequency.

Guedes Soares (84) estimated the bias and the COV of the mean square wave bending moment due to statistical and fundamental uncertainties, for different significant wave heights and heading angles. He found that the effect of statistical uncertainties is negligible compared to that of fundamental uncertainty (spectral shape variability). Thus, the results provided by Guedes Soares correspond to fundamental uncertainty. The effect of the uncertainty in wave spectra on the mean square wave bending moment, for a significant wave height of 10.0 m and for a Froude number equal to 0.15, is shown in Figure 3.1. This figure has been extracted from Guedes Soares (84). The ISSC spectrum has been used to calculate the wave bending moment. Two cases of ships with lengths 150m and 350m are considered. Results are provided for different heading angles. The average bias and the COV over all relative heading angles are also presented.

It is observed that the error due to uncertainty in spectral shape is large for small average sea periods, for which case the standard method using the ISSC spectrum is conservative. For large average sea periods, ($T > 9sec$), the error is considerably lower, with a bias roughly equal to 1.0 and a COV of 0.05.

An alternative simpler approach, which is called the simplified method, was also used by Guedes Soares . In the simplified method, it was assumed that the bias depends only on the significant wave height, H_s. The results of the simplified method are summarized by the following equations:

$$E(B_s) = \begin{cases} 1.0 & \text{for } (L \leq 250m \text{ or } H_s > 5m) \\ 2 - 0.2H_s & \text{for } (L > 250 \text{ or } H_s < 5m) \end{cases} \tag{3.1}$$

and $COV_{B_s} = 0.1.$

B_s stands for the ratio between measured and predicted mean square bending moment, $E(\cdot)$ is the mean value of the quantity in parenthesis. Clearly, for long ships ($L > 250m$) and for small wave heights ($H_s < 5m$), spectral shape variability leads to underestimation of the wave bending moment.

Kaplan (84) also studied the effect of spectral shape variability on the root mean square (rms) of the longitudinal bending moment. He used a set of measured spectra obtained by Hoffman and Miles (76) and evaluated the resulting COV of the rms bending moment. His results show the same trends as those by Guedes Soares. More specifically, the COV for high sea states ($H_s > 10m$) is significantly lower than that for low significant wave heights. Moreover, the COV is lower for head seas than for beam seas. Kaplan's conclusion was that the COV of the rms bending moment due to spectral shape variability ranges between 0.10 to 0.20 with an average value of 0.15. This value is almost identical with that estimated by Lewis (67).

Uncertainties are introduced by the directional spreading of the wave spectrum. Analysis procedures, which are recommended by all classification societies, use spreading functions to account for directional spreading. However, this approach involves simplifications, which introduce errors in the calculated loads. More specifically, it is assumed that the energy distribution in different directions is independent of the significant wave height and the frequency. This is an unrealistic assumption, because directional spreading decreases with the significant wave height increasing. Moreover, the angular distribution of wave energy is very narrow for the frequency components near the spectral peak.

Guedes Soares (84) evaluated the bias and the coefficient of variation of the mean square bending moment due to the effect of directional spreading. More specifically, he used the following equation for bias,

$$B_{sc} = \frac{R}{R_s} \tag{3.2}$$

where R is the mean square bending moment calculated by using a directionality function, which accounts for the dependency of spreading on the significant wave height. R_s is the mean square response which is calculated by using the directional spreading function which is recommended by classification societies. The latter method for calculating R_s will be called standard method. The results are plotted in Figure 3.2. Here the average bias $E(B_{sc})$ is plotted against the average sea period and the heading angle for various significant wave heights and ship lengths.

It is observed that the average bias is small, (less than 0.5), for beam seas, and it exceeds 1.0 for head and following seas. This means that standard methods overestimate bending moments for beam seas, while they are unconservative for head and following seas. Furthermore, the bias decreases with the significant wave height increasing.

The above observations can be explained as follows: The wave energy spreading, which is assumed by standard methods, is wider than the actual one. Moreover, waves with directions corresponding to heading angles of 180° (head seas) induce considerably larger bending moments than those corresponding to heading angles in the range of 90° (beam seas). Therefore, standard methods underestimate bending moments for head seas, while they overestimate them for beam seas. This can be observed in Figure 3.2. The bias for

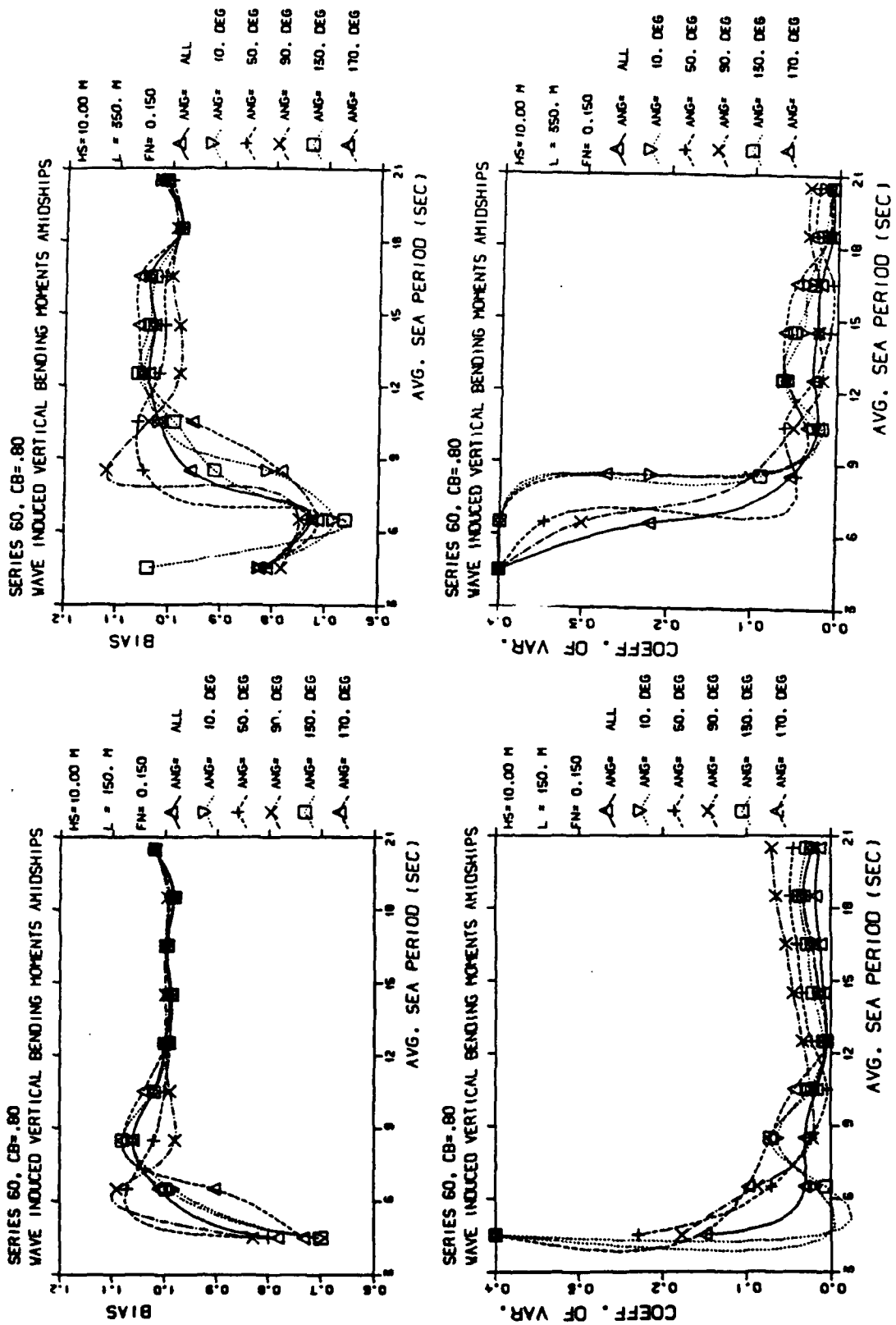


Figure 3.1 Effect of Spectral Shape Variability on Mean Square Wave Induced Bending Moment

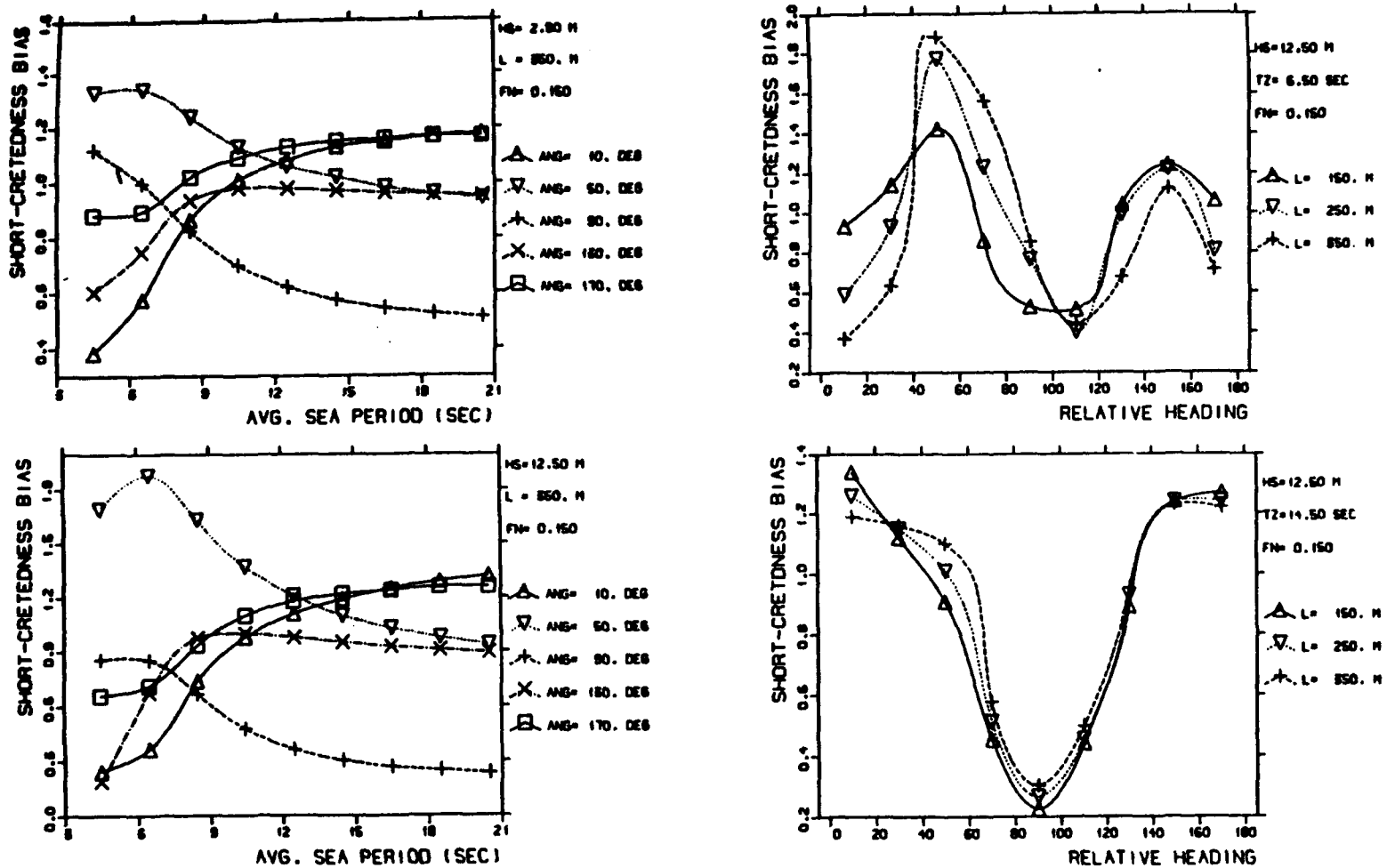


Figure 3.2 Dependence of the Short-Crestedness Bias on Various Parameters

head seas increases for high sea states because directional spreading decreases with the significant wave height increasing. The opposite is true for beam seas. It appears that, for the cases studied by Guedes Soares, the latter effect dominates and that the average bias decreases with significant wave height increasing.

Finally, Guedes Soares used a simplified approach for short crestedness bias, where the bias was assumed to be only a function of the significant wave height. The results of his approach are summarized by the following equations,

$$E(B_{sc}) = 1. - 0.0077H_s \tag{3.3}$$

$$COV_{B_{sc}} = 0.05$$

Some refined formulations of the wave spreading function, which account for the dependence of the wave energy spreading on frequency, have been proposed. However, it is impractical to use these formulations to calculate design loads because the required computational cost is too high. Moreover, it is very difficult to estimate some of the parameters involved in the spreading function models. Therefore, we did not estimate the uncertainties associated with these formulations.

Due to the systematic directional character of meteorological systems, the distribution of relative headings encountered by a ship which always travels in a certain route, is nonuniform. For example, a ship sailing eastbound and westbound in the Atlantic Ocean is more likely to encounter head than beam seas, as it was found from analysis of data on ship headings (Guedes Soares 84). On the other hand, with the exception of Bureau Veritas, methods recommended by classification societies assume that the distribution of headings is uniform (Liu, Chen and Lee 81). This might introduce considerable bias because wave induced bending moments are sensitive to relative heading angles.

Guedes Soares (84) calculated the bias in the mean square bending moment due to directionality, for ships crossing North Atlantic by sailing eastbound or westbound. The resulting bias is plotted in Figure 3.3 as a function of the significant wave height for various wave periods. It is observed that the standard method, which assumes that the distribution of relative headings is uniform, is unconservative. Moreover, the bias increases with the significant wave height increasing. This can be explained as follows. Standard methods assume that the distribution of relative headings is uniform, while, in reality, ships are more likely to encounter head seas than beam seas. Furthermore, head seas induce higher bending moments than beam seas. Consequently, the actual bending moment is larger than that predicted by standard methods. Moreover, the directional spreading of wave energy decreases with the significant wave height increasing, which makes directional effects most significant. Thus, the bias due to directionality is larger for high sea states.

The directional bias was also calculated by Guedes Soares by using a linear model which includes H_s as a parameter. For this case, directional bias, B_d, is given by the following

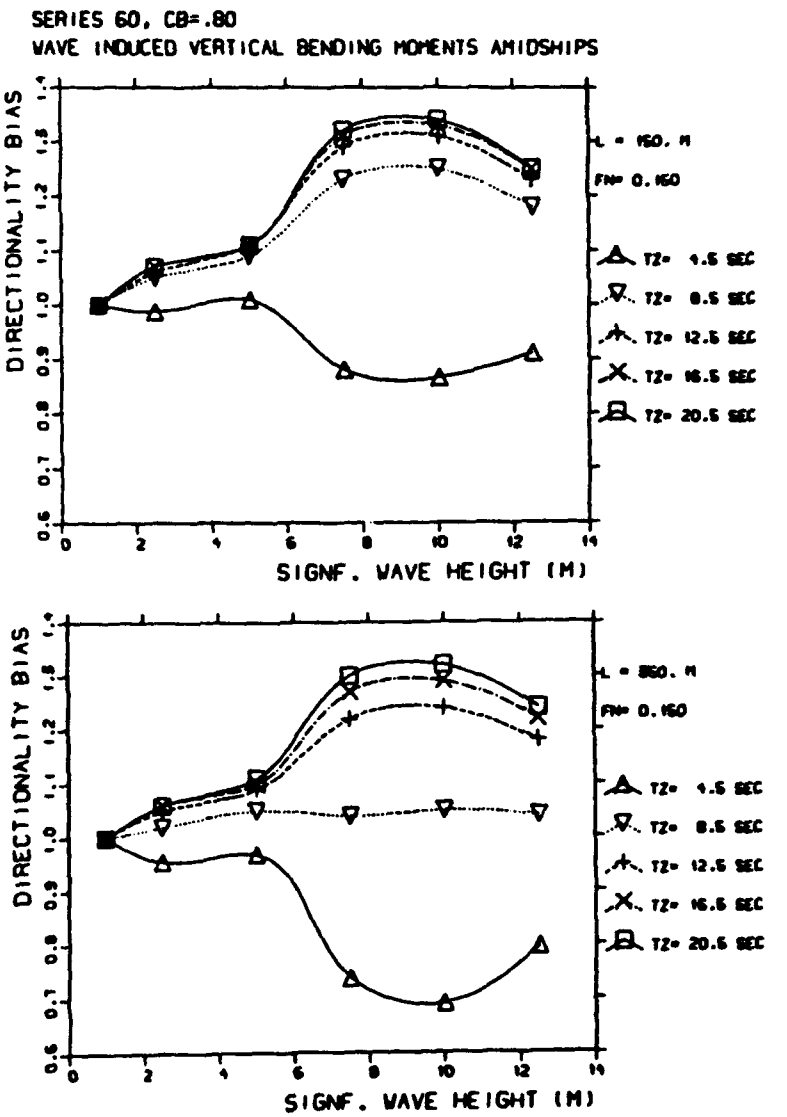


Figure 3.3 Directionality Bias

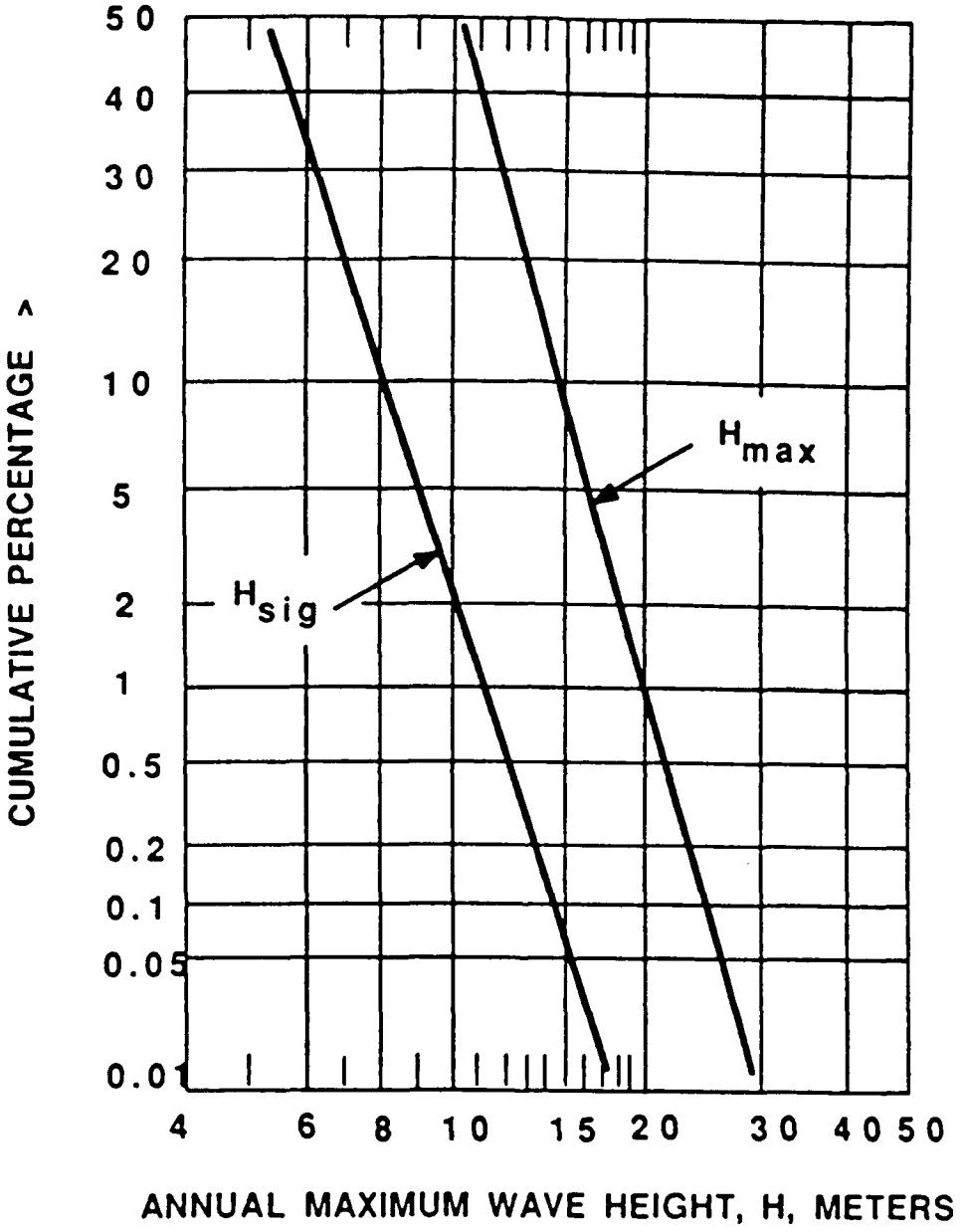


Figure 3.4 Probability Distribution of Annual Expected Maximum (Hmax) and Significant (Hsig) Wave Heights

equation,

$$E(B_d) = 0.981 + 0.018H_s. \tag{3.3}$$

The COV is equal to 0.10.

Uncertainty in visual observations of wave heights also introduces uncertainty in loads. It has been found that visual observations tend to underestimate small waves and overestimate large ones. Guedes Soares (84) recommended a linear model for obtaining the significant wave height from the visually observed wave height. This equation gives slightly different results from those obtained by the equation recommended by the International Ship Structures Congress (Hogben 67). Using Guedes Soares equations, we derived the following equation for bias due to uncertaintly visual observations,

$$E(B_H) = \frac{0.75H_s}{H_s - 2.33}. \tag{3.4}$$

The COV was found by Guedes Soares equal to 0.17.

It is important to note that the above values refer to the error in the significant wave height. The corresponding bias of the mean square bending moment is $E^2(B_H)$ and the COV is 0.34.

The effect of the correlation between subsequent wave peaks on the maximum lifetime wave height has been studied by Naess (82,83). Naess showed that the assumption of independent peaks leads to conservative estimates of the maximum wave height. Dalzell (89) reached the same conclusion but he maintains that, for long return periods corresponding to real life applications, the error in the expected maximum wave height is less than 10%.

In high sea states, the ship operator might adjust the course in order to reduce the risk of capsizing. For such cases, the relative heading angle becomes 180° which is the direction corresponding to the largest wave bending moments. Consequently, the effect of countermeasures in severe weather conditions is to increase the wave bending moments. Guedes Soares (90) performed a Monte Carlo based simulation study to assess the error from neglecting the effect of heavy weather countermeasures. He found that the resulting average bias is greater than one, and that it increases with the significant wave height increasing. Both these results should have been expected since by neglecting weather countermeasures we underestimate load effects. For a small ship with length 135m the bias ranged between 1.0 and 1.25, while for a longer ship with length 200m the bias was almost 1.0. The reason is that heavy weather countermeasures are very rarely taken for large ships.

Table 3.1 summarizes the uncertainties involved in modeling the loading environment for ships.

Table 3.1. Uncertainties in Describing Loading Environment for Ships

Type of uncertainty	Bias/COV	Study
1. Spectral shape variability	$-/0.15$	Kaplan(84)
	Figure 3.1 (complete repr.) $1/0.1$ ($L \leq 250m$ or $H_s > 5m$) $2 - 0.2H_s/0.1$($L \geq 250m$ or $H_s < 5m$) (simplified representation)	Guedes Soares(84)
2. Shortcrestedness	Figure 3.2 (complete repr.) $1 - 0.0077H_s/0.05$(simplified repr.)	Guedes Soares(84)
3. Directionality of weather systems	Figure 3.3 (complete repr.) $0.981 + 0.018H_s/0.10$(simplified repr.)	Guedes Soares(84)
4. Visual observations	$\frac{0.75H_s}{H_s - 2.33}/0.17$	Guedes Soares(84)
5. Heavy weather countermeasures	$1.0 - 1.25$	Guedes Soares(84), Guedes Soares(90)

Notes:

a) Kaplan's results refer to the effect of spectral shape variability on rms wave induced bending moment. The other results refer to mean square bending moment.

b) In complete representation, the bias is considered as a function of parameters such as the significant wave height, average wave period, and relative heading angle. In simplified representation, we consider dependence on significant wave height only.

3.2 Offshore platforms

Bea (89) investigated uncertainties in global forces on offshore platforms, which are located in the northwestern shelf of Western Australia. According to Bea's approach, the maximum annual force is proportional to the maximum annual wave height or its square. The wave energy for the particular platform, which was considered in this study, is out of the range of reasonance, in which case the period distribution is unimportant. Therefore, the effects of the loading environment were taken into account by considering the wave height only. Bea estimated both modeling and random uncertainties for the expected annual maximum wave height by comparing hindcast and measured maximum wave heights in severe cyclones. The probability distribution function of the ratio of measured and predicted annual maximum wave heights, which was used to estimate the bias and coefficient of variation for modeling uncertainties, is presented in Figure 2.1. According to this figure, the bias due to modeling uncertainties is lognormally distributed with median equal to 1.1 and COV equal to 0.13.

The variability in the expected severest sea condition over a period of one year is considered in Figure 3.4, which is extracted from Bea (89). The probability distribution function of the annual maximum significant wave height is plotted in this figure. The maximum wave height is also considered in the same figure. According to these results, the COV of the random bias of the annual maximum wave height is 0.30. Assuming that modeling and random uncertainties are independent, the COV due to both types of uncertainties is 0.33.

Uncertainty due to the facts that, a) the wave peaks do not follow the Rayleigh distribution, and b) subsequent wave peaks are correlated has been studied by Forristall (78). Based on analysis of data from the Gulf of Mexico, Forristall found that the assumption associated with the Rayleigh distribution and the independence of wave peaks can overestimate the wave heights by 10 to 20 percent. Bea (89) used Forristall's results, and recommended an average bias for the wave height equal to 0.93 and a COV of 0.08. Consequently, the bias in the mean square bending moment due to this effect is 0.86 and the COV is 0.16.

Wirsching (81) also studied the uncertainty on load and load effects due to uncertainties in modeling the loading environment. His study was confined to modeling uncertainties associated with wave loads. Data on uncertainties were also reported in Wirsching (88). According to Wirsching, the average bias ranges between 0.63 to 1.20 and the COV ranges between 0.40 to 0.60. For offshore platforms with low natural frequencies, for which dynamic effects are important, the largest component of this uncertainty is due to variability in the dominant period of the spectrum describing a sea state. Although the variability in the dominant period might be moderate (the COV ranges between 0.10 and 0.20), its effect on the resulting loads and load effects is high. The high sensitivity of a platform's response to uncertainties in dominant period has also been discussed by Moses (85). Un-

certainties in the relative frequency of occurrence of each sea state, as well as those due to directionality of weather systems have also been accounted for by Wirsching in quantifying uncertainties in environmental description. The median bias of the former type of uncertainties ranges between 0.9 and 1.00 and the COV between 0.1 and 0.3.

Guedes Soares and Moan (82) investigated uncertainties in global loads applied to a cylindrical pile in the North Sea. The COV's for the model, random and measurement uncertainties in the maximum wave height were found equal to 0.11, 0.08 and 0.09, respectively. The maximum wave height corresponds to a period of 100 years.

A linear model was postulated for the period corresponding to the maximum wave height, and the model parameters were estimated by regression. The COV's for the model, random and measurement uncertainty in the wave period were estimated equal to 0.10, 0.05 and 0.10, respectively. The total COV for the period is 0.14, and the correlation coefficient between the wave height and the period is 0.50, which implies a strong positive correlation between these quantities.

Guedes Soares and Moan also considered current loads. The COV of the current velocity was estimated 0.35. No information was provided on the probability distribution of the aforementioned variables. Furthermore, the error due to shortcrestedness of waves was not examined.

A survey was conducted under the sponsorship of ABS and Conoco in order to quantify the modeling error associated with design loads for cylinders and pontoons for tension leg platforms (Wirsching 82). The bias and the COV for the cumulative effect of wind, current and tide on the platform loads were reported equal to 0.95 and 0.12, respectively. These estimates were based on the responses of experts to a questionnaire.

Table 3.2 summarizes the uncertainties involved in modeling the loading environment for offshore platforms.

Table 3.2. Uncertainties in Describing Environment for Offshore Platforms

Type of uncertainty	Bias/COV	Source
Maximum wave height	1.0/0.30 (Random)[1] 1.1/0.13 (Modeling)	Bea (89)
Maximum wave height	$-/0.16$[2]	Guedes Soares and Moan(82)
Average period corresponding to maximum wave height	$-/0.14$[2,3]	Guedes Soares and Moan(82)
Effect of environmental uncertainties on rms stress in structural elements of a platform	$0.6 - 1.2/0.4 - 0.6$[4]	Wirsching(81)
Effect of modeling uncertainties in wind, current and tide on loads on tension leg platform	0.95/0.12	Wirsching(82)

Notes:

[1] Results refer to annual maximum wave height. Bias is lognormally distributed. Uncertainties due to the correlation of subsequent peaks and the Rayleigh distribution assumption are included in these results.

[2] Results refer to 100 year maximum wave height. The error due to short crestedness was not examined.

[3] Correlation coefficient between wave height and period is 0.5.

[4] Bias is lognormally distributed. The relation of the period to the response depends upon the natural period characteristics of the structure. Uncertainty in average wave period dominates for offshore platforms with low natural frequencies, for which there is a substantial amount of wave energy in the vicinity of their natural frequency

4.0 Loads

In this chapter, we study uncertainties in loads and load effects. For ships, we examine loads applied to the main girder as well as hydrodynamic pressure. Uncertainties in both short and long term predictions are quantified. For offshore platforms, we quantify uncertainties in base shear and overturning moment.

4.1 Ships

Here, we consider uncertainties in the most important loads applied to ships.

4.1.1 Stillwater bending moments and shear forces

Guedes Soares and Moan (88) statistically analyzed stillwater bending moments and shear forces for various ship types. In their study, stillwater load effects were assumed to vary from voyage to voyage for a particular ship, from one ship to another in a particular class of ships, and from one class of ships to another. The above sources of variability can be modeled as follows,

$$m_{ijk} = \quad m_o + m_k + m_j + \epsilon_i \tag{4.1}$$

where,

m_{ijk} is the bending moment or shear force, at the i^{th} voyage, which is applied to the j^{th} ship, which belongs to the k^{th} class,

m_o is the average load effect for all ships,

$m_o + m_k$ is the average load effect of all ships in the k^{th} class,

$m_o + m_k + m_j$ is the average load effect for the j^{th} ship of the k^{th} class,

and ϵ_i represents the variation of the load effect from voyage to voyage. Accordingly, the following variances can be defined,

a) variance of the load effect for a particular ship: σ_ϵ^2,

b) variance of the load effect for all ships in a particular class, which is specified by k: $(\sigma_\epsilon^2 + \sigma_j^2)^{1/2}$,

c) variance of the load effect for all ships: $(\sigma_\epsilon^2 + \sigma_j^2 + \sigma_k^2)^{1/2}$.

The generality of description increases from a) to c) by accounting for all ships in a class, or by accounting for all ships in all classes. Clearly, the variance increases with the generality of description increasing.

Tables 4.1 and 4.2 summarize the results from statistical analysis of data on stillwater bending moments and shear forces respectively, for seven types of ships. The values in these tables have been normalized by the corresponding values which are prescribed by classification societies. The average stillwater load effect, and the variance of this load effect for one ship, and also for all ships in a given class, are presented in Table 4.1. The results are based on the analysis performed by Guedes Soares and Moan (88), and all the numbers are normalized by the design values prescribed by classification societies. The data used in this analysis can be found in Guedes Soares and Moan (88) and in Guedes Soares (84).

Table 4.1 Variability in stillwater bending moments

Type of ship	Average load effect for all ships within a class $(m_o + m_k)$	Standard deviation for a particular ship (σ_ϵ)	Standard deviation for all ships within a class $(\sigma_\epsilon^2 + \sigma_j^2)^{1/2}$
Cargo	0.50	0.28	0.30
Containership	0.72	0.16	0.20
Bulk Carrier	-0.008	0.30	0.38
OBO	0.80	0.30	0.41
Chemical Carrier	-0.005	0.22	0.36
Ore/Oil Carrier	-0.44	0.22	0.37
Tanker	-0.12	0.21	0.44

Note:

a) Positive bending moments correspond to hogging, and negative ones to sagging.

b) the bending moments have been normalized by dividing by the values which are prescribed by classification societies.

Table 4.2 Variability in stillwater shear forces

Type of ship	Average load effect for all ships within a class $(m_o + m_k)$	Standard deviation for a particular ship (σ_ϵ)	Standard deviation for all ships within a class $(\sigma_\epsilon^2 + \sigma_j^2)^{1/2}$
Cargo	-0.17	0.20	0.31
Containership	-0.32	0.10	0.29
Bulk Carrier	0.04	0.34	0.52
OBO	0.03	0.25	0.49
Chemical Carrier	-0.06	0.20	0.30
Ore/Oil Carrier	0.12	0.25	0.75
Tanker	0.07	0.20	0.55

It is observed that cargo and containerships experience large hogging moments. Tankers and Ore/Oil Carriers are subjected to sagging moments. Although the average stillwater bending moment is small for tankers, there is a large variability in this moment. This is attributed to the large variability of the stillwater bending moment from one tanker to another.

Kaplan (84) reported some results on stillwater bending moments obtained from Akita (82). According to his study, the COV for containerships is 0.29, and for tankers it is 0.99 for ballast, and 0.52 for full load conditions. These values reflect variabilities from voyage to voyage and from one ship to another within a particular class. They indicate the same trend with Guedes Soares results. Indeed, the variability is considerably larger for tankers than for containerships. However, Guedes Soares reported a significantly larger variability for tankers (COV $\simeq$ 3.7) compared to that reported by Kaplan. This discrepancy might be due to the large spreading of sizes of the tankers which were considered by Guedes Soares. The coefficients of variation reported for containerships are almost identical.

The above results are for stillwater load effects, which occur at any time instant. The extreme values of these load effects are also important. In the following, we calculate the first two moments of the lifetime maximum stillwater bending moments, by using the results from Tables 4.1 and 4.2.

The value of a load effect at a particular voyage is given by eq. (4.1). ϵ_j is assumed to

be a zero mean gaussian random variable with standard deviation σ_ϵ. Furthermore, the values of ϵ for different voyages are assumed to be independent.

The lifetime extreme load effect for a particular ship is;

$$\max_i\{m_{ijk}\} = m_o + m_k + m_j + \max_i\ \epsilon_i \tag{4.2}$$

Subscript i below max indicates that the maximum value of the load effect refers to all voyages.

Therefore, the standard deviation of the lifetime maximum load effect for all ships in a particular class is,

$$\sigma_m = (\sigma_j^2 + \sigma_{\max\epsilon}^2)^{1/2} \tag{4.3}$$

where $\sigma_{\max\epsilon}$ denotes the standard deviation of the maximum load effect, $\max_i\{\epsilon_i\}$. The latter random variable follows the type I asymptotic extreme value probability distribution (Ochi 90),

$$F_{\max\epsilon}(\epsilon) = \exp\ (\exp\ (-a_N\ (\epsilon - b_N))) \tag{4.4}$$

where,

N is the number of voyages over the lifetime of the ship,

$a_N = N\ f\ (b_N)$,

$f\ (\cdot)$ is the probability density function followed by ϵ_i,

b_N is the most probable value of max ϵ_i, which is equal to $\Phi^{-1}\ (\frac{N-1}{N})\sigma_\epsilon$,

and $\Phi\ (\cdot)$ is the standard gaussian probability distribution.

The mean and variance of $\max_i \epsilon_i$ are,

$$E\ (\max_i \epsilon_i)\ = b_N + \frac{\gamma}{a_N}, \text{and}$$

$$\sigma_{\max\epsilon}^2 = \frac{\pi^2}{6a_N^2} \tag{4.5}$$

respectively. γ is the Euler constant.

Table 4.3 presents the results for lifetime extreme stillwater bending moments for $N = 200$.

Table 4.3 Uncertainties in lifetime extreme stillwater bending moments

Type of ship	Most probable extreme bend. moment	Stdr. dev. for variability from ship to ship within a particular class (σ_j)	Stdr. dev. of extreme bend. moment for a particular ship $(\sigma_{\max \epsilon})$	Stdr. dev. of extreme bend. moment for all ships within a class $(\sigma^2_{\max \epsilon} + \sigma^2_j)^{1/2}$
Cargo	1.27	0.11	0.12	0.16
Containership	1.16	0.12	0.07	0.14
Bulk Carrier	-0.84	0.24	0.13	0.27
OBO	1.13	0.28	0.13	0.31
Chemical Carrier	-0.66	0.29	0.10	0.31
Ore/Oil Carrier	-1.04	0.30	0.10	0.32
Tanker	-0.70	0.39	0.09	0.40

It is observed that, for the case of Chemical Carriers, Ore Carriers and Tankers, the variability in lifetime extreme stillwater bending moments is almost entirely due to the variation of bending moments from one ship to another within a particular class. Indeed, for this type of ships, the variability from one voyage to another is too small to affect the extreme bending moments.

4.1.2 Uncertainties in short term vertical wave bending due to errors in response amplitude operators

Kaplan (84) compared model data against theoretical predictions of response amplitude operators for two Series 60 ships (0.70 and 0.80 block coefficients), and also for the WOLVERINE STATE. The data, which can be found in Kaplan and Raff (72), cover different speeds and headings in regular waves. Kaplan calculated the rms of the wave bending moment by using, a) theoretically calculated response amplitude operators obtained from the SCORES seakeeping computer code, and b) measured response amplitude operators. A reference wave spectrum was used, for which the value of the power spectral density function is constant with frequency. The bias due to errors in response amplitude operators was calculated by comparing the rms values of the wave bending moment, which were calculated by using experimental and theoretical response amplitude operators.

Based on the above approach, Kaplan found that the COV of the rms wave bending moment is 0.10. No information was provided on the probability distribution of the bias or its average value.

Guedes Soares (84) separated uncertainties in response amplitude operator into those due to nonlinearities and those due to all the other simplifications and idealizations. According to his approach the bias in the response amplitude operator is given by the following equation;

$$H(\omega) = B_L \; B_{S/H} \; H_P \; (\omega) \qquad \text{for any } \omega \tag{4.6}$$

where, B_L is the bias due to all uncertainties except nonlinearities, B_S expresses the uncertainty in sagging, B_H expresses the uncertainty in hogging, H is the actual response amplitude operator, and H_p is the value of the response amplitude operator as it is predicted by a linear strip theory based method. Errors due to the flexibility of the ship hull were found to be unimportant except for very long ($L \geq 350m$), fast ships. Therefore, this source of uncertainty was neglected. Guedes Soares examined the error associated with the Salvensen, Tuck and Faltinsen (70) (S.T.F.) method. Linear models were postulated for both B_L and $B_{S/H}$, and the coefficients were found by regressing on data from model experiments. B_L was assumed to be a function of the relative heading angle α, the Froude number V, and the block coefficient C_B. The following relations were found for the bias, on the basis of regression fits:

$$B_L = 0.00631\alpha + 1.22V + 0.657C_B + 0.064 \text{ for } 0 \leq \alpha \leq 90°, \text{ and} \tag{4.7}$$

$$B_L = -0.00495\alpha + 0.42V + 0.701C_B + 1.28 \text{ for } 90° \leq \alpha \leq 180°.$$

The COV was found equal to 0.38 for both cases.

An alternative approach was also followed, in which the linear bias, B_L, was assumed to be a function of the significant wave height, H_S, only. For this case, the bias is given by the following equation,

$$B_L = 1.22 - 0.005H_S. \tag{4.8}$$

The COV was found equal to 0.35. The bias in eq. (4.8) is defined as the ratio of the average values of the measured and predicted response amplitude operators over all heading angles and average wave periods.

The effect of nonlinearities was modeled by employing a linear model which involved the block coefficient C_B as a parameter. The resulting equations, which were also derived by regression, are,

$$B_S = 1.74 - 0.93C_B \qquad \text{for sagging, and} \tag{4.9}$$

$$B_H = 0.26 + 0.93C_B \qquad \text{for hogging.}$$

The COV was found equal to 0.12 for both equations.

The following conclusions can be extracted from eq's (4.7)-(4.9):

- S.T.F. method is unconservative, when it is used to predict sagging bending moments.
- The error of the S.T.F. method is larger for beam seas than it is for head and following seas. For example, the bias, B_L, for $\alpha = 90°$, $V = 0.2$, and $C_B = 0.8$, is 1.48, while it is only 1.03 for $\alpha = 180°$ and same V and C_B.
- S.T.F. method underestimates sagging and overestimates hogging because the linear model does not distinguish between them.
- The error of the S.T.F. method due to nonlinearities is smaller for ships with large block coefficients. This is true because the assumption of vertical hull walls is realistic for ships with large C_B.
- The bias, B_L, decreases with H_S increasing.

Although a large portion of the experimental data used by Kaplan and Guedes Soares are identical, a significant discrepancy is observed between their COV's. In our opinion, the above discrepancy should be attributed to the way by which uncertainties were quantified by Guedes Soares (84). More specifically, Guedes Soares regressed on data for the ratio of measured and predicted response amplitude operators for various frequencies. A typical set of data is shown in Figure 4.1. Clearly, this approach overestimates modeling error, because it uses data from test measurements which have been contaminated with experimental errors as well as concentrating on individual frequencies. A better way to proceed is the following,

a) postulate a linear model for the rms bending moment,

b) transform the data on transfer function into data on the rms bending moment by using some sea spectrum (for example, the ISSC spectrum) and by integrating over frequency,

c) regress on the data from b), or simply estimate the COV of the ratio of measured over predicted rms bending moments.

This procedure, which has been followed by Kaplan (84), removes the experimental error as well as the individual frequency sensitivity by integrating over frequency in step b). Therefore, in our opinion, the results obtained from this approach should be more realistic.

4.1.3 Long term induced bending moments

Kaplan (84) found that the COV of the extreme lifetime vertical bending moment is 0.19. The COV of random uncertainties was found 0.065. No information was provided

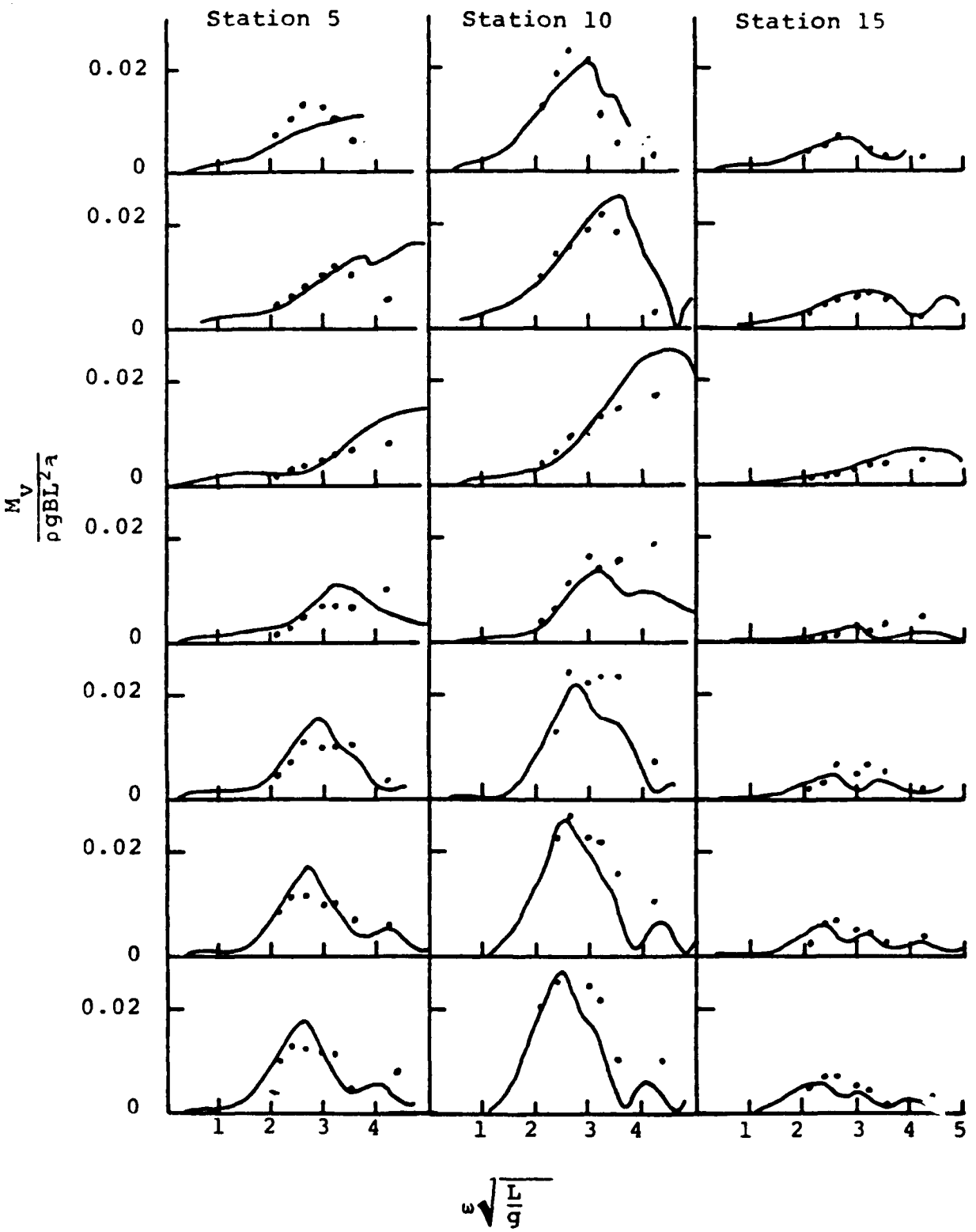


Figure 4.1 Calculated and Measured Response Amplitude Operators for a Containership (Fn=0.245)

on the probability distribution of the average value of the bias. The relative contribution of the uncertainties examined by Kaplan is presented in Table 4.4.

Guedes Soares (84) estimated uncertainties in the most probable extreme long term vertical bending moment for the following cases,

a) tankers ($C_B = 0.8$)

b) tankers in sagging,

c) containerships ($C_B = 0.6$) in hogging,

d) containerships ($C_B = 0.6$) in sagging,

e) hogging in any type of ship,

f) sagging in any type os ship,

g) the type of ship and bending moment (hogging or sagging) is unknown.

An extension of Ochi's approach was used to caluclate the long term extreme long term vertical bending moment (Ochi 78). The results from Guedes Soares study are shown in Table 4.5.

Clearly, the variability in load effects is smaller for cases that the type of ship and/or the type of moment are specified in the formulation. For example, the modeling bias for a ship with block coefficient of 0.8 is 1.13 and the COV is only 0.04. If the block coefficient is not specified, the bias is 1.10 and the COV is 0.15. This indicates that a design code, which distinguishes between various ship types and hull characteristics and specifies different load and strength factors for each case, allows the design of more efficient ships.

Another conclusion from Guedes Soares study is that theoretical predictions are almost always unconservative. This is primarily due to the unconservative errors of linear strip theory in response amplitude operators. In particular, the error in the sagging bending moments is very large for ships with small block coefficients. For example the bias is 1.28 for containerships. The reason is that nonlinearity in response is significant for these ships, due to their nonvertical sides. This unconservative error must be accounted for in design because sagging can cause buckling of the deck plates, which is an important failure mode in ship hulls.

Table 4.4 Relative Contribution of Various Types of Uncertainties to Total Uncertainties in Extreme Bending Moment (source: Kaplan (84))

Type of Uncertainty	Contribution (%)
Spectral shape variability	61
Uncertainty in transfer function	27
Random uncertainty	12

Note: Contribution is defined as the square of the ratio of the particular uncertainty over the total uncertainty.

Table 4.5 Uncertainties in Long Term Vertical Wave Bending Moment (source: Guedes Soares (84))

Case	Modeling Uncertainty Exp. Bias/COV	Random Uncertainty COV	Total Uncertainty Exp. Bias/COV
Tankers in hogging	1.13/0.04	0.07	1.13/0.08
Tankers in sagging	1.13/0.04	0.07	1.13/0.08
Containerships in hogging	0.88/0.05	0.07	0.88/0.09
Containerships in sagging	1.28/0.04	0.07	1.28/0.08
Any ship in hogging	1.0/0.15	0.07	1.0/0.17
Any ship in sagging	1.2/0.08	0.07	1.2/0.11
Any ship/hogging or sagging	1.1/0.15	0.07	1.1/0.17

Although Guedes Soares and Kaplan's results are in good agreement, we believe that modeling uncertainties were not treated properly by the former. More specifically, Guedes Soares assumed that modeling errors in mean square bending moments are independent from one sea state to another or from one heading to another (eq. 4.57, p. 278 of Guedes Soares (84)). This assumption is not realistic, because, as we mentioned in chapter 2, modeling uncertainties are systematic and as such, they are highly correlated from one sea state to another or from one heading angle to another. Therefore, the COV's reported in Guedes Soares (84) might be lower than the actual values.

Faulkner (81) reported the following COV's for lifetime extreme vertical bending moments:

a) Modeling uncertainties:

0.15 for warships

0.10 for commercial ships

b) Random uncertainties:

0.12 for both warships and commercial ships.

Faulkner considered a SL-7 containership and a large tanker in his study. He found that the uncertainty is larger for the containership than for the tanker, which agrees with Guedes Soares' conclusions.

Finally, uncertainties in both vertical and horizontal bending moments were considered in ISSC(85), for a tanker with length equal to 160m. The bias of both bending moments was assumed to be normal with a mean of 0.95 and a COV of 0.1 for the vertical bending moment. The bias and COV for the horizontal bending moment are 0.85 and 0.15, respectively. The correlation coefficient between the two bending moments was assumed to be 0.70. Unfortunately, no information was provided in ISSC(85) on how these numbers were derived. Moreover, it is mentioned in this report that these numbers are simply crude approximations.

The results from the studies considered in this section are summarized in Table 4.6.

4.1.4. Uncertainties in hydrodynamic pressure

Chen et al compared theoretically predicted hydrodynamic pressures on a ship hull against model tests results and full scale measurements. A linear strip theory based computer code (ABS/SHIPMOTION) was used to calculate pressures. Measurements were obtained for an SL-7 containership and a Great Lakes bulk carrier. The total hydrodynamic pressure, the pressure component due to the incident and diffracted waves, and the

pressure component arising from ship motions were considered in this study. Model tests were performed for head seas at Froude numbers 0.15, 0.23 and 0.32 over a range of ship length/wave length ratios from 0.65 to 1.65.

The following are the main conclusions from Chen's study:

- The calculated pressures due to ship motions correlated well with test measurements.
- Good agreement was also found between predictions and measurements for the pressure due to incident and diffracted waves.
- The agreement between predictions and measurements for the total hydrodynamic pressure was good except for the bow and stern regions. This should have been expected because three dimensional effects and nonlinearities are stronger in these regions.

Table 4.6 Summary of Results On Uncertainties in Long Term Extreme Bending Moments.

Bias/COV

Source Quantity	Kaplan(84)	Guedes Soares (84)	ISSC(85)	Faulkner(81)
V. Bend. Mom. (X_1)	−/0.19	0.88 − 1.28/ 0.08-0.17	0.95/0.1	−/0.19 warships −/0.16 containerships
H. Bend. Mom. (X_2)	−	−	0.85/0.15	−

Note: In ISSC study X_1, X_2 are normally distributed with correlation coefficient 0.7.

Table 4.7 Bounds for Bias of Response Amplitude Operator for Hydrodynamic Pressure on SL-7 Containership (Source: Chen et al. 83)

Froude number	Lower Bound	Upper Bound
0.15	0.44	1.35
0.23	0.41	1.65
0.32	0.35	1.60

Using Chen's results, we found upper and lower bounds for the bias in the response amplitude operator for hydrodynamic pressure. (The response amplitude operator is the square root of the ratio of the spectral ordinates of hydrodynamic pressure and wave elevation at the same frequency.) The results are shown in Table 4.7 and they are for the SL-7 containeship.

- Clearly, the error in predicting hydrodynamic pressures is significantly larger than that in predicting global loads (bending moments and shear forces). This is true because global force are obtained by integrating pressures over the hull. A large portion of the error is averaged out when integrating. Thus, the error in global forces is smaller than that in pressures.

4.2 Offshore platforms

In this section, we study uncertainties in short term and long term extreme loads on offshore platforms. The study focuses on global loads, i.e. base shear forces and overturning moments.

Uncertainties in analysis of fixed offshore platforms were studied in the context of the L.R.F.D. A.P.I. code (Moses, 86). The maximum annual wave height was assumed lognormally distributed. Its coefficient of variation ranges between 10 - 15% for the North Sea, 15% - 25% for the Gulf of Mexico and it is somewhat higher for offshore Alaska and California. This information was extracted from measurements reported by various authors and it is summarized on p. 2.23 of Moses (86). It was shown that the effect of the length of the exposure time on the lifetime maximum load or load effect is to reduce its COV and to increase bias. However, no information was provided on natural and subjective uncertainties. Moreover, these two types of uncertainty were not distinguished when the

lifetime distribution of the maximum wave height was derived from the distribution of the annual maximum wave height.

The lifetime maximum platform forces were assumed to be related to the maximum wave height according to the following relation,

$$F_N = AH_N^{\alpha} \tag{4.10}$$

where A is called analysis coefficient, and the exponent α is 1 and 2 for inertia and drag dominated platforms respectively. For $N = 20$ years, the bias and the COV of the analysis coefficient were assumed to be 0.93 and 0.25 respectively. These results were based on measurements, which were obtained from the Ocean Test Structure (O.T.S.) (Anderson et al 82). The latter is a drag dominated platform.

Olufsen and Bea (90), investigated the uncertainties in extreme shear force and overturning moment for two platforms located in the Gulf of Mexico and in the North Sea respectively. They considered the effects of both random (type I), and modeling uncertainties (type II). An empirical model, which as obtained by regression, was used to derive global forces from the wave elevation. The following uncertainties were taken into account:

- errors in the procedure for deriving the force from the extreme wave height,
- error in predicting the extreme wave height, and
- uncertainties due to the effect of marine fouling.

It was stressed by Olufsen and Bea (90) that the coefficient of variation in the extreme global forces is severely underestimated if modeling uncertainties are not treated properly. More specifically, modeling uncertainties, which are involved in calculating loads and their effects, are almost perfectly correlated from one load application to another. Therefore, in contrast with the random uncertainties, modeling uncertainties do not decrease with the length of the return period increasing. Hence, if we do not recognize the difference between the ways that the above two types of uncertainties propagate, we will underestimate the coefficients of variation of the extreme lifetime loads. It is striking that the new L.R.F.D. A.P.I. design code is based on a value of 0.37 for the coefficient of variation of the 20 year extreme response of a platform, which is less than one half of the corresponding value reported by Olufsen and Bea (90) (0.73 - 0.98 for the Gulf of Mexico, and 0.65 for the North Sea).

Bea (89) also studied uncertainties for a platform located in the Northwest Shelf of Western Australia. The global force to the platform F, was calculated by the following formula,

$$F = k_d \, k_u \, H^{\alpha} \tag{4.11}$$

where k_d is the coefficient in the relation between the kinematics of the water particles and F, and k_u denotes the coefficient in the relation between the former and the wave height,

H. Thus, the product $k_u k_d$ corresponds to the analysis coefficient in eq. (4.10) which was used by Moses (86). Exponent α is 1 and 2 for inertia and drag dominated platforms, respectively. Only uncertainties in annual maximum values were reported. These values are presented in Table 4.8. The bias and the coefficient of variation,which were obtained by combining the uncertainties in the quantities involved in calculating global forces (eq. (4.11)), were found to be in good agreement with the corresponding values estimated by direct comparison between measurements and theoretical predictions.

The principal component of the uncertainty in k_d, as reported by Bea (89), is uncertainty in the drag coefficient C_d in Morison's formula. Based on OTS data, Bea reported that the coefficient of variation of K_d and C_d, which corresponds to random uncertainties is 0.10 and that due to modeling uncertainties are 0.23. These values incorporate the effect of marine fouling.

We derived the uncertainties in the lifetime maximum global forces from those of the annual maximum loads by using two approaches, in order to demonstrate how important it is to treat modeling uncertainties properly. In the first approach, (approach 1, Table 4.9) we assumed that modeling uncertainties are perfectly correlated from one year to another and we used equation (2.2) for the total uncertainty. In the second approach, (approach 2, Table 4.9) we treated modeling uncertainties as independent from one year to another. The details on the calculation of the coefficient of variation are described in Appendix A. Return periods from 10 to 100 years were considered. We assumed that random variable B_I, representing random uncertainties, follows the lognormal probability distribution. Thus, the lifetime maximum value of B_I follows the asymptotic, type I, extreme probability distribution. (Appendix A). The results are shown in Table 4.9. It is observed that the second approach yields significantly lower estimates for the coefficient of variation than the first approach. This is because, in this approach, modeling uncertainties are treated as random and, therefore, the coefficient of variation of the latter decreases with N increasing. Furthermore, the component of the total uncertainties due to modeling error does not change with N in the first approach. It is observed that the coefficient of variation of the maximum force over a 20 year period is 0.66, which is significantly higher than the value which was used by the A.P.I. rules (0.37). According to the foregoing discussion, this discrepancy is due to the difference between the ways that modeling uncertainties are treated in this study and in Moses (86). However, it should be noted that the actual numerical values for extreme load might be different than the values reported in Table 4.9, because it is difficult to distinguish between random and modeling uncertainties, and to estimate the coefficients of variation for random variables B_I and B_{II}. However, the trends observed in Table 4.9 should be correct, and approach 1 is more appropriate than approach 2 for calculating uncertainties in extreme loads.

Table 4.8: Uncertainties in Annual Maximum Loads
for Drag and Inertia Dominated Platforms (Bea 89)

Platform Type	Quantity		Random (type I) EB_I	Random (type I) COV_{B_I}	Modeling (type II) EB_{II}	Modeling (type II) $COV_{B_{II}}$
Drag Dominated	Wave Height	(H)	1.0	0.30	1.1	0.13
	Kinematics	(k_u)	1.0	0.10	0.41	0.47
	Force Coef.	(k_d)	1.0	0.10	1.67	0.23
	Global Force		1.0	0.62	0.83	0.58
Inertia Dominated	Wave Height	(H)	1.0	0.30	1.1	0.13
	Kinematics	(k_u)	1.0	0.10	0.93	0.20
	Force Coef.	(k_d)	1.0	0.10	0.65	0.3
	Global Force		1.0	0.33	0.66	0.38

Table 4.9: Total Coefficient of Variation of Global Force
as a Function of Return Period

Years	Approach 1 COV_{B_I}	Approach 1 COV_B	Approach 2 COV_B
Init. Dist. (Corr. to 1 yr.)	0.62	0.85	0.85
10	0.35	0.68	0.43
20	0.31	0.66	0.38
50	0.27	0.64	0.34
100	0.25	0.63	0.31

Wirsching (81) also studied uncertainties in loads applied to offshore platforms. He represented the uncertainties in loads by the product of two coefficients denoted by B_S

and B_F. B_S corresponds to environmental uncertainties and B_F accounts for the error in load calculation. The statistics of B_S were presented in chapter 3. B_F was assumed to be lognormally distributed with an average value ranging from 0.6 to 1.1 and a COV between 0.1 and 0.3.

Guedes Soares and Moan (82) considered the uncertainties in the extreme forces applied to a vertical pile in the North Sea. The extreme forces correspond to a return period of 100 years. Table 4.10 presents the random variables which were considered in this study and their means and COV's.

The COV of the extreme load was found to be in the range between 0.34 and 0.45. The uncertainty in the extreme wave height was found to be the most important, because its effect on the global load was considerably larger than the effects of all the other uncertainties. This conclusion agrees with the conclusions from Wirsching and Bea. Therefore, the uncertainty in environmental description (the extreme wave height) is the most important for offshore platforms.

The modeling uncertainties in estimating wind, current and tide loads on tension leg platforms were quantified in the context of a study which was sponsored by ABS and Conoco (Wirsching 82). The bias associated with the effect of wind, current and tide loads was assumed to be the product of five random variables which account for uncertainties in predicting the most critical combination of wind current and tide conditions, calculation of induced loads, calculation of dynamic response, calculation of nominal member loads, and structural analysis. These r.v.'s were assumed to be lognormally distributed. The median biases and COV's of those random variables are presented in Table 4.11.

The values in Table 4.11 are based on subjective estimates of experts. It is mentioned that the estimates for the COV's might be low (Wirshing 82). The correlation between the bias in wind, current and tide and in wave loads was not estimated in the above study although it is recognized that it might be significant in developing probabilistic design rules.

The results from the studies considered in this section are summarized in Table 4.12.

Table 4.10 Uncertainties Involved in Predicting Extreme Loads on a Vertical Pile in the North Sea (Source: Guedes Soares and Moan (82))

Quantity	Mean value	COV
Extreme wave height (H)	30m	0.16
Wave period (T)	5.4 + 0.373 H (sec)	0.14
Water depth (D)	80m	2/D
Current velocity (C)	1.25 m/sec	0.35
Pile diameter (D')	4.0m	0.0
Fouling thickness (K)	0.175m	0.45
Surface roughness (R)	0.02	0.4
Drag coefficient (C_d)	Sarpkaya's data	0.1
Inertia coefficient (C_M)	Sarpkaya's data	0.1
Wave Kinematics	Stokes theory	0.25

Note: The following correlation coefficients were assumed for the above random variables:

$\rho\,(H,T) = 0.5,$

$\rho\,(H,C) = 0.4,$

$\rho\,(K,R) = 0.7,$

$\rho\,(R,C_d) = 0.5,$

$\rho\,(R,C_M) = -0.5,$

$\rho\,(C_D,C_M) = -0.9.$

Table 4.11 Uncertainties in Wind, Current and Tide Loads (Wirshing 82)

Type of Uncertainty	Bias (Median)	COV
Prediction of most critical combination of wind, current and tide loads	0.95	0.12
Calculation of induced load	0.92	0.10
Calculation of dynamic response	0.95	0.14
Calculation of nominal number loads	0.90	0.15
Structural analysis	1.0	0.05

Table 4.12 Uncertainties in Extreme Global Loads on Offshore Platforms

Source	Bias/COV	Return Period (years)
Moses (86)	0.7/0.37	20
Bea (89)	$-/0.66^{1}$	20
	$-/0.63^{1}$	100
Wirsching (81)	$0.4 - 1.3/0.41 - 0.67^{1}$	
Guedes Soares (82)	$-/0.34 - 0.45$	100
Olufsen and Bea (90)	$-/0.73 - 0.93^{1,2}$	100
	$-/0.65^{1,3}$	100

Notes:

[1] Bias is lognormally distributed

[2] Gulf of Mexico

[3] North Sea

5.0 Load Combinations

In many cases, two or more loads or load effects act on the same component of a marine structure. It is very important to estimate the extreme values of the combined load in order to evaluate the safety of the structure and make design decisions. The problem of combining loads and of finding the extreme values of the combined load might be very difficult because, for most of the cases, the loads, which must be combined, vary randomly in time and their maximum values do not occur at the same time instant. Moreover, it is difficult to determine the location in the structure where the combined load effect takes its maximum value. In this chapter, we investigate the errors associated with combining loads in ships.

Examples of loads effects, which need to be combined are the following:

a) stillwater and vertical wave bending moments,

b) vertical and horizontal wave bending moments,

c) wave bending and torsional moments,

d) wave and slamming bending moments.

Guedes Soares (84) has shown that the Ferry Borges and Castanheta (68), and Larrabee and Cornell (81) methods are almost exact for problem a). Problems b) and c) can be easily solved, provided that the cross spectral densities of the pertinent random processes are known. Although this can be easily done by using any linear seakeeping computer code, most of the studies on longitudinal ship strength do not address the issue of load combination.

Problem d) is more difficult because the load processes, which must be combined, are correlated, and the slamming bending moment is nonstationary. Moreover, it is very difficult to calculate the relative positions of the wave and slamming bending moments peaks, in the time scale.

In order to assess the uncertainties in combining slamming and wave bending moments, we followed a Monte Carlo simulation approach. More specifically, we developed a computer code, which calculates slamming and wave bending moments and combines them for a given time history of the wave elevation. The code is an implementation of the procedure suggested by Kaplan (72,87) for generating random time histories of the wave elevation, and the method described by Kaplan (72,86) for calculating the resulting slamming bending moments. We generated a large number of wave elevation time histories, and for each of them, we calculated, a) the time histories of the resulting slamming, wave, and combined bending moments, and b) the maxima of the combined bending moments. For the purpose of this study, we assumed that these are the actual values of the maxima of the combined

bending moment. We also estimated the maxima of the combined bending moment, from those of the slamming and wave bending moments, by using standard methods. These methods are, Turkstra's rule, the peak coincidence approximation, and the square root of sum of squares (S.R.S.S.) rule, and they are described in Appendix B. Then, we compared the actual maxima against those from the aforementioned methods. The results of this study are summarized in Table 5.1. The details of our approach can be found in Appendix B.

The following conclusions can be extracted from Table 5.1, and from the results presented in Appendix B:

a) Turkstra's rule is unconservative. For some cases, it may underestimate the combined bending moment by 40%.

b) The peak coincidence approximation is overconservative, and as such, it might lead to very inefficient designs.

c) The bias of the S.R.S.S. approximation was found to be almost 1.00. However, this approximation has slightly larger scatter than the other two methods. Moreover, it is conservative for some cases, while it is unconservative for some others.

d) The uncertainty associated with the combination of the above moments is significant.

e) Presently, there is no method, which can be used as a reliable engineering tool to predict the maxima of the combined slamming and wave bending moments.

Table 5.1 Bias and COV of Standard Methods for Combining Slamming and Wave Bending Moments

Method	Bias	COV
Turkstra's rule	1.17	0.11
Peak coincidence approximation	0.72	0.11
SRSS	1.01	0.12

6.0 Structural analysis

In this chapter we investigate the accuracy and the fidelity of procedures which are used to predict the response of marine structures to the applied loads. We will focus on uncertainties associated with finite element analysis (F.E.A.) procedures, but we will also examine the accuracy of traditional beam theory in estimating main girder stresses in the ship hull. Information is also provided on uncertainties associated with F.E.A. of automotive and aerospace structures.

6.1 Ships

6.1.1 Uncertainties in F.E.A.

The accuracy of F.E.A. procedures can be assessed by comparing their results against measurements from test models or actual ships. Elbatouti et al (76), Webster and Payer (77), and Westin (81) presented experimental and analytical results for the SL-7 containeship. Analytical results were obtained by F.E.A., or simplified approaches such as the Finite Beam Technique (Westin 81) and the beam theory. Experimental measurements were obtained from tests which were carried out on a steel structural model. Jan et al (79) also presented experimental and analytical results on wave bending stresses in the hull of an SL-7 containership. Here, some of the above results are analyzed to assess the uncertainties in structural analysis.

A sketch of the ship hull including the locations, at which measurements were taken in Elbatouti's study, is presented in Figure 6.1. We considered two loading cases, which are shown in Figure 6.2. In the first case, the ship was subjected to a vertical bending moment (Loading case 1). In the second case, the ship was subjected to pure torsion. (Loading case 2). A finite element model F.E.M. of the SL-7 ship hull was generated and analyzed by Elbatouti by using the ABS/DAISY computer code. This model consisted of roughly 3,000 elements, which were mostly triangular plates. Transverse bulkheads were modelled by membrane and bar elements. The model had 1800 nodes and 6700 degrees of freedom.

Figure 6.3 compares measurements and predictions of the angle of twist along the hull under loading case 2. It can be observed that the F.E.M. is stiffer than the steel model. This is a general conclusion. For the majority of the cases in all engineering applications, F.E.A. underestimates flexibility. It can also be observed that there is a sudden change in the slope of the twisting angle at point A. (This point corresponds to frame 290). This change is due to the large change in the torsional stiffness of the hull at frame 290. The discrepancy between the slopes of the measured and experimental twisting angles is large at this frame. This is probably due to the fact that hull warping is not constrained in the F.E.M. model as strongly as in the steel model. Based on the results in Figure 6.3, the bias in the twist angle was found equal to 1.4 and the COV equal to 0.18.

Figures 6.4 and 6.5 depict the normal warping stresses in frames 142 and 290, respectively under loading case 2. Analytically predicted stresses, as well as those measured from tests on a steel and a vinyl model, are plotted in these Figures. The bias for frame 142 was estimated 1.20 and the COV 0.42. These estimates are based on the analytical stresses and those obtained from tests on the steel model. For frame 290, these numbers were 1.8 and 0.67, which indicates that the error in the warping stresses was larger at this frame. This is attributed to the sudden change in the geometry and torsional stiffness of the hull at this frame. Moreover, according to the Figure 6.3 and the discussion in the previous paragraph, the F.E.M. does not represent accurately the warping constraint at frame 290.

Clearly, it is very difficult to predict the normal warping stresses in ships with large openings in their decks, by using F.E.A. Even if we use detailed F.E.M's to represent portions of the structure, at which the geometry suddenly changes, the error is still likely to be large. The reason is that we cannot accurately determine the forces applied to the boundaries of these critical portions of the hull from the rest of the ship. Analysis of frame 290 in the SL-7 containeship, is an example of a case, for which F.E.A. cannot accurately predict the normal forces on this frame due to the effect of constraining warping. (Elbatouti 76).

The shear stress distribution at frame 186 under loading case 2 is plotted in Figure 6.6. We observe that the F.E.A. results are in good agreement with measurements. The bias was found equal to 1.01, which indicates that there is no systematic trend for the predictions to be either conservative or unconservative. The COV was found 0.20, which implies that shear stress predictions are more accurate than those for warping stresses.

Finally, we compared predicted and measured normal longitudinal stresses under pure bending (loading case 1). The results are plotted in Figure 6.7 together with those from beam theory. The bias and the COV for F.E.A. results are 0.93 and 0.17, respectively. This implies that results on longitudinal bending stresses are more accurate than those for shear or warping stresses. Moreover, beam theory was found to be very accurate in predicting normal stresses. Its bias was 0.94 and its COV was 0.10.

It should be emphasized that th esults of the previous paragraphs are based on a small number of samples. Therefore, they should be used with caution. Furthermore, the SL-7 is a very difficult ship to analyze due to the extremely complex geometry of its hull. The COV's for the results from F.E.A.'s of other ships, such as tankers, are expected to be considerably lower than the values, which were estimated in this example. Moreover, the data, which were used to estimate uncertainties, were contaminated with experimental error. Unfortunately, we cannot get rid of this type of error. Thus, the values of the COV's are likely to be conservative because, they incorporate the effects of the error in both F.E.A. and experimental measurements.

Jan et al (79) compared theoretically predicted and measured stresses in the hull of

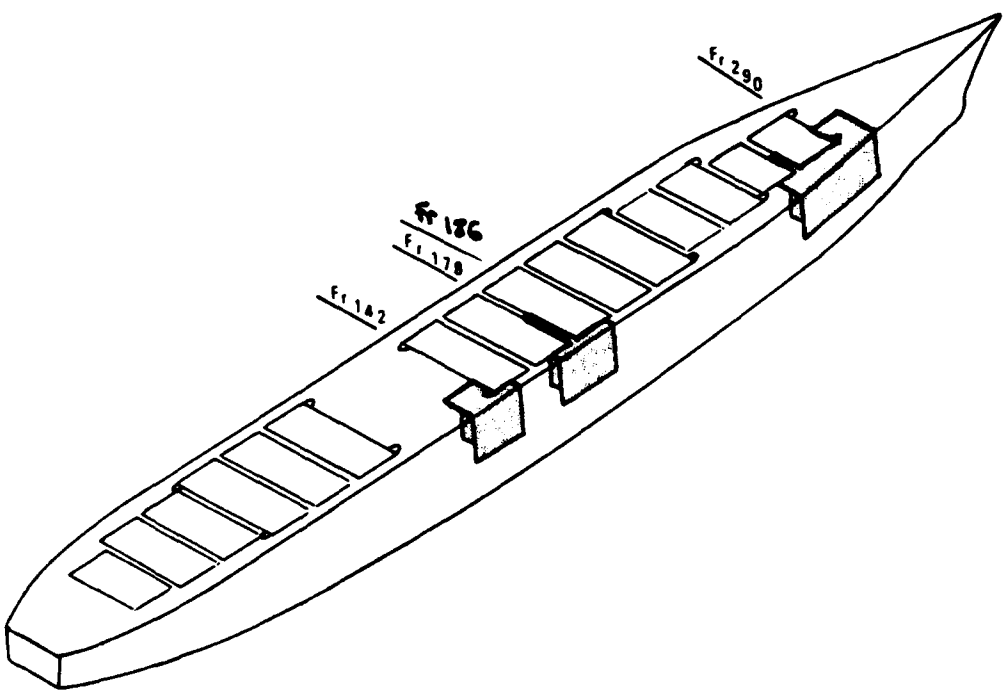
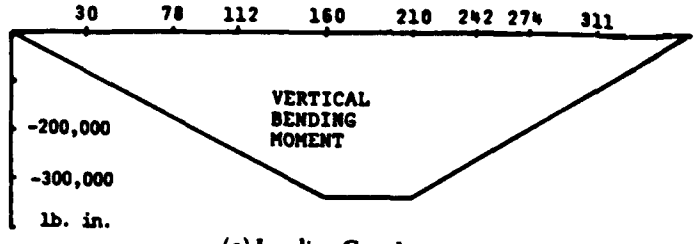


Figure 6.1 Sketch of SL-7 Model



(a) Loading Case 1

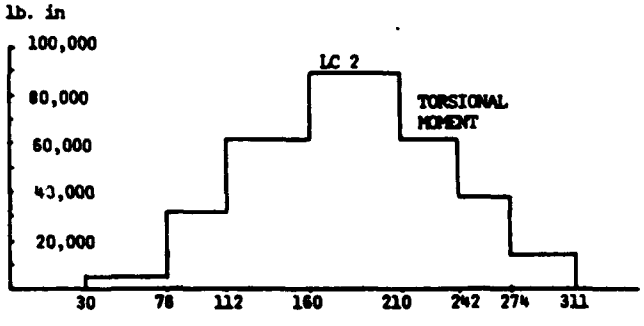


Figure 6.2 Loading Conditions

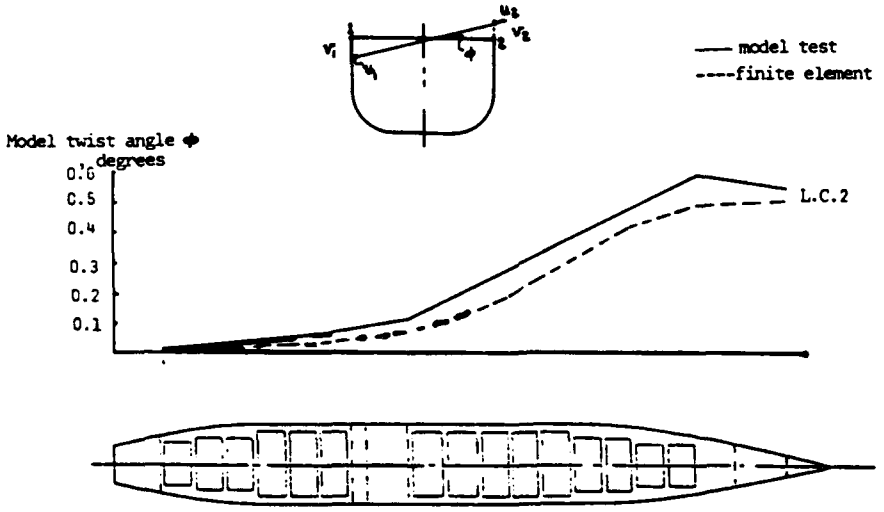


Figure 6.3 Comparison of Twisting Angles Along the Ship Hull

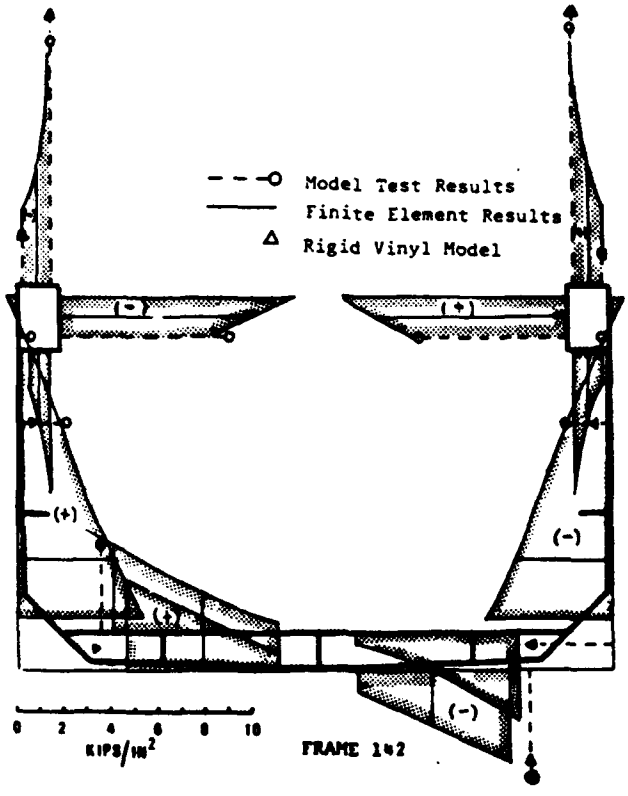


Figure 6.4 Longitudinal Warping Stresses in Frame 142

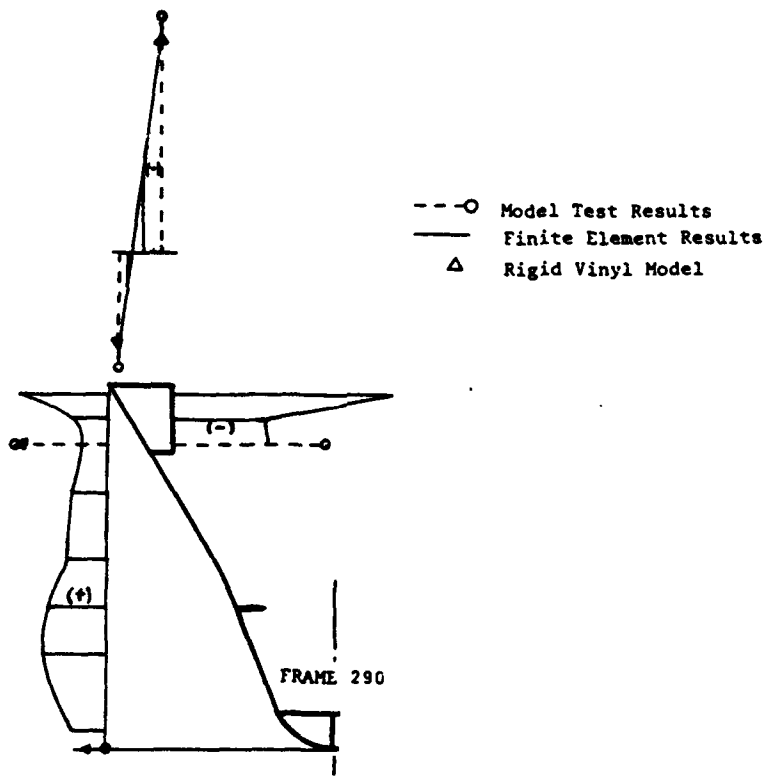


Figure 6.5 Longituding Warping Stresses in Frame 290

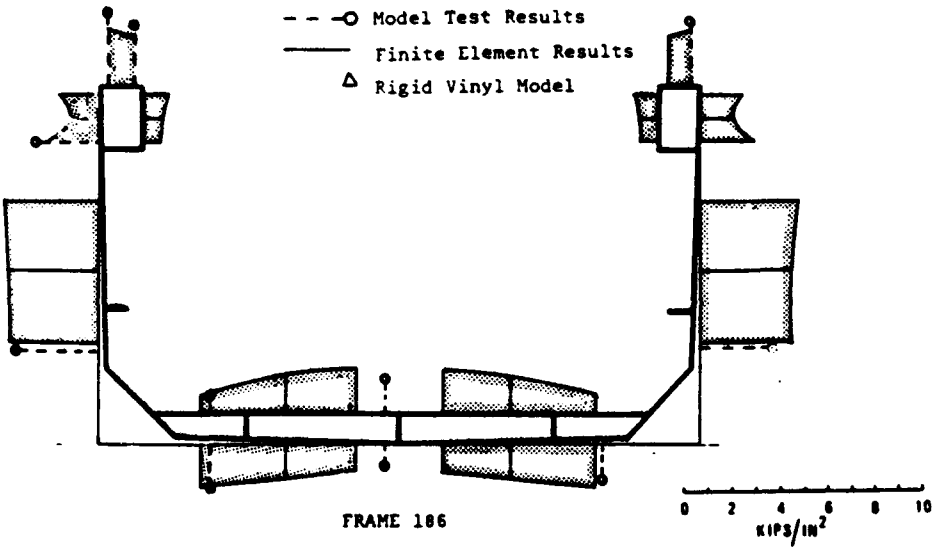


Figure 6.6 Shear Stresses at Frame 186

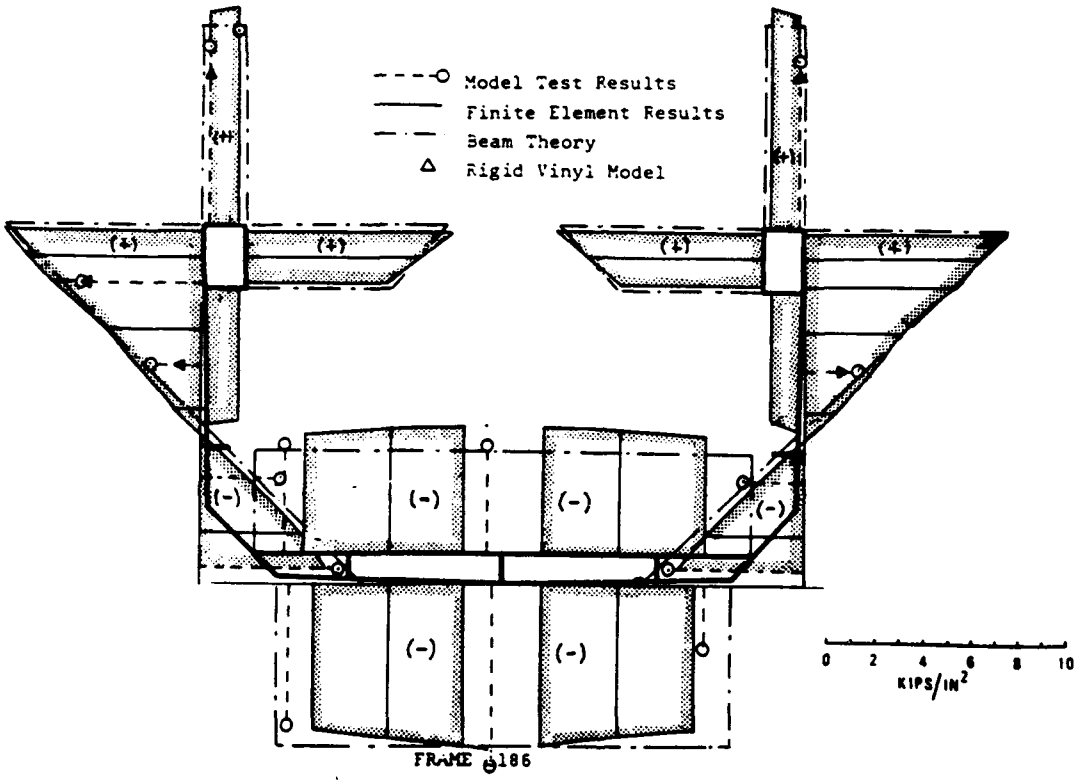


Figure 6.7 Normal Bending Stress in Frame 186

an SL-7 containership. Strip theory based computer codes (ABS/SHIPMOTION and ABS/DUNPRE) were used to predict hydrodynamic motions and loads. The ABS/DAISY code was used for F.E.A. Stress spectra and rms of wave bending stress in head and obligue seas were investigated. The predicted rms of the vertical bending stress in head seas was also compared against measurements. The stress was calculated from the spectrum of the wave elevation and the stress response amplitude operator, which was obtained analytically. The results, as well as the estimated bias for the rms of the bending stress amidships are shown in Table 6.1.

Table 6.1 Measured and Predicted Longitudinal Wave Bending Stresses Amidships (Source: Jan et al, 79)

Calculated (RMS)	Measured (RMS)	B (RMS)	Comments
8343	6743	0.81	the results in
7295	6344	0.87	columns 1 and 2
7183	5368	0.75	refer to the
3547	2990	0.84	RMS of peak
4192	3300	0.79	to trough
4544	4730	1.04	stresses on
2542	2000	0.79	main deck
4252	3410	0.80	amidships
4766	4310	0.90	
3188	3530	1.11	
4595	5800	1.26	

Based on the results in Table 6.1, the bias was found equal to 0.91 and the COV 0.16. These values incorporate errors in both the response amplitude operator between the wave elevation and wave loads, and the structural analysis of the hull. Assuming that the COV for the response amptitude operator between the wave elevation and the bending moment is 0.1 (Kaplan 84), the COV for the stress analysis is estimated 0.125. The COV is of the same order of magnitude with that found from analysis of Elbatouti's results.

The results on uncertainties in structural analysis of ship hulls are summarized in Table 6.2.

Table 6.2 Uncertainties in F.E.A. of an SL-7 Containeship

Loading Case	Quantity	Bias	COV
Pure longitudinal bending	Normal stress	0.93	0.12 - 0.17
Distributed torsional moment	Shear stress	1.01	0.20
Distributed torsional moment	Normal warping stresses	1.20	0.42
Distributed torsional moment	Twisting angle along the hull	1.4	0.18

6.1.2 Uncertainties in F.E.A. in other engineering applications

It is interesting to compare the errors in Table 6.2 with those associated with F.E.A. of other engineering structures. Sutharsana et al (90) and Newlin et al (90) reviewed the literature on F.E.A. of aerospace structures and discussed the subject with experts. Their conclusion was that F.E. stress analysis would calculate stresses to within 20% of the true value. Based on this conclusion, they assumed that the analysis bias follows the uniform probability distribution from 0.8 to 1.2. According to this assumption, the average bias is 1.0 and the COV is 0.12.

F.E.A.'s using F.E.M. with roughly 5000 degrees of freedom are routinely used to analyze automotive structures. The author had extensive discussions with experts on F.E.A. of car bodies on the correlation between analytical predictions and measurements. The following conclusions are based on these discussions: It is general consensus that F.E.A. underestimates the flexibility of a car body. This conclusion agrees with that for F.E.A. of ship hulls (Table 6.2). Moreover, the error in predicting deflections due to bending or torsional loads ranges between 10 to 20%. Finally, it is more difficult to predict the response due to longitudinal bending than that due to torsional loading.

6.1.3 Errors Due to Shear Lag

Elementary theory of bending assumes that the bending stresses in a beam are proportional to the distance from the neutral axis. This is not true for sections having wide flanges. Indeed, the parts of the flange far away from the web can carry lower stresses, which makes the actual maximum normal stress larger than that predicted by the classical beam theory.

For design purposes, this is dealt with by reducing the width of the flange so that the correct bending stress can be obtained by applying the elementary theory of bending.

In the literature, the terms, "effective breadth" and "effective width" are used interchangeably for two different phenomena:

(i) Effective width of plates subjected to compressive loads to compensate for buckling effects.

(ii) Effective width of plates subjected to lateral loads to compensate for shear lag effects.

Schade (51,53) attempted to resolve this confusion by using the terms "effective width" for case (i) and "effective breadth" for case (ii).

Here, we review various methods for estimating effective breadth. The methods are applied to some simple plate-stiffener assemblies subjected to bending, and their results are compared to test measurements in order to quantify the bias of each method. The following methods are studied:

a. Timoshenko & Goodier

A stress function is defined such that,

$$\sigma_x = \frac{\partial^2 \phi}{\partial y^2}$$

$$\sigma_y = \frac{\partial^2 \phi}{\partial x^2}$$

$$\tau = -\frac{\partial^2 \phi}{\partial_x \partial_y}$$

The stress-strain relations and the compatibility condition together result in the biharmonic equation

$$\frac{\partial^4 \phi}{\partial x^4} + 2\frac{\partial^4 \phi}{\partial x^2 \partial y^2} + \frac{\partial^4 \phi}{\partial y^4} = 0$$

An expression for $\phi(n, y)$ satisifying the boundary conditions is obtained from this equation from which the stresses are calculated. The effective breadth is then calculated by

$$\lambda = \frac{1}{\sigma_B} \int_0^b \sigma_x(y) dy,$$

where σ_B is the stress in the part of the flange close to the web. In case of a general transverse loading, the bending moment is represented by a sine series of the type:

$$M(x) = \Sigma M_n \sin\, \mathrm{n}\pi x/L$$

where

$$M_n = \frac{2}{\ell}\int_0^{\ell} M(x)\sin\frac{n\pi x}{L}dx$$

This yields the following formula for effective breadth:

$$\frac{L}{2\lambda} = \beta[\frac{M(x)}{\sum_{n=1,3,5}\frac{Mn\ \sin(n\pi x/L)}{4+(k/\beta)n\pi}} - 4] \qquad \text{where,}$$

$k = \frac{(1+\mu)(3-\mu)}{4}$,

$\beta = \frac{t \times L}{A_s}$

A_s is the stiffer area.

t is the plate thickness,

L is the beam length, and

μ is Poisson's ratio.

b. Schade

According to Schade, the effective breadth depends upon the following factors:

(a) Span of the stiffners. It increases with the span increasing.

(b) Nature of the load, but not its magnitude. It is lowest where high shear exists.

(c) The boundary conditions, particularly at the plate sides. It does not depend on thickness.

For a multiple stiffener configuration,

$$\frac{\lambda}{b} = \frac{1.1}{1+2(\frac{2b}{CL})^2}$$

where CL = distance between points of zero bending moment.

c. Bureau of Ships (BuShips)

This study assumes that the effective breadth is influenced not only by the thickness of the plating, the spacing, and the span of the stiffners but also by the shape factor of the stiffner as well as the general stress level. This approach has been presented in Schade (51) (pp. 421-422).

The equation which relates these terms is,

$$2\lambda = \frac{\sigma}{\sigma_{yp}} \times \frac{I_T}{C_C} \times \frac{1}{et}\left[\frac{\sinh\frac{\pi b}{L'}}{\sinh\frac{\pi b}{L'}(1+\frac{\rho^2}{e^2}+\frac{\pi I_S}{4e^2tL'}\{(3-\mu)(1+\mu)\cosh\frac{\pi b}{L'}-(1+\mu)^2\frac{\pi b}{L'}\cosh\frac{\pi b}{L'}\}}\right]$$

where,

t - thickness of plate,

μ - Poisson's ratio,

$2b$ - breadth of plate or flange,

2λ - effective breadth,

σ - ultimate compressive stress of panel,

σ_{yp} - yield stress,

I_T - Total Moment of Inertia,

C_C - distance of neutral axis from top fiber of plate,

e - distance from N.A. of stiffner alone to c.g. of plate,

ρ - radius of gyration of stiffner,

I_S - M.I. of stiffner, and

$2L' = L =$ Span of the Beam.

d. Modified Schade's Formula (Faulkner 75)

Schade's formula was modified as follows:

$$\frac{\lambda}{b} = \frac{1.1c}{1+2(\frac{2b}{CL})^2}$$

where c is constant equal to 0.75.

In the following we estimate the bias and scatter introduced by the aforementioned formulas.

Consider a simply supported beam under a uniformly distributed load along its length. The beam consists of a plate and a stiffener, which is attached to the beam. The dimensions

are provided in Tables 6.3 and 6.5. A comparison of the previous methods and some test results has been made in Tables 6.4, 6.6 and 6.7.

Table 6.3 Loading and Geometry Description:

Loading - Uniformly Distributed.

Span - 16'

Spacing (Plate breadth) - 24"

Stiffener Area - 6.22 sq. in.

The following table presents the effective breadth for various plate thickness.

Table 6.4 Effective Breadth For Various Plate Thicknesses
Effective Breadth

Plate Thickness (in)	Tests	Schade	Modified Schade	Timoshenko	BuShips
0.32	0.60	1.06	0.80	0.77	0.62
0.44	0.88	1.06	0.80	0.84	0.89
0.63	0.89	1.06	0.80	0.70	0.87

Test results are taken from Schade (51)

Table 6.5 Loading and Geometry Description:

Loading - Uniformly Distributed

Span - 16'

Spacing - 24"

Plate Thickness - 0.44"

The following table shows the effective breadth for various stiffeners with different cross-sectional areas.

Table 6.6: Effective Breadth For Various Stiffeners
with Different Cross-sectional Areas

Area of Stiffness in	Tests	Schade	Modified Schade	Timoshenko	BuShips
6.22	0.88	1.06	0.80	0.84	0.89
7.72	0.82	1.06	0.80	0.99	0.82
8.61	0.82	1.06	0.80	1.06	0.87
10.72	0.79	1.06	0.80	1.16	0.81

The aforementioned results were analyzed in order to estimate the bias and scatter of the effective breadth and the maximum stress as obtained from each formula. The results are presented in the following table.

Table 6.7: Bias and Scatter of Methods to Estimate Effective Breadth

Method	Stress	
	Bias	Scatter
Schade	1.35	0.16
Timoshenko	1.17	0.21
BuShips	1.02	0.03
Beam Theory	1.27	0.16
Modified Schade	1.02	0.16

Clearly, the effect of shear lag may be significant for some cases. This is particularly true for longitudinal bending of short beams (length/breadth < 5), for which case shear effects are important. Transverse bending of a SWATH ship is an example for which shear

effects must be taken into account. The results in Table 6.7 demonstrate that classical beam theory underestimates bending stresses. Empirical equations, such as the modified Schade's formula, can be used to account for shear lag in stress analysis. Moreover, one of the aforementioned empirical equations (BuShips) was found to be very effective in calculating effective breadth and the maximum stress.

6.1.4 Effect of joint flexibility and rigid beam lengths in transverse strength analysis of ships.

In strength analysis of traverse hull frames, it is assumed that the joints, which connect frame elements, are rigid. Moreover, it is assumed that transverse frames are flexible all over their length. However, in reality, joints are flexible, and portions of transverse frames in the vicinity of joints are practically rigid because they are reinforced by brackets and by the attached longitudinal beams.

Hughes (83) studied the effect of joint flexibility and rigid beam lengths. His study was based on Milchert's (72) results. It was demonstrated that an idealization of the transverse frames of a ship as continuous frames with no allowance for joint flexibility and rigid frame-length may lead to significant errors in transverse strength analysis. The results reported by Milchert (72) and Hughes (83) showed that the bending moment which is calculated by the aforementioned idealization, might be 50% larger than the actual one. Moreover, the displacements might be overestimated by 60%. However, the significance of these results is reduced by the fact that they correspond to a frame whose members are very short (the size of the joint was roughly 30% of that of the frame element). For this case, it is not necessary to be very accurate when analyzing transverse strength, because the displacements and stresses are small. Furthermore, the errors due to joint flexibility and rigid frame lengths should be considerably smaller than for frames with long elements.

The effect of joint flexibility and rigid frame lengths can be accounted for if we employ a very detailed finite element model, which models transverse frames and brackets by plate elements. The computer program MAESTRO (Hughes 83), which is for ship structural analysis, accounts for the joint flexibility and the effect of rigid frame lengths. Most of the general purpose finite element codes do not account for the above effects.

6.2 Offshore platforms.

Finite element programs, such as NASTRAN, are used to derive member forces in offshore platforms from the applied loads. Wirsching (81) reported that the bias, which is associated with the calculation of member forces, ranges between 0.8 and 1.10, while the COV is between 0.2 to 0.4. These numbers were based on discussions with experts in structural analysis of platforms.

The error in structural analysis was attributed to the effect of joint flexibility, which

is not taken into account in F.E.A., and uncertainty in damping. The COV of member force estimates due to the latter effect was estimated as 8%. Due to the joint flexibility, the actual natural period of a platform is lower than that estimated by F.E.A. Thus, joint flexibility introduces uncertainties in the natural period. Moreover, by treating joints as rigid, we overestimate bending moments and the resulting stresses in the structural members, which are attached to the joints. This effect was also observed in the analysis of transverse ship frames (Hughes, 83).

Bouwkamp et al. (80), found that the effect of joint flexibility on the structural response of an offshore platform might be significant for high offshore towers (height $>$ 500 ft). Moreover, the effect of joint flexibility on member forces is strong for tubular members whose lengths are short compared to their diameter. It is interesting that, although joint flexibility increases the deflections of a platform, classical structural analysis procedures, which model joints as rigid, might overestimate the displacements at some locations. The maximum error in deflection due to joint flexibility was found equal to 30% for the example considered in Bouwkamp (80). The corresponding maximum error in the bending moments in structural members was found to range up to 500%. The error in the first natural period was small, less than 2%. However, the error in higher natural periods was higher (for example it is 11% for the second natural period). These modest errors in natural period are important in structural analysis because they lead to large errors in the dynamic response.

Moses (85), investigated uncertainties in dynamic analysis of fixed offshore platforms with low natural frequencies, for which dynamic effects are important. He used the inertia load factor (I.L.F.) in order to account for dynamic effects. The I.L.F. is defined by the following equation;

Dynamic response = (1.0 + ILF)$\times$ static response.

The overall uncertainty of ILF was estimated by using a FOSM approximation and Taylor expansion about the mean values of the random variables, which are used to quantify uncertainties in all the steps of dynamic analysis. The COV of the ILF for member loads was found equal to 0.61. Table 6.8 summarizes the uncertainties which were considered by Moses.

Table 6.8: Uncertainties in Dynamic Analysis of Fixed Offshore Platforms

Quantity	Uncertainty (COV)	Effect on ILF	Relative contribution (%)
Natural period	0.1	0.48	62
Damping	0.3	0.10	2
Spectral shape variability	-	0.20	11
Transfer function	-	0.20	2
Member force calculation	-	0.15	6
Analysis uncertainty	-	0.25	17
Total uncertainty in ILF		0.61	

Of the above uncertainties, those due to natural period, damping, member force calculation, and analysis uncertainty can be considered as uncertainties in structural analysis. Clearly, the uncertainty in estimating the natural period is the most significant. Indeed, a small error in this quantity leads to a large error in the calculated nominal member forces, and stresses.

Thus, emphasis should be given in improving the accuracy of methods for estimating the natural period of platforms. This could be achieved by improving the accuracy of procedures for estimating the mass of a platform, by modeling the behavior of the foundation more accurately, and by accounting for the joint flexibility.

7.0 Fatigue

Fatigue is an important consideration in structural design. For many structural systems, fatigue is the most critical failure mode, and thus safety requirements associated with fatigue reliability dictate design decisions. Fatigue strength can be described by a characteristic S-N curve or by a fracture mechanics fatigue model.

A cumulative damage based approach for fatigue analysis consists of the following steps:

a) modeling the loading environment,

b) modeling loads exerted by the environment on the structure,

c) evaluation of nominal loads,

d) evaluation of stresses at all points of possible crack initiation (stress concentrations),

e) evaluation of cumulative fatigue damage over the lifetime of the structure.

Uncertainties, which are involved in steps a) to c), were studied in the previous chapters. In this chapter, we quantify errors in calculating stress concentration factors. We also combine the errors involved in all the steps of fatigue analysis and quantify uncertainties in fatigue damage, for the case that a cumulative damage approach is used. Finally, we investigate the relative importance of the uncertainties in each of the steps a) to e), and also of the random and modeling uncertainties.

7.1 Uncertainties in stress concentration factor.

Wirsching (81) reported estimates of the uncertainties in stress concentration factors for tubular joints of offshore structures. These uncertainties are for stress concentration factors obtained from parametric equations, such as those by Kuang, Potvin and Leick (77). According to Wirsching, the average bias in the stress concentration factor is in the range from 0.80 to 1.20, and the COV ranges between 0.1 and 0.50. The bounds for the bias and the COV in stress concentration factor are very wide, possibly because the parametric equations cover a large number of geometries and loading conditions.

Uncertainties in the stress concentration factor are large for other engineering structures. For example, the stress concentration factor for the fatigue analysis of a liquid propellant engine was assumed to follow the beta distribution (Sutharsana et al 90), (Moore, et al 90). The stress concentration factor is in the range from 1.2 to 3.5, and its COV is roughly 0.15.

7.2 Uncertainties in cumulative fatigue damage.

Studies on fatigue reliability of marine structures assume that the effect of random uncertainties on the cumulative damage is negligible. Thus, these studies account only for modeling uncertainties in stress evaluation processes (Wirsching and Chen 88). Although the effect of random uncertainties reduces with the number of load cycles increasing, to the best of our knowledge no study has proven that this effect is negligible.

The objectives of the exercise presented in this section are to address the above issue, estimate uncertainties in the cumulative fatigue damage over the lifetime of platforms and ships, and study the relative importance of each uncertainty.

The following are the basic assumptions:

a) Fatigue life can be estimated by using the S-N curves. The integrated Paris law gives the same form, assuming no threshold level and no sequence effects. The slope of these curves is constant for any number of cycles, N.

b) Miner's rule can be used to estimate fatigue damage.

c) The stress amplitude distribution is known.

d) The mean and standard deviation of the cumulative damage, D, can be estimated by linearizing the expression relating D with all random variables around the mean values of these variables. This is a crude approximation because the derivatives of the damage with respect to the values of the random variables are not constant. Advanced methods for fast probability integration are more accurate in this case (Madsen, Krenk and Lind 86). However, the objective of this study is to identify the most important uncertainties and obtain only rough estimates of the COV of D. Moreover, the estimates for the bias and the COV of the random variables involved in damage calculations are very crude. Thus, the benefits from using an advanced fast probability integration method are minimal.

Under the above assumptions, fatigue damage can be calculated by the following equation (Wirsching and Chen 88):

$$D = \frac{B_{II}^m \, \Sigma \, S_i^m}{A} \tag{7.1}$$

where,

B_{II} represents the modeling error in the stress at points of stress concentration,

m, is the exponent in the S-N curves,

S_i, is the predicted stress amplitude at the ith load application, and

A, is the constant at the right hand side of the S-N equations.

The summation is for all load applications.

The above equation is based on the assumption that the stress is a narrowband process. The stress might be wideband which affects the fatigue damage and the life of the structure. We may account for the above effect by using the rainflow correction factor (Wirsching 84, Wirsching and Chen 88).

The modeling bias B_{II} is given by the following equation:

$$B_{II} = B_M \cdot B_S \cdot B_F \cdot B_N \cdot B_H, \tag{7.2}$$

where,

B_M represents uncertainties in the geometry due to manufacturing imperfections,

B_S represents uncertainties in seastate description,

B_F represents uncertainties in wave load predictions,

B_N is the bias for errors in static and dynamic structural analysis, and

B_H is the bias for uncertainties in stress concentration factors.

By using a first order Taylor series expansion of the expression for D about the mean values of all random variables, we obtain the mean value of D,

$$E(D) = \frac{E^m(B_{II})\ \Sigma\ E^m(S_i)}{E(A)} \tag{7.3}$$

Assuming that the statistics of the predicted stress are the same for all load cycles, we have,

$$E(D) = \frac{E^m(B_{II})\ N \cdot E^m(S_i)}{E(A)} \tag{7.4}$$

where N is the number of cycles over the lifetime of the ship.

The coefficient of variation of fatigue damage D in (7.1) is,

$$COV_D = (m^2 COV_{B_{II}}^2 + COV_A^2 + COV_{\Sigma S^m}^2)^{1/2}, \qquad \text{where} \tag{7.5}$$

$COV_{B_{II}}$ is the COV of modeling bias,

COV_A is the COV of A, and

$COV_{\Sigma S^m}$ is the COV of the sum ΣS_i^m.

Note that subscript i has been dropped.

The first term in the expression with the square root, on the right side of (7.5), represents the effect of modeling uncertainties. The second term is associated with uncertainties in S-N curves and the third represents the effect of random uncertainties.

As it was mentioned earlier, equations (7.4) and (7.5) are approximate. The reasons for using them have been mentioned earlier in this section.

7.2.1 Relative importance of random uncertainties.

All studies on fatigue reliability of marine structures neglect the effect of random uncertainties on the fatigue damage without justifying this approximation. Here, we compare the effect of random uncertainties against that of modeling uncertainties in order to assess the importance of random uncertainties. We also investigate the effect of the correlation between the maxima of the stress process.

We considered two cases. In the first case the maxima of the stress, S_i, follow the Rayleigh distribution, while in the second they follow the Weibull distribution. We assume that the correlation coefficient between the *ith* and the *kth* stress maxima, S_i and S_k, is,

$\rho_{S_i S_k} = \rho_{S_i S_{i+1}}^{|i-k|}$, where $\rho_{S_i S_{i+1}}$ is the correlation coefficient between two subsequent peaks. In our study we considered different values for $\rho_{S_i S_{i+1}}$ in the range from 0. to 0.99. In the following discussion subscripts will be dropped. After some algebra, the following equation was derived for the COV of random uncertainties:

$$COV_{\Sigma s^m} = \frac{COV_S m(\frac{1+\rho}{1-\rho} - \frac{2\rho}{N(1-\rho)^2})^{1/2}}{N^{1/2}} \tag{7.6}$$

where COV_S is the COV of a local maximum.

It is observed from (7.6), that the COV increases with the correlation coefficient between subsequent maxima increasing. Moreover, the COV for random uncertainties decreases, with the number of load cycles, N, increasing. The $COV_{\Sigma s^m}$ is almost zero for large values of N (say 10^7), for any value of ρ less than one.

The COV for random uncertainties is presented in Table 7.1, for three cases. In the first case, the stress amplitude follows the Rayleigh distribution, while in the latter two cases, it follows the Weibull distribution (Ochi 90) with Weibull exponent c equal to 0.7 and 1.0, respectively.

Table 7.1 Coefficient of Variation of Cumulative Fatigue Damage Due to Random Uncertainties ($N = 10^6$)

Distribution of Stress Amplitude	COV of Cumulative Damage				
	Correlation Coefficient of Subsequent Peaks				
	0.0	0.5	0.8	0.9	0.99
Rayleigh	0.0	0.0	0.01	0.01	0.03
Weibull (c = 1.0)	0.01	0.01	0.01	0.02	0.06
Weibull (c = 0.7)	0.01	0.01	0.02	0.03	0.10

It is observed that the effect of random uncertainties is small. Moreover, a similar calculation for $N = 10^8$, which is a typical number of load applications over the lifetime of a marine structure, showed that the COV due to random uncertainties is practically zero. Since the distributions considered for the stress peaks represent real life situations, we conclude that random uncertainties can be neglected in fatigue reliability analysis without losing any accuracy. This is true even for the case for which the adjacent stress maxima are strongly correlated. Hence, the value of ρ is also unimportant provided that the number of load cycles is large (say 10^7).

7.2.2 Relative contribution of various types of uncertainty on fatigue damage.

The equations of the previous sections allow to quantify the uncertainties in the cumulative fatigue damage. Eq. (7.4) can be used to estimate the average bias while eq. (7.5) is for the COV. We used the above equations to calculate the average bias and COV of fatigue damage for typical marine structures. We also studied the relative contribution of various uncertainties to the overall uncertainty in fatigue damage.

The data on various uncertainties, which are involved in fatigue analysis, are presented in Table 7.2. The COV's in the first column are based on discussions with experts from the offshore industry. (Wirsching 81). Bea's data are for offshore platforms while Kaplan's data are for ships. Kaplan (84) and Bea (89) provided estimates for B_S and B_F only. In addition, the value of COV_{B_N} for ships was estimated in Chapter 6. The COV of the other variables were assumed to be equal to the corresponding values specified in the first column.

Finally, exponent m was taken to be 4.38.

Table 7.2 Uncertainties Involved in All Steps of Fatigue Analysis

Type of Uncertainty		COV	
		Bea (89)	Kaplan (84)
B_M	0.2	0.2	0.2
B_S	0.5	0.58[a]	0.15
B_F	0.2		0.19[b]
B_N	0.3	0.3	0.12
B_H	0.3	0.3	0.3
B_A^c	1.0	1.0	1.0

Notes:

a) This COV refers to the cumulative effect of environmental and load evaluation uncertainties, i.e. to the product of B_S and B_F.

b) This COV represents modeling uncertainties in the combined wave and slamming bending moment. The estimate was based on COV's of 0.1 and 0.16 for the uncertainties in wave and slamming bending moments, respectively.

c) B_A is the bias for the constant A at the right hand side of the S-N equations.

There is uncertainty in stress calculations due to the fact that the peaks of the wave elevation do not follow the Rayleigh distribution. This uncertainty introduces conservative bias in the stress predictions.

Table 7.3 presents the overall uncertainty in cumulative damage, as well as, the relative contribution of all types of uncertainties to the cumulative damage.

Table 7.3 Uncertainties in Cumulative Fatigue Damage and Relative Contribution of Each Uncertainty in Table 7.2

Source	COV_D	COV_M	COV_S	COV_F	COV_N	COV_H	$COV_{\Sigma S^m}$	COV_A
	3.29	0.07	0.45	0.07	0.16	0.16	0.0	0.09
Bea (89)	3.42	0.07	0.55		0.15	0.15	0.0	0.08
Kaplan (84)	2.21	0.16	0.09	0.14	0.06	0.35	0.0	0.20

The following conclusions can be extracted from Table 7.3.

a) Uncertainty in cumulative damage is very large for both ships and offshore platforms. The reason is that fatigue damage is extremely sensitive to the amplitude of the applied stress. In other words, a small change in the amplitude results to a large change in the fatigue damage and the expected fatigue life.

b) As indicated by our example, uncertainty in fatigue damage is smaller for ships than for offshore structures.

c) Uncertainty in describing the loading environment is the most important for offshore platforms. This means that even a small reduction in this uncertainty will result to a large reduction in the overall uncertainty in fatigue damage.

d) For the case of ships, uncertainty in the stress concentration factor is the most important. The next important uncertainty is that in A, which is the constant in the right hand side of the expression for the S-N curves.

e) The effect of random uncertainties is negligible because these uncertainties are averaged out in the procedure for evaluating fatigue damage. Moreover, the statistical correlation between consecutive stress peaks is unimportant in fatigue.

8.0 Conclusions

The following are the main conclusions from our study.

1. In both ships and offshore platforms, it is important to distinguish between natural (random) and modeling uncertainties and between their effects on lifetime extreme loads and load effects. Since the latter uncertainties are systematic, they do not decrease with the length of the exposure period increasing. Therefore, if we treat modeling uncertainties as if they were random, we may grossly underestimate uncertainties in extreme loads. In our opinion, approach 1 in Table 4.9 is more appropriate than approach 2.

2. We believe that modeling uncertainties have not been treated correctly (i.e. according to the method described in the previous paragraph) in the new Load and Resistance Factor Design code of the American Petroleum Institute. As a result, the coefficients of variation of load effects have been grossly underestimated.

3. An effective way to reduce uncertainties is to distinguish between different classes of ships with different characteristics and operational schedules, and quantify uncertainties for each class, separately.

4. Moreover, we may consider the dependence of modeling errors on some parameters, such as the significant wave height, and the relative heading angle. Then, we can employ regression to determine relations between the error and the above parameters. Such relations can be used to improve theoretical predictions of loads and load effects. From work dealing with this approach, it was demonstrated that we can reduce uncertainties by a significant amount.

5. There is significant variability in stillwater load effects in different voyages of a ship. There is also significant variation between similar ships and between different ship types.

6. Different effects lead to underestimation of overestimation of loads or load effects on ships. For example, if we neglect nonlinearities, wave directionality, and heavy weather countermeasures, then we will underestimate load effects in ships. On the other hand, we overestimate load effects, if we do not account for errors in visual observations of wave heights, and for the dependence of short-crestedness on sea severity.

7. The coefficient of variation for extreme wave moments in ships is roughly 0.20. The bias (ratio of actual over predicted value) is greater than one, which means that theoretical estimates of wave loads are lower than the actual values. However, the magnitude of this exceedence above one depends upon the type of ship as well as consideration of the particular type of bending (ie. sagging or hogging).

8. The coefficient of variation in extreme global loads (overturning moments and base shear forces) on offshore platforms ranges between 0.60 to 0.90. While these numbers

are large, and their precise magnitude may be questioned, the actual values are expected to be considerably larger than that in A.P.I. code. The trend indicated by these numbers appears to be proper.

9. A large uncertainty is involved in combining slamming and wave bending moments in ships. This problem cannot be treated properly by using Turkstra's rule, or the peak coincidence approximation, although a reasonable value appears to be indicated by the square root of sum of squares approach.

10. No reliable validated method presently exists for calculating slamming bending moments, and local hydrodynamic pressures on the ship hull due to impact with waves. These loads are very significant in reliability analysis of ships. Therefore, the necessary resources should be allocated for expanding the state of knowledge on slamming.

11. Linear seakeeping methods cannot estimate hydrodynamic pressures on the ship hull with acceptable accuracy. This is particularly true in the vicinity of the bow and the stern of the ship hull. These methods are more effective in calculating global loads and wave bending moments.

12. Nonlinear effects are more important for ships with small block coefficients, such as containerships, than for ships with large block coefficients such as tankers and bulk carriers.

13. The probability distribution of wave peaks is not exactly Rayleigh, and subsequent peaks are statistically dependent. This introduces conservative error in the estimates for extreme wave height. The bias (as defined in this report) due to this effect is roughly 0.93 and the coefficient of variation is 0.08.

14. Random uncertainties are unimportant in fatigue reliability analysis of both ships and offshore platforms. Moreover, the statistical correlation between subsequent wave peaks is also unimportant.

The following conclusions refer to the relative importance of the uncertainties involved in stress analysis.

15. It is general consensus that, in offshore structures, the uncertainty in describing the loading environment is the most important. For those fixed platforms, for which dynamic effects are insignificant, the largest part of this uncertainty is due to errors in estimating the long term maximum wave height. The uncertainty in estimating the long term severest sea condition over the lifetime of the platform is primarily responsible for the above errors.

16. Uncertainties in the value of the drag coefficient in Morison equation are also important, especially when calculating the forces on small cylindrical members of offshore platforms.

17. Uncertainties in describing the loading environment (wave height and period) are the most important in fatigue analysis of offshore platforms. Errors in stress concentration factor and in structural analysis follow in terms of relative importance. It should be mentioned that errors in structural analysis are primarily due to errors in estimating the natural period of a platform.

18. The following are the most important uncertainties in stress analysis on ships:

 - uncertainties in slamming bending moments,
 - spectral shape variability,
 - errors in combining wave and slamming bending moments,
 - variability in stillwater load effects,
 - model uncertainty in the response amplitude operator for wave bending moments. Note that the order in which the above uncertainties are presented, is not associated with their relative importance.

19. Uncertainty in stress concentration factor is the most important factor in fatigue analysis of ships.

9.0 Research Plan for Future Efforts to Reduce Uncertainties, in Estimated Load Effects on Marine Structures

On the basis of the information given in the preceding chapters of this report, future research should be directed toward various projects that would have benefit in reducing the most important uncertainties in load effects on marine structures. A five year research program plan is provided in the present section which is based on the relative importance of the various tasks, while also considers the associated factors of cost and risk.

The tasks are briefly described, together with their relative ranking, the rationale for such a prioritizing, and the basis for assigning the cost, benefit, and risk characterization to each task. Initially, a listing of the tasks is given with their associated characterization (and related comments) in a summary form, which is then followed by the task descriptions in the following paragraphs. The topic of cost is considered in terms of the required man-hours to complete the particular task, with the following associated definitions:

	Costs
Low	1,000 - 1,500 man-hours
Medium	2,500 - 3,500 man-hours
High	4,000 - 6,000 man-hours

A proposed schedule for carrying out the work proposed in this research program plan is appended at the end of this section.

Table 9.1 List of Tasks for Reducing Uncertainties

Task	Import-ance	Cost	Risk	Comments
1. Impact loads on ships (local effects)	+	o	o	
2. Slam loads (hull grinder responses)	+	-	-	Should be initiated after completing 1
3. Extreme impact loads	+	o	o	Should be initiated after partially completing 2
4. Combination of loads-load effects	+	o	o	
5. Nonlinearities in in wave loads	+	-	-	Will complement SR-1304 project
6. Nonlinear systems under random excitation	+	o	+	
7. Modeling uncertainties	+	+	+	
8. Breaking waves	+	+	+	
9. Effects of routing, heavy weather countermeasures	o	o	-	
10. Torsional loads in ships	o	o	o	
11. Ship-superstructure interaction	o	o	-	Very important for ships with large superstructures. (Naval, passenger ships)
12. Hydrodynamic loads in offshore platforms	+	o	+	
13. Natural period of offshore platforms	+	+	+	

Task	Import-ance	Cost	Risk	Comments
14. Flexibility of joints	o	-	-	Important in transverse strength analysis of bulk, ore carriers, and tankers.
15. Development of designer oriented computer code for stress analysis	o	+	-	Should be initiated after completing most of the previous tasks.

Notation: + : High

o : Average, medium

- : Low

Note: Order reflects priority ranking.

Task: Impact loads on ships (local effects)

Importance: +
Cost: o
Risk: o
Priority: 1

Objective: Compile state-of-the-art knowledge on impact hydrodynamic loads, and also extend existing approaches to establish reliable methods for predicting hydrodynamic pressures on ship hulls due to bottom slamming, and bow flare impact.

Impact pressure due to slamming and bow flare impact is important in design of high speed vessels such as containerships, SWATHS, patrol vessels, and combatants. Indeed, impact loads are known to induce significant damage, usually in the form of excessive permanent set, to the front panels. Evaluation of impact pressure is a very difficult and complex task, which might require to take into account the interaction between the deformation of the hull panels and the surrounding water. For this reason, our ability to predict this type of load and its effects is limited. A comprehensive review of various approaches to the problem of analyzing hydrodynamic impact loads was presented in ISSC (88) (committee I.2), as well as in previous reports of the same committee. Most theoretical approaches to the problem are based on a momentum equation which relates the impact force to the change of momentum of the water surrounding the hull (Kaplan 87). A serious problem associated with these methods is due to flat bottom surfaces which sometimes introduce some subjective considerations into the analysis. Kaplan developed an approach which circumvents the problem by use of a quasi-three dimensional method to determine the total impact force on large flat surfaces. That method avoids the infinite force values found in two-dimensional sections with flat bottoms. However, no associated pressure information was developed in that approach. In addition, the incorporation of the treatment of flat portions of a ship hull bottom region together with the remaining part of the immersed ship sections could also have to be accomplished.

Empirical models which presume a linear relation between the impact pressure and the square of the impact velocity have been extensively used by Ochi (73), Mansour (82), and Ferro (85). It should be noted that the high variability in the value of the coefficient relating the impact pressure to the square of impact velocity, (Mansour 82), is indicative of the uncertainty associated with this approach. The impact pressure has also been measured from tests in which plates, wedges, or cones drop in the water (Takemoto 84), or from actual ships (Rask 86).

In this task, it will be necessary to assess the state of knowledge in predicting slamming induced hull pressures and many existing theoretical and empirical approaches to produce a reliable method for predicting these loads. The work should also investigate the effect of structural deformation due to the loads, assess its significance, and possibly the class of

ship hulls for which it should be accounted for.

Clearly, this is a difficult and complex task. Therefore, the associated cost and risk might not be low. However, this task is very important because it is necessary to predict impact loads in a reliable way, in order to design safe and efficient ships. This particular task, or a somewhat similar type program, is also included in the FY-90 and FY-91 recommended Ship Structure Committee research programs (pp. 36-37)

Task: Slam loads (hull girder responses)

Importance: +
Cost: -
Risk: -
Priority: 2

Objective: Develop a methodology for evaluating slam-induced bending moments, and stresses in ships.

As it was demonstrated in this report for high sea state conditions, slam-induced stresses may be of the same order of magnitude as those due to longitudinal wave bending moments. Furthermore, as has been demonstrated by Vulovich et al (89), bending stresses due to slamming are significant at forward locations where lower stresses are normally expected. As such, the slamming-induced stresses play an important role in design of certain classes of ships (container ships, naval vessels, and different advanced marine vehicle concepts).

There is uncertainty in calculating hull girder responses primarily due to the difficulties in predicting the slam impact local loads and pressures (as described in Task 1 above). On this basis, it is suggested that a study using the results of Task 1 be undertaken to improve the ability to calculate slam-induced hull girder stresses. Hull flexibility, and its influence in determining vibratory responses, should be included using the methods of Kaplan (72), Vulovich (89) or other similar approaches that represent the ship structure as a prismatic beam. By means of such an approach, it is not anticipated that there will be great difficulties in response determination as long as the task on local impact forces (Task 1) has been successfully accomplished.

Task: Extreme impact loads.

Importance: +
Cost: o
Risk: o
Priority: 3

In structural reliability evaluations, it is not sufficient to know the statistics of the values

of loads or load effects at any time instant. We also need to know the extreme values over certain exposure periods. Therefore, it is important to predict the extreme values of impact loads and their effects.

The problem of determining the extreme value statistics of impact loads is considerably harder than the corresponding problem for low frequency wave induced loads, because of the nonlinear behavior of the ship. More specifically, even if the wave elevation were treated as a Gaussian stationary process, the whipping stress would not be Gaussian. Therefore, its local peaks would not follow the Rayleigh or the Rician distribution.

An estimate of the extreme value statistics can be obtained by expressing the impact loads or load effects in terms of a second-order Volterra series and by following an approach introduced by Naess (85). The basic idea behind this approach, which uses the Kac-Siegert (47) technique, is to expand the quadratic impulse response function in terms of its eigenfunctions. This allows to represent the response as a weighted sum of squares of known stationary processes, and to evaluate the average upcrossing frequency of some known threshold. We believe that this approach is suitable for this problem because, as it has been observed in experiments, the hydrodynamic impact pressure as well as the impact force are proportional to the square of the impact velocity.

For the reasons explained above, we believe that this is an important task. Furthermore, it requires the adaptation and extension of a highly sophisticated approach, which is reasonably well understood. On this basis we expect that the cost required is medium. There is also some risk that the resulting extreme value predictions might not correlate well with measurements, requiring the development of an alternate method.

Task: Combination of loads and load effects.

Importance: +
Cost: o
Risk: o
Priority: 4

Objective: Improve our ability to statistically combine loads and their effects in ships, and to predict their extreme values.

In many cases, two or more loads or load effects act simultaneously on the same structural element. Therefore, in probabilistic analysis and design, we must superimpose these loads and estimate the extreme values of the combined load process. Examples of loads or load effects that must be combined are vertical and horizontal bending moments, stillwater and wave bending moments, slamming and wave induced bending moments, and axial forces and lateral wave pressure applied to hull plates.

In general, the local maxima of the loads to be combined do not occur at the same time instant. Furthermore, the loads might be correlated or even nonstationary. This is the case for slamming and wave-induced bending moments. Therefore, the load combination problem is very complex, and for some cases it has not been solved in a satisfactory way.

Some simple procedures for combining loads and load effects are Turkstra's rule (Turkstra 70), the square root of sum of squares law (Mattu 80), and an approach which assumes that the load processes coincide. The aforementioned approaches are fairly straightforward and as such they are popular to practioners. They have also been used by several researchers. Turkstra's rule has been used by Ferro (85) to combine slamming and wave induced bending moments in ship hulls. Kaplan (84) has also used the square root sum of squares law to solve the same problem. Unfortunately, these approaches are based on some very strong assumptions, which in many practical situations are unrealistic. Turkstra's rule, for example, is accurate only for the case that the processes to be combined are statistically independent. Similar considerations will apply to the square root of sum of squares relation.

More advanced sophisticated methods are also available. These methods calculate the upcrossing rate of a safe domain in the space of random load and strength variables by a vector defined by the loads to be combined. This can be used to estimate the extreme value statistics of the combined process Madsen et al. (86). Bounds for the upcrossing rate, which are inexpensive to calculate can be found by the point crossing method introduced by Larrabee and Cornell (84). This method was extended by Winterstein and Cornell (84). However, the point crossing method, in the form described in the above references, cannot account for the correlation between loads.

Wen (77), and Wen and Pierce (83) introduced the load coincidence method. This method accounts for the correlation between the random processes to be combined by calculating and using the average coincidence rate. It also estimates the average crossing rate of a safe region. One of the disadvantages of the load coincidence method is that it is not directly applicable to the case of nonstationary loads. Moreover, the average coincidence rate, which is required by the method, is not always known or easy to calculate.

As it was demonstrated in this report, the accuracy of the approach employed for load combination affects significantly the estimates of the extreme loads. Clearly, the issue of load combination is critical in probabilistic analysis and design. Therefore, it is worth undertaking a study whose objective is to improve the ability to predict the extreme values of two or more stochastic load or load effect processes acting simultaneously on the same structural component. This will be accomplished by selecting, adapting, and extending existing approaches for load combination. The following are a few cases that must be analyzed:

a) low frequency wave and slamming induced longitudinal ship hull bending stresses,

b) wave induced, and stillwater bending moments in ships,

c) horizontal, vertical and torsional wave induced bending moment in ships,

d) dead, live, and wave loads in offshore platforms.

This task should improve our ability to establish the statistics of extreme loads and design loads for code calibration. For this reason, this task is important. We do not anticipate any problems in completing this task. Therefore, the associated cost and risk are low.

Task: Nonlinearities in wave loads.

Importance: +
Risk: o
Cost: o
Priority: 5

Objective: Review methods for nonlinear analysis of wave loads and select and recommend the most practical ones.

It is recognized that linear strip theory gives only a rough approximation of low frequency wave bending moments, and that its results might be misleading when it is applied to estimate load in extreme sea states. Indeed, nonlinear effects are important in high sea states, in which case linear strip theory underestimates wave loads (Jensen 81, Vulovitch 89).

The proposed project will synthesize the bibliography, including the results of the SR-1304 project on strategies for nonlinear analysis of marine structures, (sponsored by SSC) and identify the most practical approaches for prediction of nonlinear loads.

The following sources of nonlinearity should be considered,

- hydrostatic and hydrodynamic effects due to flaring of ship sections,

- viscous effects,

- large rolling motion, which introduces coupling between vertical and horizontal forces and their effects on loads,

- steep waves.

Perturbation and nonlinear simulation methods, based on strip theory, should be con-

sidered in this project. Presently, three-dimensional methods cannot be easily applied for load prediction in practical design problems. (ISSC Comm. I.2, 1988). However, there is an existing Accelerated Research Program on Nonlinear Ship Motion, that is supported by the U.S. Navy Office of Naval Research (ONR), which is aimed at developing techniques for calculating nonlinear hydrodynamic loads. This 5 year program (which started recently) also includes model testing and validation efforts, with the results expected to provide some useful applications for the present area of structural load prediction (without any extensive efforts by the Ship Structure Committee programs).

This is an important task because nonlinearities may play a dominant role in determination of design loads. We believe that the project can be accomplished at low cost and the risk associated with this endeavor (from the perspective of the Ship Structure Committee programs) is also low, based upon the efforts being carried out separately in the ONR program.

Task: Nonlinear systems under random excitation.

Importance: +
Risk: +
Cost: o
Priority: 6

Objective: Review and recommend methods for random vibration analysis of nonlinear ship responses.

In probabilistic analysis of dynamic systems, we need to derive the statistics of the response, and its extreme values from the known statistics of the driving exitation. For the case of nonlinear systems, this is a very challenging problem because the response is non-gaussian even if the driving excitation is a stationary gaussian stochastic process. Due to the nonlinear character of the ship response in high sea states, where the exciting forces are expected to be nonlinear also, it is very important to determine the statistics of the response.

This project, which will be initiated after completing the task on nonlinear loads, will review and recommend methods for determining the statistics of ship responses, loads, and load effects. It should also review the results from a pertinent project sponsored by the Ship Structure Committee (Chakrabarti 87) in terms of their utility.

The following methods should be studied:

- equivalent linearization techniques,

- Markov based approaches,

- methods based on Volterra series expansion of the response,

- Monte Carlo time domain simulation.

The investigator of this project must have a good understanding of random vibrations and level crossing problems. As a consequence, the associated cost might not be low. Some problems may also be encountered if the analytical results do not correlate well with those from Monte Carlo simulation or measurements. Furthermore, the large computational cost required by most of the aforementioned methods might be a problem.

Task: Modeling uncertainties.

Importance: +
Cost: +
Risk: +
Priority: 7

Objective: Develop a philosphophically consistent and practical method to model quantify, and account for modeling uncertainties in reliability analysis, design, and code calibration.

It is important to distinguish between natural and modeling uncertainties. Indeed, various studies on reliability analysis and design of marine structures yield erroneous results because they treat modeling uncertainties incorrectly (Bea 89, Olufsen 90). Unfortunately, there is no consensus on how to distinguish modeling uncertainties from natural ones, and how to treat them properly.

We should study modeling uncertainties closer and in more detail. The proposed project should address the following issues:

a) should we take modeling uncertainties into account in reliability analysis, design, and design code calibration?

b) what is the best way to account for modeling uncertainties?

c) how do the errors in various steps of stress analysis procedures propagate when estimating lifetime extreme loads and their effects?

d) are the existing databases on measured responses of marine structures sufficient to quantify modeling uncertainties?

e) what experiments should we conduct, and what measurements should we take, in order to quantify modeling uncertainties?

Clearly, it is important to answer the above fundamental questions before delivering a reliability based design code to practitioners. Otherwise, we take the risk of developing a code which prescribes designs with highly inconsistent safety levels (Bea 89, Olufsen 90). For this reason, this task is important. On the other hand, this is obviously very difficult and it requires significant resources. Also, due to the philoshophical nature of the questions related with this task, and the poor understanding of the nature of modeling uncertainties, there is a high risk that this task may not be completed in a satisfactory way.

Task: Breaking waves

Importance: +
Risk: +
Cost: +
Priority: 8

Objective: Study forces due to breaking waves.

Breaking waves can cause significant impact loads in both ships and offshore structures. Unfortunately, our ability to predict these loads is limited. (ISSC 85, Committee I.2). Ochi and Tsai (84) published results for the case of vertical walls of cylinders in breaking waves. Other related work of this nature was also carried out by Kjeldsen and Dean (86), where the forces measured in breaking waves were much larger than for non breaking wave conditions.

This task will critically review the literature in the area of breaking waves and it will provide methods for predicting the resulting loads. Data for structures other than cylinders would have to be obtained for application to a larger range of marine structures.

This is an important task because of the loads associated with breaking waves are large and they might dominate in design. Due to the complexity of the nature of breaking waves, and the poor understanding of the associated phenomenon, the cost is likely to be high and significant difficulties are expected in this study. Experimental measurements in controlled laboratory tests would be a main source of data for configurations not considered in previous work, which is another reason for expecting a high cost.

Task: Effects of routing, heavy weather countermeasures, and cargo load distribution in design

Importance: o
Risk: -
Cost: o
Priority: 9

Objective: Develop a method for predicting extreme loads and load effects in ships, which accounts for the effects of routing, heavy weather countermeasures and cargo load distribution in design.

The statistics of the lifetime extreme loads and their effects can be obtained by combining the short term statistics at all environmental and operational states weighted by the corresponding probability of occurrence of each state. In principle, this is a simple operation. However, the long term extreme loads are affected by many factors such as countermeasures taken under extreme weather conditions, weather routing, load distribution, and navigation errors. Petrie (86), Guedes Soares (90), and Hutchinson (86), investigated the effects of some of the above factors. Their results demonstrated that it is important to account for these factors, since these factors can increase critical load effects such as wave bending moments (Guedes Soares 90).

The objective of the proposed project is to review existing approaches for taking into account the effects of the aforementioned factors and integrate them into procedures for predicting long term extreme values of loads and their effects.

This objective can be accomplished by using Guedes Soares (90) approach. The key idea is to derive the conditional probability density function of operational parameters, such as relative ship heading, conditioned upon environmental parameters, such as the significant wave height, by simulating operational decisions by Monte Carlo simulation.

We believe that this task can be accomplished at moderate cost and we do not anticipate any problems or risks in completing it.

Task: Torsional loads in ships

Importance: o
Risk: o
Cost: o
Priority: 10

Objective: Develop methods for predicting torsional loads and their effects. Torsional

loads are important for design of ships with large hatch openings such as containerships. The uncertainty involved in estimating torsional moments is considerably higher than that in longitudinal bending moments. The reason is that the dynamic system, whose input is the wave elevation and output the resulting torsional loads, involves considerable nonlinearities associated with roll motion.

A study should be undertaken in order to reduce uncertainties in estimating torsional loads. This effort should allow us to predict torsional loads their statistics as well as their statistical correlation with the vertical and horizontal bending moments. It is important to know this correlation in order to be able to estimate the Von Mises stresses at critical locations in the deck.

The approach we propose to improve our ability to predict torsional loads will involve along the following,

a) more precise determination of line of action of lateral shear forces,

b) inclusion of nonlinear roll motion terms, in equivalent linearized form, in load equations,

c) more precise determination of distribution of vertical CG of distributed mass of analyzed ship.

The above actions are consistent with present analysis methods, and can be accomplished by efforts that require a moderate (average) cost. The expected risk is also moderate, in view of prior experience where torsional moments have not been predicted with sufficient accuracy.

Task: Ship-superstructure interaction

Importance: o
Risk: -
Cost: o
Priority: 11

Objective: Improve accuracy of structural analysis procedures by taking into account the interaction between the ship hull and the superstructure.

In analysis of ships with long superstructures, the interaction of the latter with the ship hull is important. Ordinarily, analysis methods do not model the superstructure and neglect its effects because it is believed that this is a conservative idealization. However, this is not true for all cases. Large stresses and resulting cracks have been observed at locations in the hull, which are near the superstructure. These have been attributed to sudden changes in the geometry and the flexibility along the ship hull. These sudden

changes are due to the presence of the superstructure.

For this reason we propose to modify and extent computer codes for structural analysis so that the superstructure is analyzed together with the hull.

This should be a relatively simple task which should also improve the effectiveness of stress analyses procedures. The associated cost and risk are deemed to be low.

Task: Hydrodynamic loads in offshore platforms

Importance: +
Risk: +
Cost: o
Priority: 12

Objective: Improve accuracy of load calculation methods in offshore platforms.

One of the conclusions from this study is that the uncertainty in hydrodynamic loads in fixed offshore platforms is the most important of all loads acting on such structures. Therefore, research efforts should be directed toward reducing this type of uncertainty.

For fixed jacket platforms, Morison's equation is usually employed to find loads. We should improve our ability of predicting wave particle kinematics, and of estimating the values of the coefficients in Morison's equation. We should also investigate alternative ways to estimate loads. For floating structures first order diffraction approaches should be further validated via comparisons with test data. Second order diffraction approaches should also be further developed and their results compared with measurements particularly for low frequency drift forces and also high frequency springing effection TLP and other moored structures.

The proposed project will address the above issues. This project is very important because uncertainties in hydrodynamic loads in offshore structures are critical. This should be a long term effort and the required cost could be considerable. The risk is also high due to the extreme complexity and length of the effort. However, even a small improvement in the accuracy of the load calculation procedures should lead to significantly more efficient designs (ISSC 85, Committee V2). In view of extensive efforts by the offshore engineering industry, most of the work will be accomplished by these private sources rather than through Ship Structure Committee studies.

Task: Natural period of offshore platforms

Importance: +
Risk: +
Cost: +
Priority: 13

Objective: Reduce the error in procedures for calculating the natural period of deep water fixed offshore platforms.

The uncertainty in the natural period of fixed offshore platforms is the most critical in dynamic analysis. (Moses 83). This uncertainty is primarily due to variations in the platform weight and the added hydrodynamic mass, and the uncertainty in the platform stiffness. The latter is due to the flexibility of the joints and errors in modelling the foundation. Therefore, we should reduce this critical uncertainty by focusing on the above sources of variability.

The cost required to complete this task might be high from the point of view of total effort devoted to this type of study. The reason is that it will be necessary to develop a model for the behavior of flexible joints and the behavior of the foundation which might be very complex and nonlinear. It is sometimes also difficult to estimate accurately the added mass of the platform, depending upon its specific design. However, in view of the efforts of the offshore industry, such work would be accomplished primarily by these private sources rather than via Ship Structure Committee studies. The risk in this area may be small, since a design allowance for variability in amplification ratios is usually considered in platform design.

Task: Flexibility of joints and rigid length of transverse webs in ships

Importance: o
Risk: -
Cost: -
Priority: 14

Objective: Extent computer codes for ship structural analysis so that the joint flexibility and the effect of rigid length of transverse webs is accounted for.

Hughes (83) (pp. 302-315), demonstrated the importance of taking into account the joint flexibility and the rigid behavior of portions of transverse webs in ship hulls. He also established simple finite element models which account for these effects. However, these models have not incorporated in any finite element code for ship structural analysis. As a result, existing codes which treat joints as rigid might and frames as flexible all over their

length result in considerable errors in transverse stress analysis.

We believe that the accuracy of available codes (MAESTRO, DAISY) can be significantly improved by implementing the method developed by Hughes. Furthermore, the increase in the complexity of the analysis, and the computer cost should be low. The improved codes should be particularly effective for analyzing commercial ships such as tankers, ore carriers, and bulk carriers, because transverse strength plays an important role in their design. The cost and risk associated with this task are low because the necessary finite element models and theoretical derivations have been already completed.

Task: Development of designer oriented computer code for stress analysis

Importance: o
Risk: -
Cost: +
Priority: 15

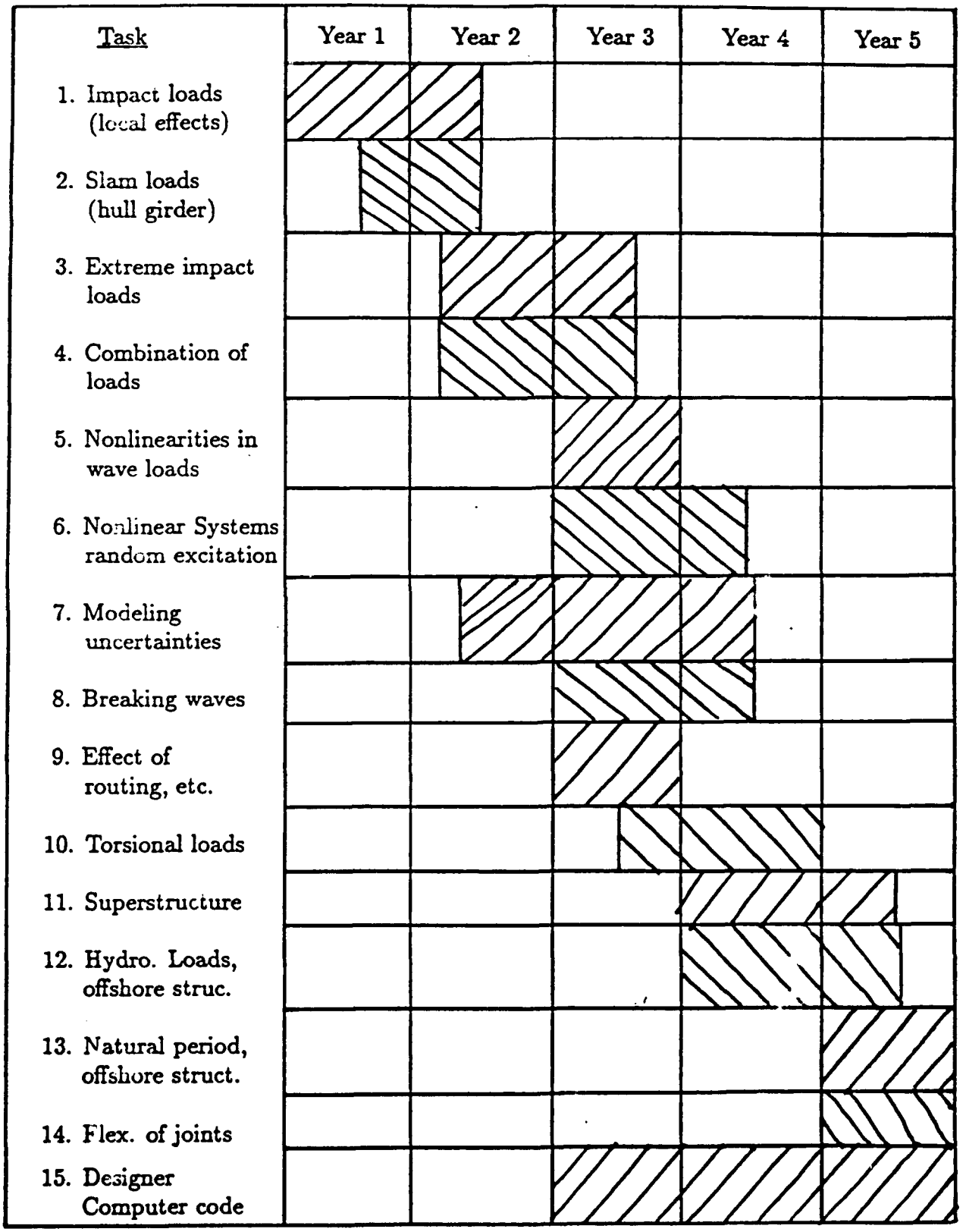
Objective: Combine computer codes on seakeeping, hydrodynamic load evaluation, structural analysis, load combination, analysis of long term extreme loads, and fatigue analysis, to produce a design oriented integrated computer package.

The completion of some of the previous tasks will result in significant advancements in the state of knowledge in the area of ship strength. We should translate these advancements into improvement in the effectiveness and the accuracy of stress analysis. Furthermore, we should make the methods developed in the previous tasks available to practitioners. Therefore, we propose to initiate a project, which will integrate the methods and the software developed, to produce an integrated computer package for stress analysis in ships. Existing computer codes for seakeeping, such as SCORES or ABS/SHIPMOTION, and for structural analysis, such as MAESTRO or DAISY, can be used. The final product will be a fully documented, user friendly computer program which can be used by practioners in ship design.

We believe that this is an important task. The cost associated with the task is expected to be considerable but not excessive. We do not expect any risks associated with this project.

Schedule

Proposed 5 year Research Program - Reduction of Uncertainties in Load Effects



10.0 References

Akita, Y., "Lessons Learned from Failure and Damage of Ships," *Joint Session I, 8th International Ship Structures Cong.*, 1982.

Anderson, W. D., Silbert, M. N., and Lloyd, J. R., "Reliability Procedure for Fixed Offshore Platforms," *Journal of the Structural Division, ASCE*, Vol. 108, No. ST 11, 1982, pp. 2517-2538.

Ang, A H-S, Cornell, A. C., "Reliability Bases of Structural Safety and Design," *Journal of the Structural Division, ASCE*, Vol. 100, No. ST9, Sept. 1974, pp. 1755-1769.

Bea, R., G., "Reliability Based Evaluations of Hydrodynamic Loadings on Coastal and Ocean Structures," *Institution of Engineers, Australia, Civil College Overseas Speaker Program*, 1989.

Bouwkamp, J. G., et al., "Effects of Joint Flexibility on the Response of Offshore Towers," *12th Annual Offshore Technology Conference*, Houston, Texas 1980, paper No. OTC 3901, pp. 455-464.

Chakrabarti, S.K., "Strategies for Nonlinear Analysis of Marine Structures, *Ship Structure Committee*, Report #347, 1987.

Chen, H. H., et al, "Correlation of Theoretical and Measured Hydrodynamic Pressures for the SL-7 Containership, and the Great Lakes Bulk Carrier S. J. CORT," *Ship Structure Committee*, Rpt. SSC-325, 1983.

Das, P.K., "The Reliability Analysis of Stiffened Cylinders Using Deterministic and Stochastic Methods," *The Royal Institution of Naval Architects*, 1986.

Dalzell, J. F., "The Ship in a Seaway," *Principles of Naval Architecture*, Vol. III, Chapter VIII, Section 4, pp. 84-109, 1989.

Ditlevsen, O., "Model Uncertainty in Structural Reliability", *Structural Safety*, 1, 1982, pp. 73-86.

El Batouti, A.M.T., Jan, H.Y., and Stiansen, S.G., "Structural Analysis of a Containership Steel Model and Comparison with Test Results," *Trans. SNAME*, Vol. 84, 1976.

Faulkner, D., "A Review of Effective Plating for Use in the Analysis of Stiffened Plating in Bending & Compression", *Journal of Ship Research*, Vol. 19, No. 1, March 1975, pp. 1-17.

Faulkner, D., "Semi-Probabilistic Approach to the Design of Marine Structures," *Extreme*

Loads Response Symposium, S.N.A.M.E., Arlington, 1981.

Faulkner, D., Birrell, N.D. and Stiansen, S.G., "Development of a Reliability Based Code for the Structure of Tension Leg Platforms," *Proceedings of the Fifteenth Offshore Technology Conference*, paper #4648, Vol. 3, 1983, pp. 575-586.

Ferro, G. and Mansour, A.E., "Probabilistic Analysis of the Combined Slamming and Wave Induced Responses," *Journal of Ship Research*, Vol. 29, No. 3, 1985, pp. 170-188.

Ferro, G., "Advances in the Calculation of the Maxima of Ship Responses," *Euromech Colloquium 155, Reliability Theory of Structural Engineering Systems, Engineering Academy of Denmark*, DIALOG 5-82 June 1982.

Ferry Borges, J., and Castanheta, M., *Structural Safety*, Laboratorio Nacional de Engenharia Civil, Lisboa, 1968 (2nd Edition, 1971).

Forristall, G, Z., "On the Statistical Distribution of Wave Heights in a Storm", *Journal of Geophysical Research*, Vol. 83, No. C5, May 1978.

Guedes Soares, C. and Moan, T., "On the Uncertainties Related to the Extreme Hydrodynamic Loading of a Cylindrical Pile," *Reliability Theory and Its Application in Structural and Soil Mechanics*, The Hague, Netherlands, Martinus Nijhoff Publ., 1982, pp. 351-364.

Guedes Soares, C., *Probabilistic Models for Load Effects in Ship Structures*, The Department of Marine Technology, The Norwegian Institute of Technology, Trondheim, Norway, Report #UR-84-38, 1984.

Guedes Soares, C. and Moan, T., "Uncertainty Analysis and Code Calibration of the Primary Load Effects in Ship Structures," in *Proceedings, 4th International Conference on Structural Safety and Reliability*, (ICOSSAR '85), Kobe, Japan, Vol. 3, 1985, pp. 501-512.

Guedes, Soares, C., "Assessment of the Uncertainty in Visual Observations of Wave Height," *Ocean Engineering*, Vol. 13, No. 1, 1986, pp. 37-56.

Guedes Soares, C., "Reliability of Marine Structures", Proceedings of the *ISPRA-Course*, Madrid, Spain, 1986.

Guedes Soares, C. and Moan, T., "Statistical Analysis of Still-water Load Effects in Ship Structures," *1988 SNAME Annual Meeting*, paper #4.

Guedes Soares, C., "Effect of Heavy Weather Maneuvering on the Wave-Induced Vertical Bending Moments in Structures", *Journal of Ship Research*, Vol. 34, No. 1, March 1990, pp. 60-68.

Haver, S., and Moan, T., "On Some Uncertainties Related to the Short Term Stochastic Modelling of Ocean Waves", *Applied Ocean Research*, Vol. 5, 1983, pp. 93-108.

Hoffman, D. and Miles, M., "Analysis of a Stratified Sample of Ocean Wave Records at Station "India"," *S.N.A.M.E. Tech. and Res. Bull.*, No. 1-35, May 1976.

Hogben, N. et al, "Environmental Conditions", Report of Committee 1, *Proc. 3rd International Ship Structures Congress*, Oslo, 1967.

Hughes, O.F., *Ship Structural Design*, John Wiley and Sons, 1983.

Hutchinson, B. L., "Cargo Mechanics (Application of Seakeeping-Revisited)", *Marine Technology*, Vol. 23, No. 3, 1986, pp. 230-241.

"Applied Design," Report of Committee V.2, *9th International Ship Structures Congress*, Geneva, 1985.

"Environmental Forces", Report of Committee I.2, *10th International Ship and Offshore Structures Congress*, Denmark, 1988.

Jan, H. Y., Chang, K. T., and Wojnarowski, M. E., "SL-7 Stress Calculations Compared with Full-Scale Measured Values," *Ship Structure Committee*, Report #282, 1979.

Jensen, J. J., and Pedersen, P. T., "Bending Moments and Shear Forces in Ships Sailing in Irregular Seas," *Journal of Ship Research*, Vol. 25, No. 4, December, 1981, pp. 243-251.

Kaplan, P. and Raff, A.L., "Evaluation and Verification of Computer Calculations of Water-Induced Ship Structural Loads," *Ship Structure Committee*, Rpt. SSC-229, 1972.

Kaplan, P., "Analysis and Assessment of Major Uncertainties Associated with Ship Hull Ultimate Failure," *SSC-332*, 1984.

Kaplan, P. "Analysis and Predictions of Flat Bottom Slamming Impact of Advanced Marine Vehicles in Waves", AIAA 8th Advanced Marine Systems Conference, San Diego, California, 1986. Also in *International Shipbuilding Progress*, Vol. 34, No. 391, March 1987.

Kaplan, P. et al, "Wave Effects Included in Simulation-An Extension of Capability for Harbor and WaterWay Development", *Proceedings of S.N.A.M.E. Spring Meeting*, 1987, Philadelphia, PA.

Kjeldsen, S. P. and Dean, R. G., "Wave Forces on Vertical Piles caused by 2- and 3-Dimensional Waves", *20th International Conference on Coastal Engineering*, November, 1986.

Kuang, J. G., Potvin, A. B., and Leick, R. D., "Stress Concentrations in Tubular Joints", *Journal of Petroleum Engineers*, August, 1977, pp. 287-299.

Larrabee, R. D., and Cornell, C. A., "Combination of Various Load Processes", *Journal of Structural Division, ASCE*, Vol. 107, 1981, pp. 223-239.

Lewis, E.V., "Predicting Long Term Distribution of Wave Induced Bending Moments in Ship Hulls", *S.N.A..M.E. Spring Meeting*, 1967.

Liu, D., Chen, H., and Lee, F., "Application of Loading Predictions to Ship Structure Design: A Comparative Analysis of Methods," *Extreme Loads Response Symposium, S.N.A.M.E.*, Arlington, Virginia, 1981, pp. 249-260.

Madsen, H. O., Krenk, S., and Lind, N. C., *Methods of Structural Safety*, Prentice-Hall, Edglewood Cliffs, NJ, 1986.

Mattu, R. K., "Methodology for Combining Dynamic Responses", *NUREG-0484, Rev. 1*, Office NRR, U.S. NRC, May 1980.

Mansour, A. E., and Lozow, J., "Stochastic Theory of the Slamming Response of Marine Vehicles in Random Seas", *Journal of Ship Research*, Vol. 26, No. 4, Dec. 1982, pp. 276-285.

Milchert, T., "Further Studies of Web Frames and their Beam Connections," Report No. E-42 *Royal Institute of Technology, Div. of Naval Architecture, Stockholm*, 1972.

Moore, N., et al., Interim Technical Report - Certification Process Assessment Task, *Jet Propulsion Laboratory, California Institute of Technology*, April, 1990.

Moses, F., "Implementation of a Reliability-Based API RP2A Format," Final Report, *API PRAC 83-22*, American Petroleum Institute, January 1985.

Moses, F., "Development of Preliminary Load and Resistance Design Document for Fixed Offshore Platforms," Final Report, *API PRAC 85-22*, American Petroleum Institute, January 1986.

Naess, A., "Extreme Value Estimates Based on Envelope Concept," *Applied Ocean Research*, 1982, No. 3, Vol. 4.

Naess, A., "Extreme Values of a Stochastic Process Whose Peaks are Subject to the Markov Chain Condition," *Norwegian Maritime Research*, No. 1, pp. 16-21, 1983.

Naess, A., "Statistical Analysis of Second-order Response of Marine Structures", *J. of Ship Research*, Vol. 29, No. 4, 1985, pp. 270-284.

Newlin, L., et al., "Probabilistic Low Cycle Fatigue Failure Analysis with Application to Liquid Propellant Rocket Engines", *Proceedings of the AIAA/ASME/AHS/ASC, 31st Structures, Structural Dynamics and Materials Conference*, pp. 1115-1123, 1990.

Ochi, M. K., and Motter, L. E., "Prediction of Slamming Characteristics and Hull Responses for Ship Design," *S.N.A.M.E. Transactions*, 1973, pp. 144-176.

Ochi, M. K., "Wave Statistics for the Design of Ships and Ocean Structures," *S.N.A.M.E. Transactions*, Vol. 86, 1978, pp. 47-69.

Ochi, M. K., "Extreme Values of Waves and Ship Responses Subject to the Markov Chain Condition", *Journal of Ship Research*, Vol. 23, No. 3, Sept. 1979, pp. 188-197.

Ochi, M. K., and Tsai, C. M., "Prediction of Impact Pressure Induced by Breaking Waves on Vertical Cylinders in Random Seas", *Journal of Applied Ocean Research*, Vol. 6, No. 3, 1984.

Ochi, M. K., *Applied Probability and Stochastic Processes*, John Wiley and Sons, New York, 1990.

Olufsen, A., and Bea, R. G., "Uncertainties in Extreme Wave Loadings on Fixed Offshore Platforms", *O.M.A.E. '90 Proceedings.*

Petrie, G. L., MacLean, W. M., Cojeen, H. P., Schudel, L. G., "The Usefulness of Response Monitoring for Estimation of Bow Structural Loadings", *Marine Technology*, Vol. 23, No. 3, July 1986.

Rask, I., "Slamming Pressure in Short-Crested and Obligue Seas", Report No. 105, *Dept. of Marine Structural Engineering*, Chalmers University of Technology, Göteborg, 1986.

Rosenblatt, M., "Remarks on a Multivariate Transformation", *The Annals of Mathematical Statistics*, Vol. 23, 1952, pp, pp. 470-472.

Salvensen, N., Tuck, E. O., and Faltinsen, O., "Ship Motions and Sea Loads", *S.N.A.M.E. Transactions*, Vol. 78, 1970, pp 250-287.

Schade, H. A., "The Effective Breadth of Stiffened Plating Under Bending Loads", *S.N.A.M.E. Transactions*, Vol. 59, 1951.

Schade, H. A., "The Effective Breadth Concept in Ship Structures", *S.N.A.M.E. Transactions*, Vol. 61, 1953, pp. 410-430.

Sutharshana, S., et al., Probabilistic High Cycle Fatigue Failure Analysis with Application to Liquid Propellant Rocket Engines", *Proceedings of AIAA/ASME/ASCE/AHS/ASC,*

31st Structures, Structural Dynamics, and Materials Conference, pp. 1105-1114, 1990.

Takemoto, M., "Wave Impact Test of a Wedge with Rectangular Plates and Analysis", *Journal of Society of Naval Architects of Japan*, Dec. 1984.

Thayamballi, A. and Jan, H.Y., "The Effect of Model Uncertainty on Design Fatigue Life Estimates of Offshore Structures," *Proceedings, Offshore Mechanics and Arctic Engineering Symposium*, Houston, Vol. III, 1987, pp. 375-383.

Timoshenko, S. P., and Goodier, J. N., *Theory of Elasticity*, Third Edition, 1970, pp. 262-268.

Timoshenko, S. P., *Strength of Materials*, Part II, Third Edition, 1983, pp. 64-68.

Turkstra, C.J., *Theory of Structural Safety*, SM Study No. 2, Solid Mechanics Division, University of Waterloo, Waterloo, Ontario, 1970.

Vulovich, R., Hirayama, T., Toki, N., and Mizuno, M., "Characteristics of Hull Stresses Measured on a Large Containesship in Rough Seas", *SNAME Transactions*, 1989.

Webster, W. C., and Payer, H. G., "Structural Tests of SL-7 Ship Model", *Ship Structure Committee*, Report SSC-269, 1977.

Watson, G. S., "Extreme Values in Samples from m-dependent Stationary Stochastic Processes", *Ann. Math Statistics*, Vol. 25, 1954, pp. 798-800.

Wen, Y. K., "Statistical Combination of Extreme Loads", *Journal of Structural Division*, ASCE, Vol. 103, No ST5, May 1977, pp. 1079-1093.

Wen, Y. K., and Pearce, H. T., "Combined Dynamic Effects of Correlated Load Processes", *Nuclear Engineering and Design*, Vol. 75, 1982, pp. 179-189.

Westin, H., "Analysis of Torsional Response of the SL-7 Hull Structure by the Use of the Finite-Beam Technique and Comparison with Other Techniques," *Journal of Ship Research*, Vol. 25, No. 1, pp. 62-75, Mar., 1981.

Winterstein, S. R., and Cornell, C. A., "Load Combinations and Clustering Effects", *Journal of Structural Engineering*, Vol. 110, No. 11, 1984, pp. 2690-2708.

Wirsching, P. H., "Probability Based Fatigue Design Criteria for Offshore Structures", *The American Petroleum Institute*, Report PRAC 80-15, Dallas, Texas, 1981.

Wirsching, P. H., "Final Report Questionnaire on Non-Statistical Uncertainties in Design Loads For Tension Leg Platforms," *American Bureau of Shipping*, Paramus, N.J, unpublished study, 1982.

Wirsching, P.H., "Fatigue Reliability for Offshore Structures," *Journal of Structural Engineering*, Vol. 110, No. 10, 1984, pp. 2340-2356.

Wirsching, P.H. and Chen, Y.N., "Consideration of Probability-Based Fatigue Design for Marine Structures," *Proceedings of the Marine Structural Reliability Symposium*, 1987, pp. 31-43, also in *Marine Structures*, Vol. 1, No. 1, 1988, pp. 23-45.

Appendix A: Calculation of Uncertainties in Lifetime Maximum Loads or Load Effects

The bias B, of the annual maximum load has a lognormal probability distribution. Therefore,

$$f_B(b) = \frac{1}{\sigma\sqrt{2\pi}b} e^{-\frac{(\ell nb - \lambda)^2}{2\sigma^2}}$$

where,

$$\sigma = (\ell n(1 + COV_B^2))^{1/2},$$

$$\lambda = \ell n(EB) \ - \frac{\sigma^2}{2},$$

and EB and COV_B are the mean and the coefficient of variation of B, respectively. The lognormal distribution belongs to the exponential class of probability distributions because it satisfies von Mises' condition (Ochi 90). Therefore, the maximum value of B, over an N year period $B^{(N)}$, follows the Type I asymptotic extreme value probability distribution,

$$F_{B^{(N)}}(b) = exp\ (-e^{-a_N(b - \bar{B}_N)})$$

where, $\bar{B}_N$ is the most probable maximum over the N year period, and

$$a_N = \quad N \cdot f_B(\bar{B}_N).$$

The most probable maximum, $\bar{B}_N$, satisfies the following equation,

$$P(B \geq \bar{B}_N) = \frac{1}{N},$$

which is equivalent to,

$$P(\ell nB \geq \ell n\bar{B}_N) = \frac{1}{N}$$

Therefore, since ℓnB is normally distributed with mean λ and standard deviation σ,

$$\bar{B}_N = exp\ (\Phi^{-1}(\frac{N-1}{N})\sigma + \lambda)$$

where $\Phi(\cdot)$ denotes the probability distribution function of a standard Gaussian random variable. Finally, the coefficient of variation of $B^{(N)}$ is

$$V_{B^{(N)}} = \frac{\pi/\sqrt{6}}{a_N\bar{B}_N + \gamma}$$

where α is the Euler's constant (0.577).

Appendix B: Combination of Slamming and Wave Induced Stresses: A Simulation Study

B.1 Introduction

The objective is to investigate the uncertainty of state-of-the-art methods for superimposing slamming, and wave induced stresses. For this purpose, we conducted a Monte-Carlo simulation study to compare the maximum combined slamming and wave induced bending moment against that estimated by three approximate methods for load combination. The first method is Turkstra's rule and it has been utilized by Ferro and Mansour (85). The second method assumes that the maxima of the two loads coincide. This method will be called peak coincidence approximation. The last method, which is called square root of sum of squares (SRSS), has been suggested by Mattu (80). The SRSS method has also been employed by Kaplan (84) to combine slamming and wave bending moments.

Other generic methods for combining loads are the load coincidence (LC) method, which was introduced by Wen (77, 82), and the point crossing method proposed by Winterstein and Cornell (84). LC method is more advanced than the first three methods, which were mentioned in the previous paragraph, and it accounts for the statistical dependency of the load processes to be combined. However, it requires some information on the load processes which is difficult to be estimated for the case of slamming and wave bending combination. For example, it is very difficult to calculate the mean rate of coincidence of the aforementioned loads, or the conditional probability distribution of the maxima of the combined load process, given that the maxima coincide. Therefore, LC method is not readily applicable to the problem of combining bending moments. Moreover, to the best of our knowledge, it has never been applied to the problem of slamming and wave bending combination. Therefore, we did not consider this method in this study. On the other hand, Winterstein's method assumes that the load processes are statistically independent, which is not a realistic assumption. We also did not consider this method in our study.

The procedure, which was used in this study, consists of the following steps:

a) Select a representative ship.

b) Select a ship speed and a significant wave height.

c) Simulate a time history of the wave elevation, by using a random number generator.

d) Evaluate the resulting wave bending time history using the SCORES seakeeping computer code. Find the extreme value.

e) For the time history which was generated in step c, calculate the time history of the resulting slamming bending moment. Find the extreme value.

f) Superimpose the wave and slamming bending moments, which were generated in tasks d and e, to obtain the combined bending moment.

g) Find the extreme value of the combined bending moment. Consider this value as the actual maximum combined bending moment.

h) Use Turkstra's rule, the peak coincidence approximation, and the S.R.S.S. approach to estimate the extreme combined bending moment from the time histories of the slamming and wave bending moment, which were generated in tasks d and e.

i) Compare the estimated combined bending moment against the actual bending moment (task h). Steps c) - i) are repeated in order to obtain a sufficiently large number of samples.

The data used in this study are presented in Table B.1. The computer program SCORES was employed to obtain information which was necessary for the simulation, such as two dimensional properties, and response amplitudes and phases for bending moment, relative motion, and velocity as function of frequency. Random time histories for the wave elevation were generated according to the procedure suggested by Kaplan (72, 87). The method described by Kaplan (72, 86) was employed to calculate the slamming bending moment in task e. Finally, we assumed that the hull is rigid in calculating the slamming bending moment as the response to impact forces. This assumption might lead to underestimation of the slamming bending moment because it neglects the effects of the hull flexibility and vibratory responses. However, it is acceptable in the context of our study, because the objective is to assess the error in combining slamming and wave bending moments and not to find the exact values of these quantities.

Table B. 1. Data for Simulation Study

Ship Length (m):	193
Displacement (tons):	36100
Beam (m):	27.6
Draft (m):	11.0
Block Coefficient:	0.6
Speed (knots):	15, 18, 20, 25

Type of Wave Spectrum: Pierson Moskowitz (1964)

Significant Wave Height (m): 6.1, 9.6, 13.1

Length of Simulated Time Period (min): 10

B.2. Results and discussion

The estimates of the maximum combined bending moment over a time interval of 10 min are presented in Tables B2-B7. Results from Monte-Carlo simulation, Turkstra's rule, peak coincidence approximation, and the SRSS law are presented in the above tables. These results are for ship speeds from 15 to 25 knots and for significant wave heights in the range from 6 to 13 m. The bias and scatter of the maximum combined bending moment are also presented. These estimates have been derived from 200 simulated time histories of the combined bending moment.

The maximum bending moment for ship speed equal to 15 knots is plotted as function of the significant wave height in Figure B1. This figure compares the maximum simulated bending moment against that estimated by Turkstra's rule, peak coincidence approximation, and SRSS law. The shaded regions correspond to the range enclosed by, a) the expected maximum combined bending moment, and b) the same quantity plus one standard deviation.

The characteristic design value of the combined bending moment at a risk level α, is defined as the threshold which corresponds to a probability of at least one upcrossing equal to α. The characteristic design values for probability levels 0.05 and 0.01, which were obtained by simulation and by the two approximate methods are presented in Figure B2. The results in this figure correspond to a ship speed of 15 knots and significant wave height ranging from 6.14 m to 13 m.

It is observed that the peak coincidence approximation is conservative and that its estimates are consistently higher than the values obtained by simulation. The bias of the peak coincidence approximation is roughly 0.85 which means that the actual combined bending moment is 15% lower than the estimated value. This trend of the peak coincidence approximation to overestimate loading can be explained as follows. The maximum slamming and wave bending moment do not occur simultaneously. This can be observed from Figure B3 which depicts a simulated time history of the combined bending moment. Apparently, the maximum of the combined bending moment highly depends on the phase lag, δ, which corresponds to the elapsed time between the occurence of a slamming and a wave bending moment peak. The most hazardous case is when δ is zero which means that the peaks of the two loadings coincide. It is known, that a slam almost always occurs when the bending moment changes from hogging to sagging. Moreover, phase lag, δ, is not likely to be zero (Ochi 73). Consequently, the peaks of the two loadings are not likely to coincide. Therefore, the peak coincidence approximation, which is based on the aforementioned unrealistic assumption, yields conservative results. SRSS law ignores the trend of δ to take values within a narrow range and therefore its estimates are also in error. In our study, the error was lower than that from the peak coincidence approximation. Furthermore, the results from SRSS law did not show any trend of being conservative of unconservative. This observation agrees with the conclusions of Wen (82).

In general, Turkstra's rule is not conservative. However, its results were conservative for high risk levels. The large scatter of the estimates, which were found roughly equal to 20-25%, explains this observation. The histograms of the maximum combined loading from simulation and from Turkstra's rule (Figure B4) show that, although the average value of the latter is lower than that of the former, the estimates from Turkstra's rule are more likely to exceed a high threshold because, the corresponding histogram is more dispersed. This relatively high scatter of Turkstra's rule estimates can be explained by the equation defining this rule for the case of two load processes:

$$max_T\{b_T(t)\} \simeq max\Big\{max_T\{b_w(t)\} + b_s(t), b_w(t) + max_T\{b_s(t)\}\Big\},$$

where $b_T(t), b_s(t)$, and $b_w(t)$ represent the combined slamming, and wave induced bending moment, and $max_T\{\cdot\}$ denotes the maximum value of the bracketed process over a time period of length T. In general, the coefficients of variation of random variables $b_s(t)$ and $b_w(t)$ are considerably higher than the coefficients of variation of $max_T\{b_w(t)\}, max_T\{b_s(t)\}$, and $max_T\{b_T(t)\}$. In particular, if the length of time interval T is large, then the coefficients of variation of the maxima are very low compared to that of $b_s(t)$ and $b_w(t)$. As a result, the coefficient of variation of the random function on the right hand side of Turkstra's rule equation is larger than that of the actual maximum of the combined stress process, $max_T\{b_T(t)\}$.

Finally, the effect of the number of simulated time histories on the estimated bias is shown in Figure B5. It is observed that the number simulated time histories considered in this study is sufficient for estimating the above statistics with good accuracy.

B.3. Conclusions

The following are the main conclusions from our study:

a) The results of simplified approaches, which are used to combine the slamming and wave induced bending moments, may lead to serious errors in the estimated design loads. Note that the bias introduced by these approaches is systematic, and as such, it will not decrease even if the length of the time interval, which is considered, becomes very high (say 20 years).

b) The peak coincidence approximation is conservative with a bias in the range from 0.60 to 0.80.

c) The results from SRSS law and Turkstra's rule do not consistently lie on the same side, conservative or nonconservative, of the actual load value. Thus, we cannot bracket the expected maximum combined bending moment using one of these approaches together with the peak coincidence approximation.

d) The design load estimates from Turkstra's rule have significantly larger variability

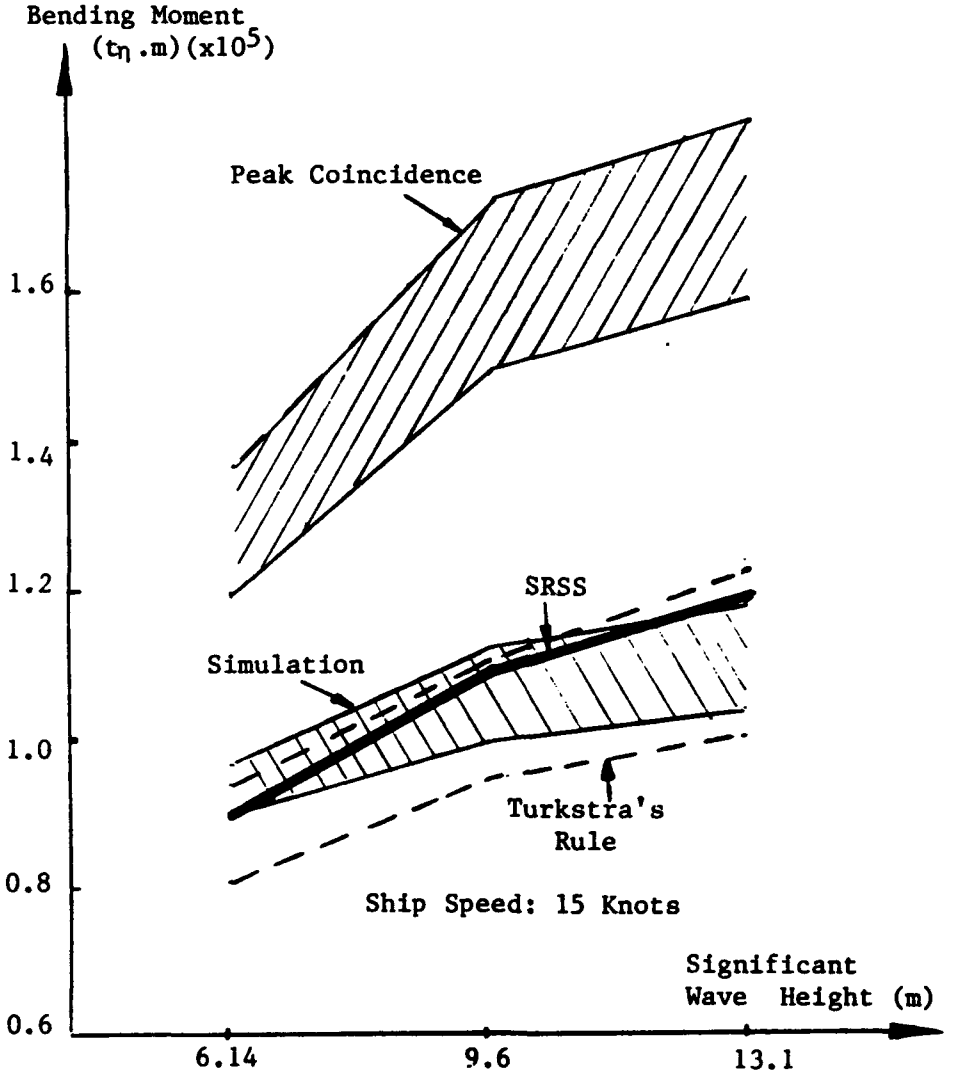


Figure B1: Maximum Wave Bending Moment vs. Significant Wave Height

Note: For each set of curves lower one corresponds to expected value, upper one corresponds to expected value plus one standard deviation.

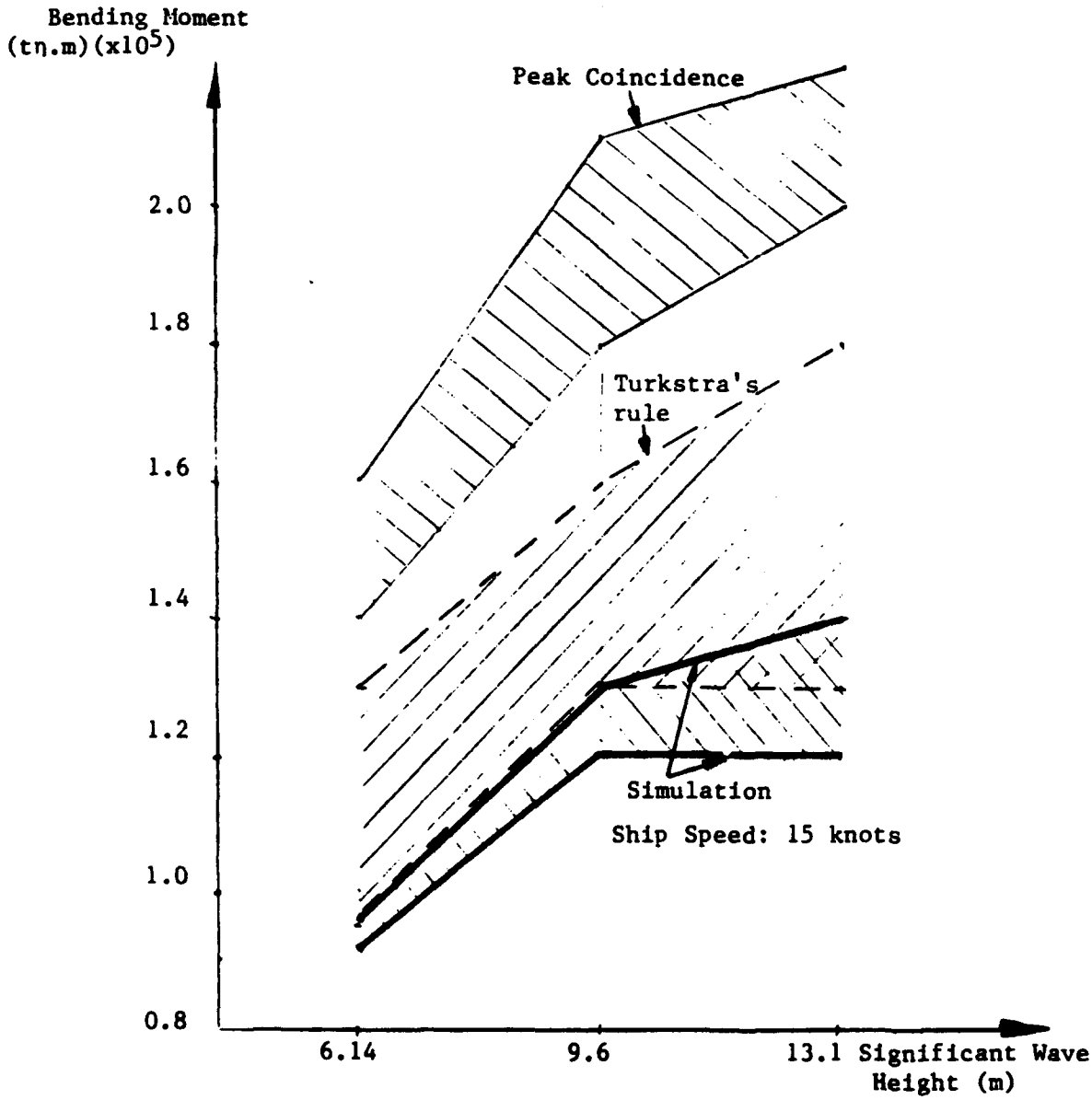


Figure B2: Design Bending Moment vs. Significant Wave Height
Note: For each set of curves, the lower one corresponds 5% risk level, and the upper one to 1% risk level.

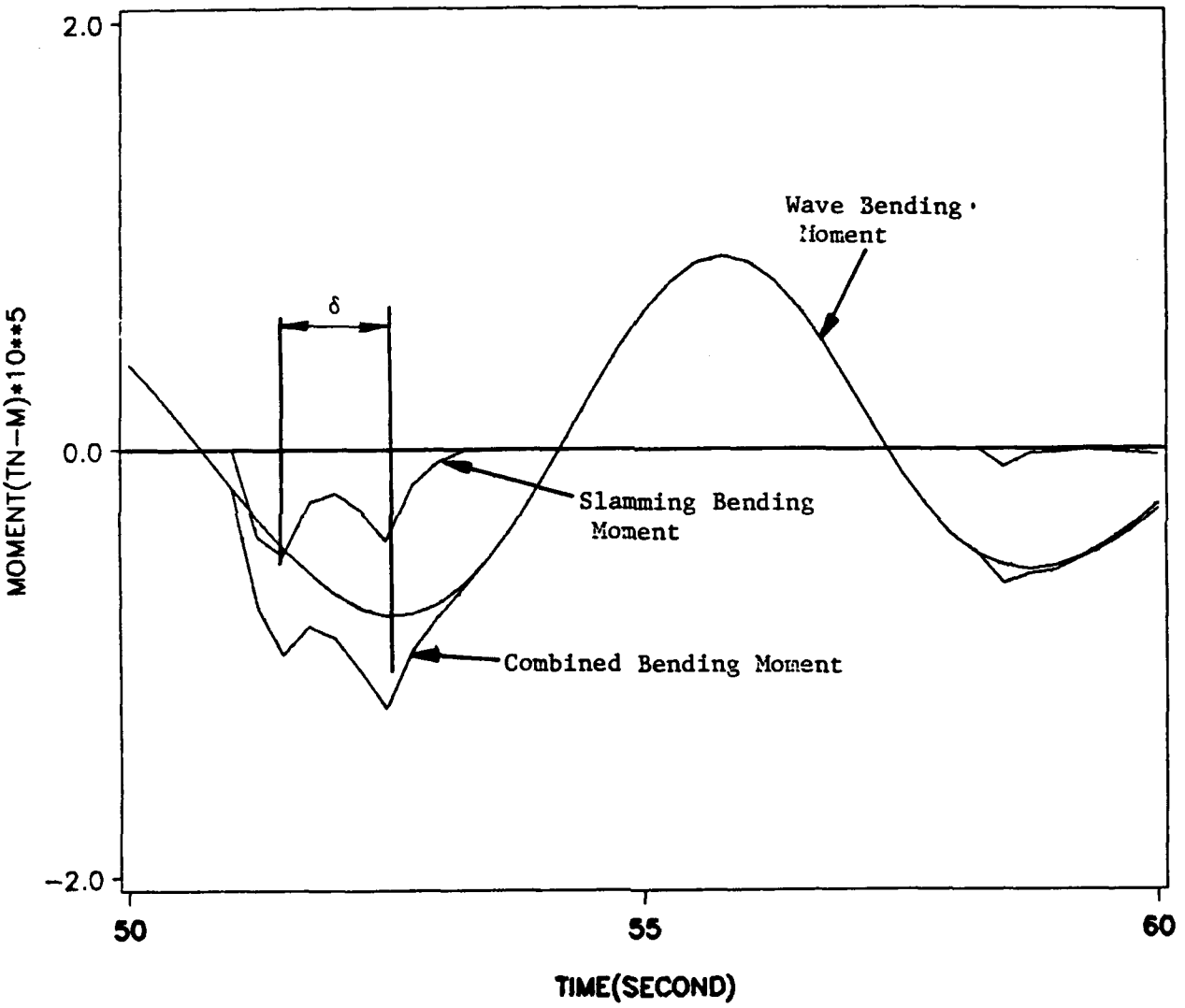


Figure B.3: Wave, Slamming and Combined Bending Moment Time History

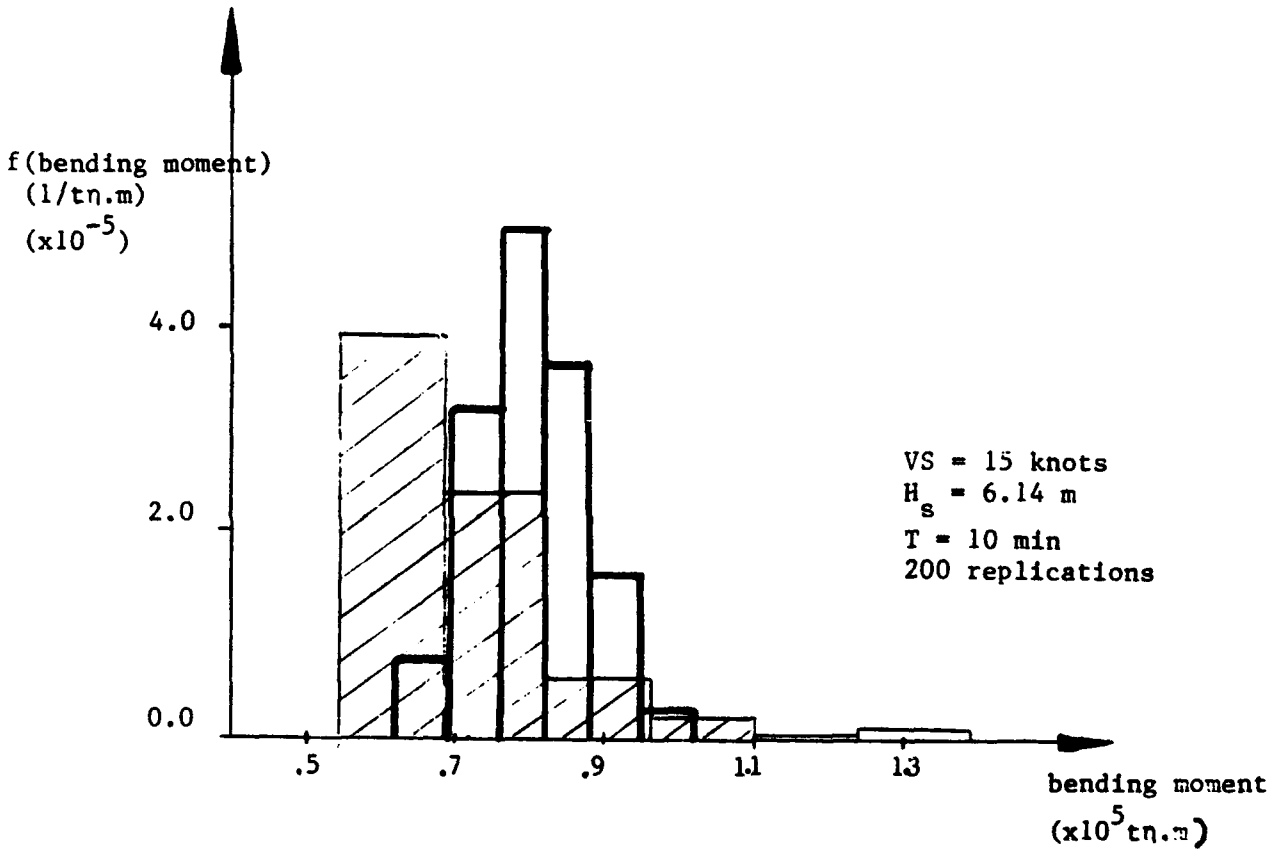


Figure B4: Maximum Combined Bending Moment Histograms
(The histogram traced by the thick line corresponds to simulation results, and histogram traced by the thin line corresponds to Turkstra's rule)

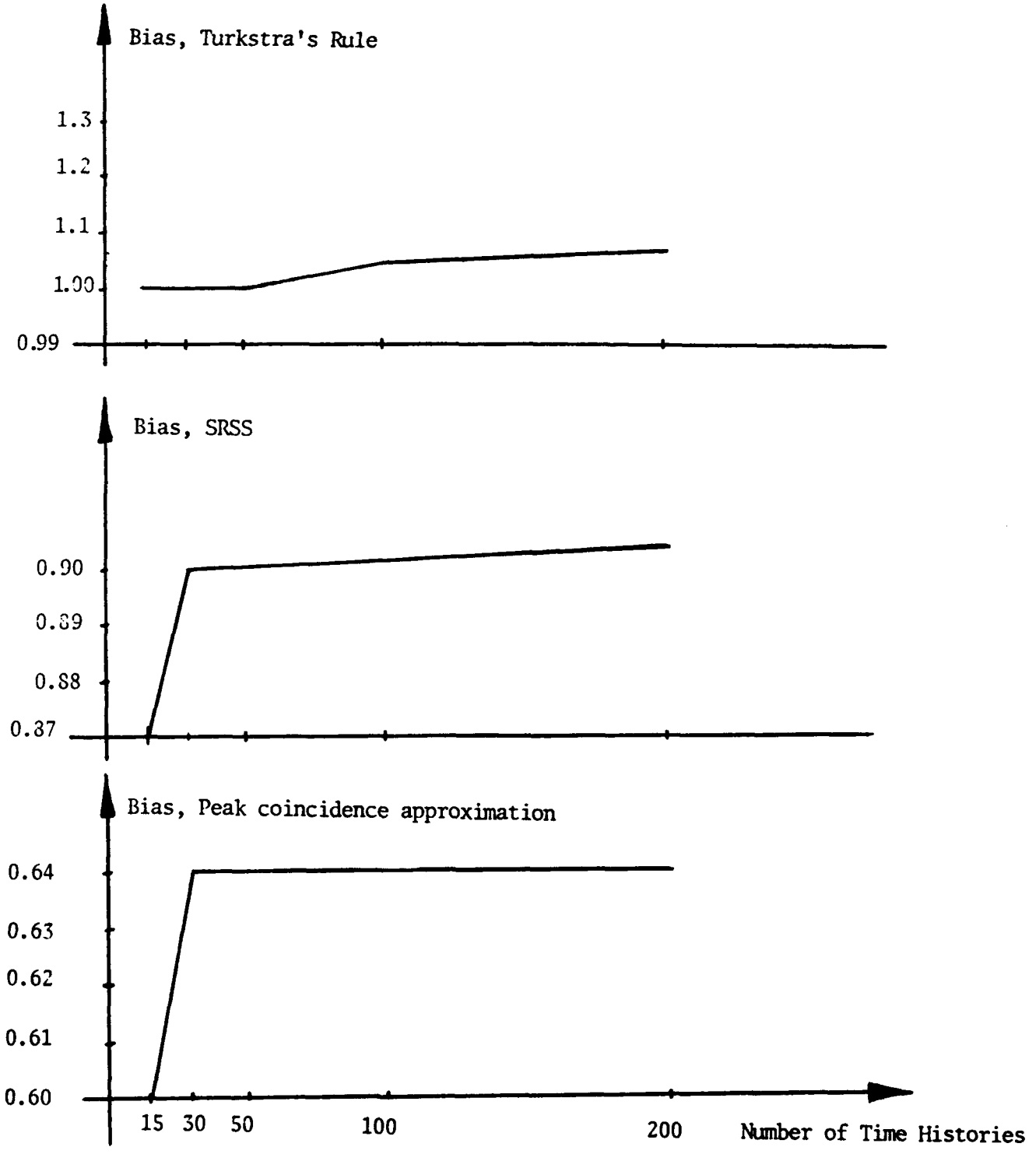


Figure B.5 Estimated Bias vs. Number of Simulated Time Histories

than the actual load. This means that this approximate rule introduces both bias and variability, which is added to the statistical variabil

Table B2. Statistics of Maximum Value
of Combined Bending Moment for Significant
Wave Height: 6.14m, Ship Speed: 15 knots

Method/ Quantity	Simulation	Turkstra's Rule	Peak Coincidence Rule	SRSS
Mean (tn.m)	0.8×10^5	0.71×10^5	0.11×10^6	0.8×10^5
Bias	1.0	1.1	0.71	1.0
Scatter	0.09	0.19	0.15	-
Char. Design Value ($\alpha = 0.1$) (tn-m)	0.89×10^5	0.86×10^5	0.13×10^6	-
Char. Design Value ($\alpha = 0.05$) (tn-m)	0.92×10^5	0.95×10^5	0.14×10^6	-
Char. Design Value ($\alpha = 0.01$) (tn-m)	0.96×10^5	0.13×10^6	0.16×10^6	-

Average Maximum Wave Bending Moment (tn.m) = 0.648×10^5

Average Maximum Slamming Bending Moment (tn.m) = 0.472×10^5

Note: All bending moments correspond to sagging

Table B3. Statistics of Maximum Value
of Combined Bending Moment for Significant
Wave Height: 9.6(m), Ship Speed: 15 knots

Method/ Quantity	Simulation	Turkstras Rule	Peak Coincidence Rule	SRSS
Mean (tn.m)	0.9×10^5	0.85×10^5	0.14×10^6	0.996×10^5
Bias	1.0	1.1	0.64	0.9
Scatter	0.143	0.26	0.162	-
Char. Design Value ($\alpha = 0.1$) (tn-m)	0.10×10^6	0.11×10^6	0.17×10^6	-
Char. Design Value ($\alpha = 0.05$) (tn-m)	0.12×10^6	0.13×10^6	0.18×10^6	-
Char. Design Value ($\alpha = 0.01$) (tn-m)	0.13×10^6	0.17×10^6	0.21×10^6	-

Average Maximum Wave Bending Moment (tn.m) = 0.72×10^5

Average Maximum Slamming Bending Moment (tn.m) = 0.695×10^5

Note: All bending moments correspond to sagging

Table B4. Statistics of Maximum Value
of Combined Bending Moment for Significant
Wave Height: 13.07m, Ship Speed 0 Knots

Method/ Quantity	Simulation	Turkstra Rule	Peak Coincidence Rule	SRSS
Mean (tn.m)	0.95×10^5	0.91×10^5	0.15×10^6	0.11×10^6
Bias	1.0	1.04	0.62	0.88
Scatter	0.15	0.25	0.16	-
Char. Design Value ($\alpha = 0.1$) (tn-m)	0.11×10^6	0.12×10^6	0.18×10^6	-
Char. Design Value ($\alpha = 0.05$) (tn-m)	0.12×10^6	0.13×10^6	0.20×10^6	-
Char. Design Value ($\alpha = 0.01$) (tn-m)	0.14×10^6	0.18×10^6	0.22×10^6	-

Average Maximum Wave Bending Moment (tn.m) = 0.75×10^5

Average Maximum Slamming Bending Moment (tn.m) = 0.77×10^5

Note: All bending moments correspond to sagging

Table B5. Statistics of Maximum Value
of Combined Bending Moment for Significant
Wave Height: 6.14m, Ship Speed: 18 knots

Method/ Quantity	Simulation	Turkstras Rule	Peak Coincidence Rule	SRSS
Mean (tn.m)	0.1×10^6	0.83×10^5	0.14×10^6	0.99×10^5
Bias	1.0	1.2	0.72	1.0
Scatter	0.15	0.21	0.17	-
Char. Design Value ($\alpha = 0.1$) (tn-m)	0.12×10^6	0.11×10^6	0.17×10^6	-
Char. Design Value ($\alpha = 0.05$) (tn-m)	0.14×10^6	0.12×10^6	0.19×10^6	-
Char. Design Value ($\alpha = 0.01$) (tn-m)	0.15×10^6	0.15×10^6	0.2×10^6	-

Average Maximum Wave Bending Moment (tn.m) = 0.7×10^5

Average Maximum Slamming Bending Moment (tn.m) = 0.71×10^5

Note: All bending moments correspond to sagging

Table B6. Statistics of Maximum Value
of Combined Bending Moment for Significant
Wave Height: 6.14m, Ship Speed: 20 knots

Method/ Quantity	Simulation	Turkstras Rule	Peak Coincidence Rule	SRSS
Mean (tn.m)	0.12×10^6	0.98×10^5	0.16×10^6	0.11×10^6
Bias	1.0	1.3	0.76	1.09
Scatter	0.22	0.30	0.19	-
Char. Design Value ($\alpha = 0.1$) (tn-m)	0.16×10^6	0.13×10^6	0.2×10^6	-
Char. Design Value ($\alpha = 0.05$) (tn-m)	0.18×10^6	0.15×10^6	0.23×10^6	-
Char. Design Value ($\alpha = 0.01$) (tn-m)	0.21×10^6	0.20×10^6	0.25×10^6	-

Average Maximum Wave Bending Moment (tn.m) = 0.763×10^5

Average Maximum Slamming Bending Moment (tn.m) = 0.848×10^5

Note: All bending moments correspond to sagging

Table B7. Statistics of Maximum Value
of Combined Bending Moment for Significant
Wave Height: 6.14m, Ship Speed: 25 knots

Method/ Quantity	Simulation	Turkstras Rule	Peak Coincidence Rule	SRSS
Mean (tn.m)	0.18×10^6	0.13×10^6	0.21×10^6	0.15×10^6
Bias	1.0	1.4	0.83	1.20
Scatter	0.21	0.26	0.16	-
Char. Design Value ($\alpha = 0.1$) (tn-m)	0.23×10^6	0.17×10^6	0.25×10^6	-
Char. Design Value ($\alpha = 0.05$) (tn-m)	0.25×10^6	0.18×10^6	0.27×10^6	-
Char. Design Value ($\alpha = 0.01$) (tn-m)	0.28×10^6	0.22×10^6	0.30×10^6	-

Average Maximum Wave Bending Moment (tn.m) = 0.94×10^5

Average Maximum Slamming Bending Moment (tn.m) = 0.117×10^6

Note: All bending moments correspond to sagging

COMMITTEE ON MARINE STRUCTURES

Commission on Engineering and Technical Systems

National Academy of Sciences - National Research Council

The COMMITTEE ON MARINE STRUCTURES has technical cognizance over the interagency Ship Structure Committee's research program.

Stanley G. Stiansen (Chairman), Riverhead, NY
Mark Y. Berman, Amoco Production Company, Tulsa, OK
Peter A. Gale, Webb Institute of Naval Architecture, Glen Cove, NY
Rolf D. Glasfeld, General Dynamics Corporation, Groton, CT
William H. Hartt, Florida Atlantic University, Boca Raton, FL
Paul H. Wirsching, University of Arizona, Tucson, AZ
Alexander B. Stavovy, National Research Council, Washington, DC
Michael K. Parmelee, Ship Structure Committee, Washington, DC

LOADS WORK GROUP

Paul H. Wirsching (Chairman), University of Arizona, Tucson, AZ
Subrata K. Chakrabarti, Chicago Bridge and Iron Company, Plainfield, IL
Keith D. Hjelmstad, University of Illinois, Urbana, IL
Hsien Yun Jan, Martech Incorporated, Neshanic Station, NJ
Jack Y. K. Lou, Texas A & M University, College Station, TX
Naresh Maniar, M. Rosenblatt & Son, Incorporated, New York, NY
Solomon C. S. Yim, Oregon State University, Corvallis, OR

MATERIALS WORK GROUP

William H. Hartt (Chairman), Florida Atlantic University, Boca Raton, FL
Fereshteh Ebrahimi, University of Florida, Gainesville, FL
Santiago Ibarra, Jr., Amoco Corporation, Naperville, IL
Paul A. Lagace, Massachusetts Institute of Technology, Cambridge, MA
John Landes, University of Tennessee, Knoxville, TN
Mamdouh M. Salama, Conoco Incorporated, Ponca City, OK
James M. Sawhill, Jr., Newport News Shipbuilding, Newport News, VA

SHIP STRUCTURE COMMITTEE PUBLICATIONS

SSC-347 Strategies for Nonlinear Analysis of Marine Structures and Criteria for Evaluating the Results by Subrata K. Chakrabarti 1988

SSC-348 Corrosion Experience Data Requirements by Karl A. Stambaugh and John C. Knecht 1988

SSC-349 Development of a Generalized Onboard Response Monitoring System (Phase I) by F. W. DeBord, Jr. and B. Hennessy 1987

SSC-350 Ship Vibration Design Guide by Edward F. Noonan 1989

SSC-351 An Introduction to Structural Reliability Theory by Alaa E. Mansour 1990

SSC-352 Marine Structural Steel Toughness Data Bank by J. G. Kaufman and M. Prager 1990

SSC-353 Analysis of Wave Characteristics in Extreme Seas by William H. Buckley 1989

SSC-354 Structural Redundancy for Discrete and Continuous Systems by P. K. Das and J. F. Garside 1990

SSC-355 Relation of Inspection Findings to Fatigue Reliability by M. Shinozuka 1989

SSC-356 Fatigue Performance Under Multiaxial Load by Karl A. Stambaugh, Paul R. Van Mater, Jr., and William H. Munse 1990

SSC-357 Carbon Equivalence and Weldability of Microalloyed Steels by C. D. Lundin, T. P. S. Gill, C. Y. P. Qiao, Y. Wang, and K. K. Kang 1990

SSC-358 Structural Behavior After Fatigue by Brian N. Leis 1987

SSC-359 Hydrodynamic Hull Damping (Phase I) by V. Ankudinov 1987

SSC-360 Use of Fiber Reinforced Plastic in Marine Structures by Eric Greene 1990

SSC-361 Hull Strapping of Ships by Nedret S. Basar and Roderick B. Hulla 1990

SSC-362 Shipboard Wave Height Sensor by R. Atwater 1990

None Ship Structure Committee Publications - A Special Bibliography 1983